
Sound control in windy weather

Master Thesis
Jonas Buchholdt

Aalborg University
Electronic Engineering and IT

Copyright © Jonas Buchholdt, Electronic Engineering and IT P10, Aalborg University 2019
This report is compiled in L^AT_EX. Additionally Mathworks MATLAB[®], Inkscape, and Xfig
are used to draw figures and charts.



Electronic Engineering and IT
Aalborg University
<http://www.aau.dk>

AALBORG UNIVERSITY
STUDENT REPORT

Title:
Sound control in windy weather

Abstract:
Will come later

Theme:
Signal Processing and Acoustics

Project Period:
MSc, 10th Semester 2019

Project Group:
Jonas Buchholdt

Participants:
Jonas Buchholdt

Supervisor:
Sofus Birkedal Nielsen

Number of Pages: 214

Date of Completion:
?th June 2019

The content of this report is freely available, but publication may only be pursued with reference.

Preface

This report is composed by Jonas Buchholdt during the 10th semester of Electronic Engineering and IT at Aalborg University. The general purpose of the report is *Signal Processing and Acoustics*.

For citations, the report employs the Harvard method. If citations are not present by figures or tables, these have been made by the authors of the report. Units are indicated according to the SI standard.

Aalborg University, May 23, 2019

Jonas Buchholdt
<Jbuchh13@student.aau.dk>

Contents

Preface	v
Glossary	1
1 Introduction	3
1.1 Live venue sound challenges	3
I Problem Analysis and Requirements	7
2 Analysis of sound propagation in outdoor venue	9
2.1 Ideal geometric spreading loss	9
2.2 Homogeneous atmospheric conditions	11
2.3 Inhomogeneous atmospheric conditions	18
2.4 sound pressure level doing a concert	26
3 Summary of Problem Analysis	27
4 Problem statement	29
4.1 Delimitation	29
II Test Design	31
5 Preknowledge of outside measurement	33
5.1 Measuring in inhomogeneous atmosphere	33
5.2 Ground reflection	33
5.3 Wind noise	33
6 Proposal solution	35
6.1 proposal of solution to the wind problem	35
6.2 Optimality condition	35
6.3 Proposal solution to crosswind	36
6.4 Proposal solution to parallel wind	38
7 Test of Proposal Solution	39
7.1 Test of proposal solution	39
7.2 Description of the used line source array	39
7.3 Designing the measurement	43

7.4	Data logging system	55
8	Test of measuring design	61
8.1	Test of measuring design	61
8.2	research of the problems	71
8.3	Update to the final measurement	72
III	Measurement	75
9	Measurement	77
9.1	The measurement	77
9.2	Wind noise doing measurement	77
9.3	Crosswind measurement	80
9.4	parallel wind measurement	88
IV	Results	95
10	Results	97
10.1	Result	97
10.2	Crosswind data analysis	97
10.3	Parallel wind data analysis	99
11	Discussion and conclusion	101
11.1	Conclusion	101
V	Appendix	103
A	cross wind effect on line source array	105
B	Design of windscreen	113
C	Windscreen concept measurement	119
D	Windscreen attenuation measurement	129
E	Windscreen attenuation measurement	143
F	Windscreen attenuation measurement	153
G	Outline ET 250-3D turntable control	159
H	Weather measurement	163
I	Impulse response measuring software	167
J	The directionality of L-acoustics KUDO	171
K	cross wind effect on line source array	177
L	Line source array angle measuring design	185
M	Windscreen influence of frequency response	187
N	Wind noise in designed windscreen	199
O	Hardware	205

P Questionnaire	207
Bibliography	211

Glossary

ADC Analog to Digital Converter. 57

DLL Dynamic Link library. 159

DSP Digital Signal Processor. 78

FDTD Finite-Difference Time-Domain. 15

FFT Fast Fourier Transform. 56

FIFO First In First Out. 57

FOH Front Of House. 5, 26

IFFT Inverse Fast Fourier Transform. 56

IP Internet Protocol. 159

PA Public Address System. 3, 4

PCB Printed Circuit Board. 59

SPL Sound Pressure Level. 3, 4, 5, 9, 10, 11, 12, 16, 17, 20, 23, 24, 25, 26, 27, 28, 29, 35, 36, 37, 39, 40, 41, 44, 45, 49, 54, 56, 63, 66, 68, 69, 70, 71, 73, 80, 89, 107, 108, 109, 115, 116, 133, 172, 191, 192, 193, 194, 197, 202, 204

TTL Transistor–Transistor Logic. 159

UDP User Datagram Protocol. 159

USB Universal Serial Bus. 55, 58

Chapter 1

Introduction

1.1 Live venue sound challenges

This section explores the challenges of producing sound in an outdoor environment. The challenge of producing a good sound experience for the audience highly depend on the calibration method and the atmosphere condition. It is well known that acoustically wave propagation is strongly affected by the inhomogeneous atmosphere doing the outdoor sound propagation. This inhomogeneous atmosphere shifts the calibration of the sound system which affects the intelligibility. In section 1.1.1 an overview of high Sound Pressure Level (SPL) Public Address System (PA) system is discussed.

1.1.1 Acoustics as live venue

An outdoor PA system is an essential sound reinforcement concept today. It is used to address information, music or just entertainment where the number of audiences is large, sometimes more than 10.000 audiences. The number of the audience makes it difficult to address the information to a large number of the audience without the reinforcement of the information. The reinforcement is nearly always done from a stage with a sizeable PA system and sometimes delay unit in the middle of the audience area. The stage lifts the artist while the PA system is designed to cover the audience area with sound. The optimal PA system covers the area with a linear frequency spectrum in the audible frequency range with a homogeneous SPL. Today, the used speaker is a line source array flown in both side of the stage and is therefore only close to the audience in front of the stage. The line source array is an array of small identically wide speakers attached to each other, to form a vertical line of speakers. An example of a line source array is shown in Figure 1.1

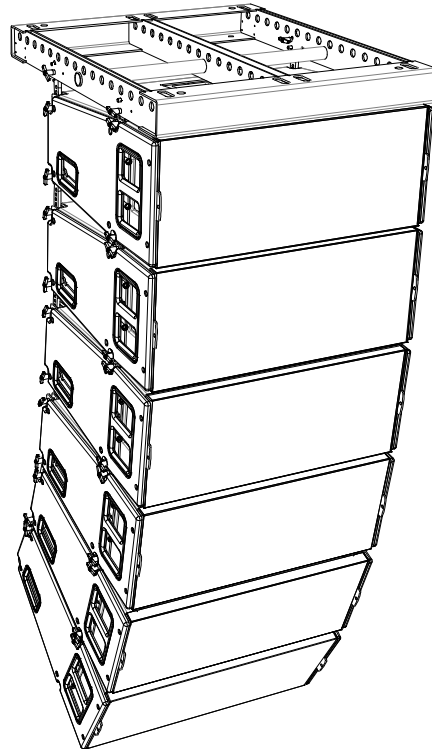


Figure 1.1: The figure shows an illustration of a KUDO line source array from L-Acoustics [L-Acoustics, a]

Every speaker or a small group of the line source array can be controlled individually, both in sound coverage area angle and SPL. The benefit of using the line source array design is that the coupling between the speaker makes a line acting source. With an optimised control system of the line source array, the audience area is covered with sound such that all audience can hear the information without damage the ear of the frontal audience. An optimised line source array has, for example, an optimised main lobe such that the lower part of the main lobe lays flat along the audience area. The following Figure 1.2 shows a graphical illustration of the outdoor PA venue concept.



Figure 1.2: The figure illustrate the concept of outdoor PA venue

As shown in Figure 1.2, the distances from one element in the line source array to the receiving audience dependent on the audience position. The distance indicates that the signal to every line source element has to be set individually to cover the audience area with homogeneous SPL. The individual control of the source is necessary because of the wave amplitude decay with distances. This phenomena is addressed in section 2.1. The adjustment is not as simple as just supply the upper speaker with more power. A sound wave is a mechanical movement of the particle in the air, which condense and compress the air molecule, then low pressure and high pressure respectively. The movement of the molecule depends on the medium, and in this thesis, the medium is limited to air. The SPL is the pressure divination of the instantiates atmospheric pressure. The atmospheric pressure, therefore, set a lower bound on the condensation while very high pressure changes the speed of sound and distort the wave as it propagates. To ensure that the information is communicated to the audience without distortion, the limitation is addressed in section 2.2.3. The medium in the air is not constant and varies over time regarding pressure, wind, humidity and temperature. The analysis starts with the experience for live concert of the author in section 1.1.2, next section 2.2 address the impact of homogeneous atmospheric effect on sound propagation. Then section 2.2 address the impact of inhomogeneous atmospheric effect on sound propagation.

1.1.2 Author experience of live concert

The Author of the thesis has experience with live concert both as an audience and as a sound engineer. The aspect of being the sound engineer and an audience to a live concert is very different. As a sound engineer, the area for controlling the sound is a secured area with a tent as protection. The tent roof often shadows for the high frequency, and the walls make standing waves of the low frequency because the distance between parallel tent walls fits with the wavelength for the low frequency. The sound engineer control area is defined as the Front Of House (FOH). The FOH is often equipped with an additional speaker, and the sound engineer does not fully know how it sounds outside the FOH, but base there mixes on experience ???. The aspect of being an audience depends on where the audience is regarding the stage. In close hand to the stage the SPL is high and often too high especially in the low frequency. The low frequency is often made as a vertical array at the ground or two end-fire arrays and shall be able to exhibit all audience by an audible low frequency spectrum typically from 25 Hz but one company extends down to 13 Hz. Therefore the SPL just in front of the subwoofer has a very high SPL. This position is not comfortable to be at in longer period, and the high SPL mask the higher frequency. The optimal audience position is in the centre of the stage and not as long from the stage as the delay towers. The average SPL is often less than 102 dB SPL since the sound engineer try to keep a maximum average SPL at 102 dB SPL just in front of the FOH. Moreover, it is the stereo sweet spot. This position is the only position where the stereo image is optimal. The stereo perspective problem is a hot topic nowadays, both L-Acoustics [L-Acoustics, 2019] and D&B Audiotechnik [d&b audiotechnik,

2019] have made there own solution to the problem. The idea is to fly many small line source array above the stage and assign every musician to there own line source array. The concept minimises the interference between two line source array playing the same mono signal. Near the delay towers or approximately 50 m from the main stage, the low frequency spectrum is still sharp and audible but something happens to the high frequency. Often the high frequency disappears for a few seconds and gets back. This phenomenon altering through the full concert. Behind the delay towers, the line source array in the delay tower reproduces the sound such that the audience in the back also gets the high frequency spectrum. The question is why does the high frequency disappear for a short period when the low frequency does not? This analysis focus on finding the atmospheric condition which cause the phenomena.

Part I

Problem Analysis and Requirements

Chapter 2

Analysis of sound propagation in outdoor venue

2.1 Ideal geometric spreading loss

When a line source generates a sound wave, the wave field exhibits two fundamental difference spatially directive regions, near-field and far-field. In near-field, the wave propagates as a cylindrical wave wherein the far-field the wave propagates as a spherical wave. When the wave propagates as a cylindrical wave, the wave propagates only in the horizontal plane, and therefore the attenuation is 3 dB Sound Pressure Level (SPL) per doubling of distance. For a spherical wave propagation, the wave propagates in all direction. Therefore the attenuation is 6 dB SPL per doubling of distance. The near-field and far-field attenuation are based on non-absorption homogeneous atmospheric conditions. The border between the near-field and far-field depends on the hight of the array and the frequency. The distance can be calculated with Fresnel formula Equation 2.1, where the wavelength λ is approximated to $\frac{1}{3f}$ [Bauman et al., 2001]

$$d_B = \frac{3}{2} f \cdot H^2 \sqrt{1 - \frac{1}{(3f \cdot H)^2}} \quad (2.1)$$

Where:

d_B	is is the distance from the array to the end of near field	[m]
f	is the frequency	[kHz]
H	is the hight of the array	[m]

In equation Equation 2.1 it can be calculated that less than 80 Hz radiate directly intro spherical wave on the exit of the speaker no matter the hight of the line source array. The following Figure 2.1 shows a horizontal cut of the near-field, far-field from a line source array.

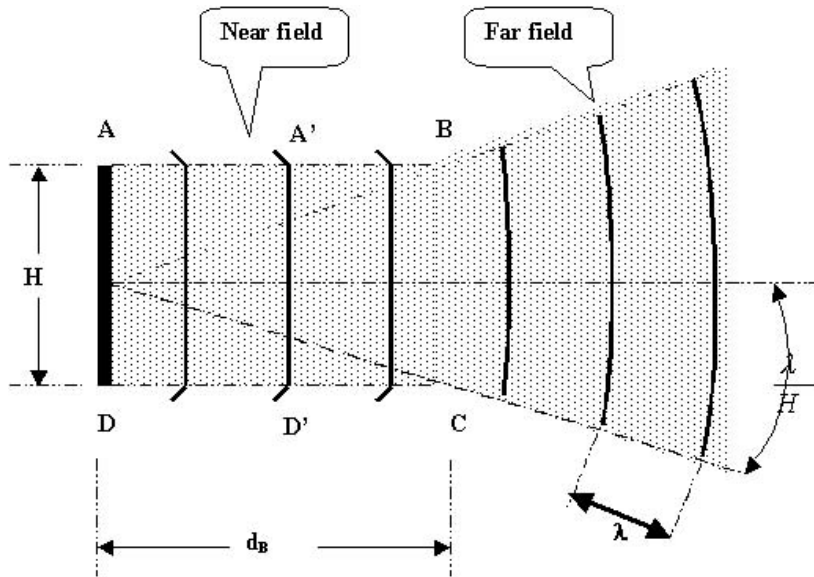


Figure 2.1: The figure shows horizontal cut of a SPL radiation pattern of a line source array [Bauman et al., 2001].

As seen in Figure 2.1, the wave propagating as a plane cylindrical wave in the near-field, where the coverage area for every double of distance is twice as big. Since the coverage area is twice as big, the SPL is the half for the doubled distance. When the wave excites distance d_B , the wave propagates into far-field where the coverage area is four times higher while travelling the double of distance and therefore the SPL is four times less. In far-field, the wave propagates as a spherical sound source. The following Figure 2.2 gives two examples with different height.

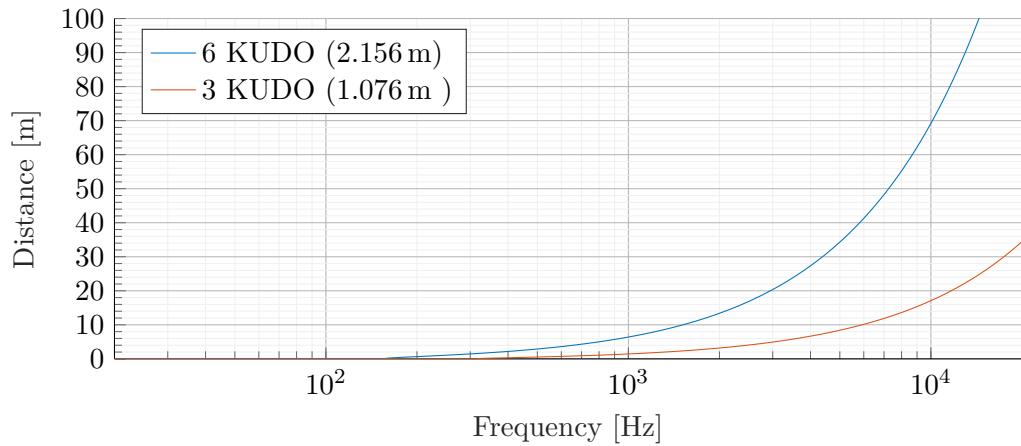


Figure 2.2: The figure shows two height example calculated from Equation 2.1.

As seen in Figure 2.2, while the height is the double, the far-field is moved four times as far back.

2.2 Homogeneous atmospheric conditions

This section aims to analyse the sound wave propagation in homogeneous atmospheric conditions. It is well known that the sound wave propagation is highly depending on the atmospheric conditions. The propagation depends on the atmospheric pressure, wind, temperature and humanity, where the two latter moreover is frequency dependent. The attenuation difference in frequency for temperature and humanity can be above 80 dB SPL [Corteel et al., 2017]. The following sections introduce a brief discussion of homogeneous atmospheric conditions effect on sound propagation.

2.2.1 Humidity and temperature impact

The temperature and humidity have three impacts on wave propagation from a line source array, directionality of the speaker, the speed of sound and a lowpass effect. The following description starts with the latter.

Lowpass effect The effect of humidity and temperature on wave propagation act as a lowpass filter while the wave propagates. The low frequency remains without any additional attenuation where the high frequency highly depends on the atmospheric condition. In other words, attenuation in the high frequency range does not only depends on the spreading loss but also temperature and humanity. Therefore, for long distance, the atmospheric conditions have a high influence on the frequency spectrum delivered to the audience. Humanity and temperature attenuation are already well studied and standardised. Standard [ISO 9613-1:1993] gives an overview of calculating the SPL attenuation concerning the frequency, distance, temperature and humanity. The article [Corteel et al., 2017] gives some examples of attenuation at a distance of 100 m. The article shows that if humanity increases proportionally to the temperature, the lowpass effect is small. If the change in temperature and humanity is the opposite of each other, for example, high temperature but dry, the attenuation in high frequency is significant. The following Figure 2.3 shows the worst-case scenario from [Corteel et al., 2017].

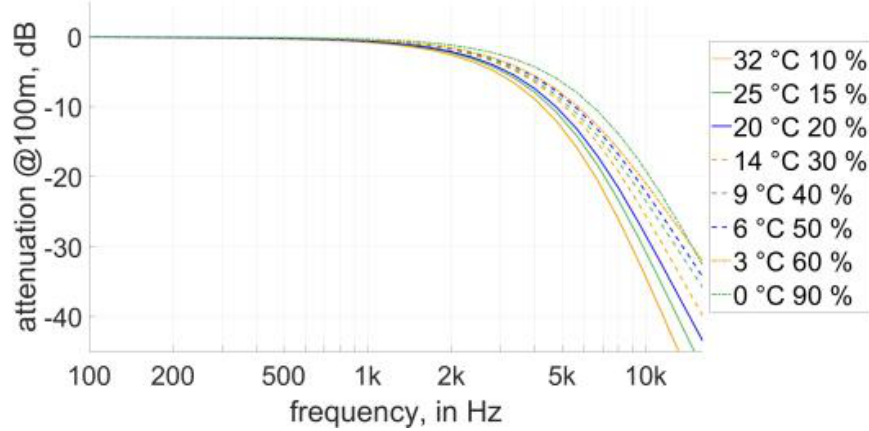


Figure 2.3: The graph shows the attenuation in dB with respect to frequency, humanity and temperature [Corteel et al., 2017].

As shown in Figure 2.3 the attenuation in the high frequency is significant and exceeds 30 dB SPL within the audible frequency range. The attenuation is such markedly that applying more power does not cover the attenuation without an extreme high-pressure driver. That driver might be possible to design in theory but not in practice. Extreme high-pressure drivers introduce high distortion as is explained in section 2.2.3

Speed of sound The second consequence is the speed of sound. At temperature range from 0 °C to 40 °C the speed of sound with respect to humanity change is sparse and mostly only depend on temperature change. At 0 % humidity, the speed of sound increases with 0.6 m/s for every increasing degree °C. At humanity higher than 0 % the speed of sound increase with respect to humanity, depends on temperature. At 0 °C the speed of sound increases with approximately 0.8 m/s when the humidity raises from 0 % to 100 %. At 30 °C the speed of sound increases with approximately 2.7 m/s when the humidity raises from 0 % to 100 % [Wong and Embleton, 1985] [Bohn, 1987]. The wave propagation speed starts at 331.5 m/s at 0 °C and 0 % humanity. The following Figure 2.4 shows the speed of sound with respect to humanity and temperature.

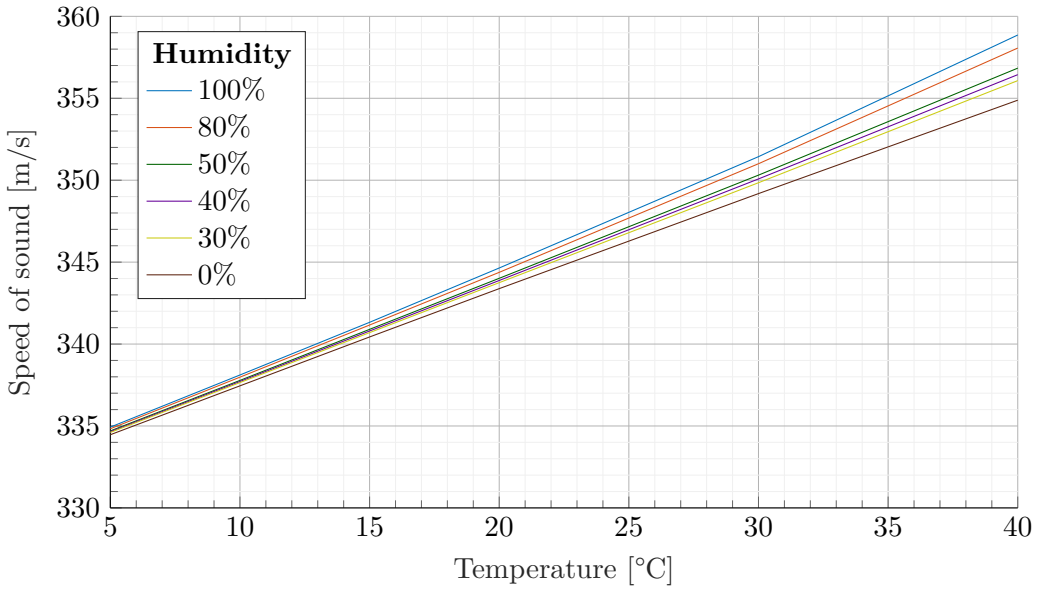


Figure 2.4: The figure shows the increase of sound speed with respect to humanity and temperature [Bohn, 1987]

As seen in Figure 2.4, the effect of humidity is negligible compared to the effect of temperature changes, but as the temperature increases the humidity gets significant. At a temperature of 40 °C the speed of sound is changed 4 m/s from 0% humidity to 100 %

Directivity The directivity of a line source array in the mid and high frequency is always controlled mechanically by a horn because the wavelength is short compared to the size of the speaker. At low frequency, the wavelength is too long to be controlled mechanically by a horn. Therefore the directional pattern is controlled via cancellation from a backwards pointing speaker. The directivity of both the low frequency and the high frequency driver suffers from temperature increased. At the high frequency, the main lobe gets narrower when the mechanical horn gets warmer, and the effect is notable when the sun directly heats up the horn. When the surface of the horn heats up by the sun, the temperature can get much warmer in the horn than the air temperature. Therefore the surface of the horn affect the directivity of the high frequency by radiate warm air from the surface. The reason that main lobe gets narrower is that the wavelength gets shorter at higher temperature [Levine et al., 2018]. The directivity of the low frequency is affected as in the high frequency with the temperature increase. The difference is not as significant as in the high frequency since there is no surface heat. The directivity is then not affected due to the sunlight, but only the temperature increasing and decreasing. As in the high frequency temperature differences change the wavelength, and then the length be-

tween the speaker in a cardioid low frequency does not match the optimised distance between the speaker more.

2.2.2 Wind impact

The wind influence is depending on the angle of the wind direction with respect to the direction of sound propagation. A homogeneous wind is a laminar wind flown with the same homogeneous speed. The following analysis assumes homogeneous laminar wind flow from one direction. The analysis is of both oblique wind and parallel wind with respect to the frontal direction of the line source array. The analysis starts with the latter.

Parallel to sound propagation When the wind flows in the same direction as the sound wave propagation, the wind flow in m/s is an addition to the speed of sound. When the wind flows in the opposite direction, it is a negative addition. In other cases, the influence is complicated since the wind deflect the sound waves.

oblique- and crosswind The effect of homogeneous oblique- and crosswind on sound propagation from a speaker is rarely studied, and the effect on high frequency seems to be unclear. One author has addressed the problem in a simulation of a low frequency source [Ostashev et al., 2005] where the author of [Ballou, 2008] have practical experience with high power sound system and indicate that crosswind effect might be frequency dependent. The author indicates that the frequency dependency might be due to the directionality of the high frequency drivers. The author of [Ostashev et al., 2005] has simulated a homogeneous crosswind effect on an omnidirectional source at 100 Hz. The author of [Prospathopoulos and Voutsinas, 2007] implemented a ray tracing method with a vector based interpolation as shown in Figure 2.5.

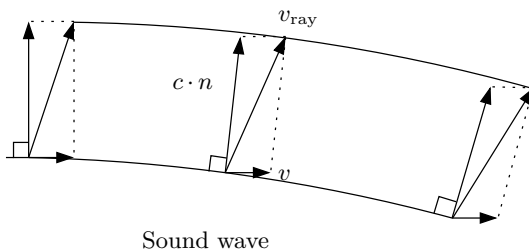


Figure 2.5: The figure shows a geometrical ray tracing calculation scheme of calculate the resulting wave direction at crosswind [Prospathopoulos and Voutsinas, 2007], [Ostashev et al., 2005]

Where:

c	is the speed of sound	[m/s]
n	is the normal unit vector	[m]
v	is the speed of wind	[m s]
v_{ray}	is the resulting sound ray	[m]

As seen in Figure 2.5, the ray vector v_{ray} is an addition of the sound speed vector $c \cdot n$ and the speed of wind v . The wave speed and wavelength, therefore, depend on the speed of the wind and the angle between the wind and the sound propagation. The following Equation 2.2 calculate the speed of sound in the v_{ray} direction with respect to the wind speed and angle.

$$c_r = c + \|v\|_2 \cdot \sin(\theta) = \|c \cdot n + v\|_2 = \|v_{\text{ray}}\|_2 \quad (2.2)$$

Where:

θ	is the angle of the wave with respect to the wind	[°]
c_r	is the resulting speed of sound	[m/s]

As the wave propagating, the resulting v_{ray} increases in the direction of the wind. The article [Ostashev et al., 2005] simulates the effect of crosswind in a Finite-Difference Time-Domain (FDTD) simulation with a wind speed of 102.9 m/s. For the acceptable condition to a concert, the wind speed is less than 20 m/s. Otherwise, the audience is escorted from the stage to the exit, and the speaker system is taken down to ensure safety. The following Figure 2.6 shows a simulation result from [Ostashev et al., 2005], where the source is an omnidirectional 100 Hz spherical source while the wind has a constant uniform wind speed from left. The simulation is done in two dimensions.



Figure 2.6: The figure shows a simulation of a 100 Hz omnidirectional source with a uniform constant wind speed from left with speed of 102.9 m/s [Ostashev et al., 2005].

As seen in Figure 2.6, the homogeneous crosswind does not affect the direction of the wave from a low frequency spherical source. It only affects the time of arrival to the audience.

2.2.3 Pressure impact

The influence of atmospheric pressure change is low compared to the effect of wind, humidity and temperature. The average atmospherical absorption from 4.0 kHz to 16.0 kHz with fixed temperature and variable humidity, increases with 2 dB SPL while going from 101.33 kPa to 54.02 kPa. The atmospheric pressure then only have a negligibility influence on sound propagation and is generally not frequency dependent.

Beside the small impact of pressure difference in the atmosphere, the high pressure generated by the speaker does have a tremendous influence on the sound propagation. There are three states in the propagation way that can produce distortion concerning the pressure. The design of the high frequency horn [Czerwinski et al., 1999], the

port design of the low frequency driver [Vanderkooy, 1998] and the influence of the sound path. The following description starts with the latte.

Sound path In the sound path, two factors distort the wave doing propagating in air. As described in section 1.1.1 a sound wave is condensation and compresses of the air particle. The air medium, therefore, has a lower limit that cannot be less than vacuum. The higher bound of SPL is then depending on the atmospheric pressure. As an example, at 54.02 kPa the highest SPL before distortion caused by vacuum is 188.6 dB SPL and at 101.33 kPa the highest SPL before distortion caused by vacuum is 194.1 dB SPL.

There is, therefore, a higher limit determined by the atmospheric pressure to vacuum, but distortion occurs much before the limit of vacuum. High pressure in the compression also distorts the sound because of the lack of linear dependency between the particle velocity and stiffness in the sound wave. The stiffness or density increases while the air particle is closer to each other. Therefore SPL increases more than the density of the sound wave which causing the compression of the sound wave to be stiffer and therefore propagate faster than in the condensation of the wave. This speed differences, therefore, produce harmonic distortion, and is even present in SPL less than 120 dB SPL [Czerwinski et al., 1999]. The speed differences transform the sinusoid into a sawtooth as it propagates which transfer energy to the harmonic of the propagation frequency. The distortion is not only SPL dependent, but also depend on the frequency. The higher the frequency is, the faster the sinusoid transforms into a sawtooth, therefore, the distortion increases with frequency for constant SPL. The harmonic frequency is higher than the fundamental frequency and therefore, as explained in section 2.2.1, the harmonic has higher attenuation with respect to the distance and viscosity. In most cases, the attention is not as high as the increase of the harmonic distortion, and therefore the distortion of the wave propagation is not fully compensated by the viscous losses in the air. [Czerwinski et al., 1999]. The distortion made by air propagation is much less than the distortion in the mouth of the speaker which leads to the next distortion problem produced by high-pressure [Czerwinski et al., 1999].

Driver throat and mouth design High pressure in both horn phase plug, sealed enclosures, vented enclosures and reflex enclosures for low frequency driver cabinet produces distortion as they act as nonlinear components. The latter produce distortion because high pressure makes air turbulence in the vent. In the optimal design, the distortion of air turbulent is low but is always present in high-pressure [Roozen et al., 1998]. The air turbulence is not only caused in the vent of the low frequency driver, but it also occurs in the phase plug of the compression driver if the SPL is high [Czerwinski et al., 1999]. The distortion depends on the moving mass, the stiffness and the viscous losses in the air on the diagram displacement and the SPL. As the air in the high frequency driver compress, it becomes heavier, stiffer and thicker which make nonlinear wave propagation. It typically occurs when the compression chamber

exceeds approximately 170 dB SPL. At a higher level, the particle velocity resistance to the air flow increases and the laminar air flow turns into turbulent air flow. The distortion is also depending on the length of the horn and the expansion rate of the horn flare. To keep the distortion as low as possible for the high frequency driver the displacement of the diaphragm should be kept significantly lower than the height of the compression chamber [Voishvillo, 2004]. Therefore, to keep the displacement of the high frequency driver as low as possible, the frequency range should be limited.

2.2.4 Ground absorption and reflection

In a concert area, ground absorption and reflection is complicated because there are two very different situations. Before the concert, the area is a local plan area often with mown grass and with ground reflection. An example of a frequency response over mown grass where the measuring height of the microphone is in the height of the ear is given in [Piercy et al., 1977]. The measurement shows that the ground reflection affects the frequency response with high interference. A measurement in Appendix A and ?? is performed where the ground reflection clearly have a big influence on the received frequency response. In this measurement inhomogeneous airflow is present, but the interference is similar in homogeneous airflow [Piercy et al., 1977]. Doing the concert the interesting part is not such ground reflection effect but the audience reflection or absorption. The area along the concert is packed by the audience and therefore, the reflection is not easy to calculate. The absorption and reflection in an outside concert area with a group of audience is rarely studied, but absorption for the audience inside a concert hall is highly studied [Beranek, 2006]. The absorption of the audience is founded to be high in all measured concert hall from 1.0 kHz octave band to 4.0 kHz octave band [Beranek, 2006]. The average absorption a_{Sabine} coefficient is calculated to be above 0.80. The method and result can be founded in [Beranek, 2006]. The reflection in the high frequency in the audience area doing concert is therefore assumed to be low. At low frequency, the article [Beranek, 2006] indicate that the absorption decay with frequency beneath 250 Hz, but The octave band for low frequency driver, which is 31.5 Hz, is not measured by [Beranek, 2006]. The low frequency absorption at 31.5 Hz octave band is therefore assumed to low. The low frequency driver is mostly located in front of the stage on a line or in end-fire settings, often with a maximum distance of half the wavelength from acoustical centre to acoustical centre. The distance between the low frequency driver is determined by the half wavelength of the highest frequency, such that they radiate a plan wave [Bauman et al., 2001]. A higher distance between the acoustical centre causes interference in the low frequency in the audience area.

2.3 Inhomogeneous atmospheric conditions

This section aims to analyse the sound wave propagation in inhomogeneous atmospheric conditions. In an inhomogeneous atmosphere, the pressure and speed is a

function of position. By this fact, the modelling of a sound wave is very complex and depend on various variables such as temperature and wind speed. The following sections give a short introduction to the effect of inhomogeneous atmospheric conditions.

2.3.1 Atmospheric refraction

When the wind speed, the temperature and humanity is assumed to be homogeneous in the sound field, the sound is travelling in a straight plan wave. Often this is not true, the wind speed increases logarithmically with the hight from the ground to the geostrophic wind [Yang, 2016] in the free troposphere [Rossing, 2014], and the temperature and humanity are inhomogeneous. The geostrophic wind in the free troposphere is located in a hight from approximately 1 km above the ground [Rossing, 2014], [Association, 2003]. The inhomogeneous atmospheric condition makes the speed of sound to depend on the hight from the ground. This inhomogeneous atmospheric condition results in a curved sound path and is defined as atmospheric refraction. For small distances, the atmospheric refraction has a spars effect on the sound travelling path, because the speed of sound is much faster than the speed of the wind and the temperature change. Generally distance up to 50 m is often assumed to have no significant refraction effect [de Oliveira, 2012]. For distances larger than 50 m the refraction is assumed to have a significant influence, especially when the sound source and the receiver are close to the ground. Refraction is frequency and distance dependent and is measured in dBexcess attenuation. The means of excess attenuation is that only the effect of wind or temperature is considered, all other atmospherical effect is excluded. A measurement is given in [Piercy et al., 1977] for a point source where the wind speed is 5 m/s. At a distance of 110 m, it is observed that frequency above 400 Hz is refracting where frequency below is rarely effected of refraction. Moreover, at a distance of 615 m the refraction is present in the full measured frequency range from 50 Hz to 3.2 kHz. In the perspective of a live concert the interesting distance is the 110 m from the line source array to the audience rather than the 615 m. Both the downwards and upwards refraction is interesting. In the upwards refraction the audience might be in the shadow zone where for the downwards refraction the high frequency reflection from the ground is assumed to be low when the concert area is full of audience. Therefore the high frequency is refracted down intro the frontal audience, and only sparse reflection of the high frequency propagate to the back part of the audience. The following Figure 2.7 display the phenomena of upwards refraction.

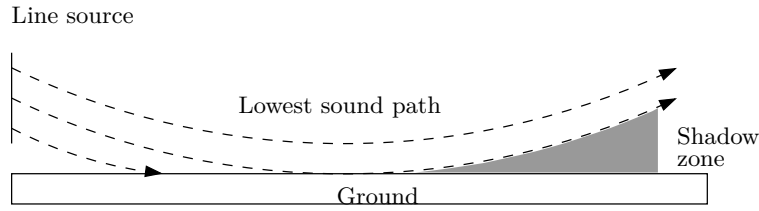


Figure 2.7: The figure illustrates that the shadow zone occurs from an upwards refraction. A line source speaker array contains of many couplet point sources. Every lowest sound path dashed line indicate the lower directional angle of one point source in the line source array.

The following description is based on the distance of 110 m and upwards refraction. As explained in [Piercy et al., 1977] the refraction at a distance of 110 m is highly frequency dependent. At a frequency below 400 Hz the effect is sparse but above the effect is high and may result in 20 dB SPL attenuation at the audience. The reason that the refraction is frequency dependent is that the scale of the wind gradient and temperature gradient close to the ground is small compared to the wavelength of the low frequency [Piercy et al., 1977]. This theory does not follow the shell's law of refraction. Shell's law describes the refraction as a layer change in the medium of propagation. Shell's law of refraction is defined as Equation 2.3

$$\frac{\cos(a_1)}{c_1} = \frac{\cos(a_2)}{c_2} \quad (2.3)$$

Where:

a_1	is the input angle in the horizontal plan	[°]
c_1	is the sound of speed in the medium of arrival	[m/s]
a_2	is the output angle in the horizontal plan	[°]
c_2	is the sound of speed in the medium of destination	[m/s]

As shown in shell's law Equation 2.3 the frequency dependency is not a factor and are therefore maybe only valid for a laminar wind flow profile. The article [Piercy et al., 1977] only explores frequency up to 3.2 kHz but since the refraction depends on the wavelength, the distance of refraction wave might be smaller for higher frequency. The attenuation with respect to refraction seems to have a saddle attenuation at 20 dB SPL. A measurement in [Piercy et al., 1977] shows the attenuation for the center frequency of 1.2 kHz with $1/3$ octave band filtered airplane noise over mown grass. The measurement is interesting with respect to a concert area and is therefore shown in Figure 2.8



Figure 2.8: Excess attenuation measured for aircraft noise in the 1.2 kHz $\frac{1}{3}$ octave band for the ground-to-ground configuration. The vector component of the wind velocity in the direction of propagation for \blacktriangle is 5 m/s, \square is 0 m/s, and \triangledown is -5 m/s. The temperature profile is neutral. F_s is the shielding factor, B is the shadow boundary [Piercy et al., 1977]

The following two paragraphs explain the difference between wind refraction and temperature refraction.

Temperature Temperature decreases with respect to the hight at day time and increases at the night time. The increase or decrease is usually approximated as a logarithmic function. In the day time, the sun heats the ground even on a cloudy day, and the concert area is full of audience. Therefore, the eath and audience radiate warm air, which makes the temperature at a low hight warmer than the temperature at higher hight. These phenomena are named lapse where the opposite is defined as inversion. As explained in section 2.2.1, the speed of sound depends on the temperature. Therefore, at day time, the speed of sound in this situation decay with respect to hight. The speed change can be modelled as a change of layer for a plane wave. The output angle of the layer change follows the shell's law when the frequency dependency is excluded. Therefore when the temperature profile is logarithmic, the layer change is a function of hight and change the wave direction. The wave direction of the descript weather condition results in an upwards refraction. Since the temperature is a scalar quantity uniformly over a large area and a function of hight, an identical temperature profile is applicable all around an omnidirectional sound source. Therefore the upwards refraction is uniform all along the speaker in the horizontal plane. The following Figure 2.9 illustrate the phenomena where the temperature decay with respect to the hight and the line source array is omnidirectional in the horizontal plane. The omnidirectionality of the line source array is only present in the low frequency typically below 200 Hz.

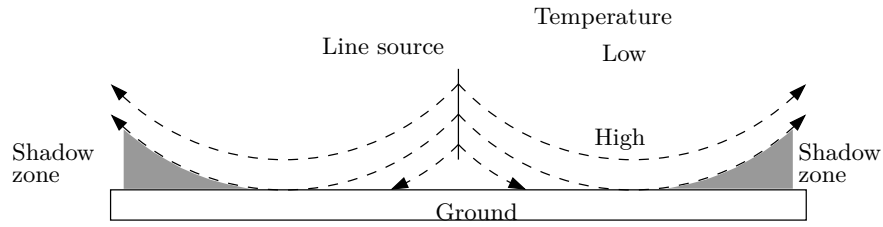


Figure 2.9: Wave refraction of a horizontal omnidirectional line source array in inhomogeneous temperature with lapse profile

When the temperature profile is reversed, the refraction is downwards.

Wind With respect to the wind speed, a concert area is often a protected area with for example barrier, stage and building. This blockage and the ground friction slows down the wind speed near the ground and cause turbulence. Moreover, from nature itself, the wind speed is often logarithmically increased with respect to the height. When the wave is propagation in the same direction as the wind, the atmospheric refraction refracts the sound wave downwards. When the wave propagates against the wind, the atmospheric refraction refracts the sound wave upwards. The following Figure 2.10 illustrate the phenomena with a logarithmic increasing wind from left, and the line source array is omnidirectional in the horizontal plane.

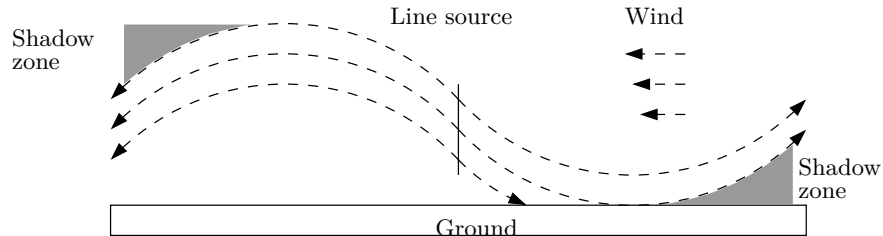


Figure 2.10: Wave refraction of a horizontal omnidirectional line source array in inhomogeneous logarithmically increasing wind profile where the wind gradient points towards left

As shown in Figure 2.7 the refraction is upwards when the wind flows in the opposite direction as the wave propagation. Behind the line array source, the refraction is downwards and is therefore different than for temperature refraction. The refraction of wind is the most dominant at a distance of 110 m. The following Figure 2.11 shows an excess attenuation plot of both inhomogeneous wind and lapse temperature profile.

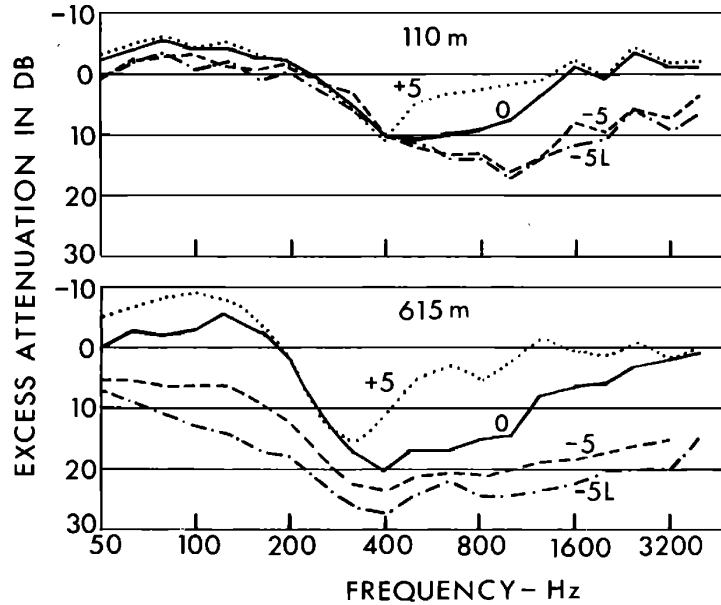


Figure 2.11: Observed attenuation of aircraft noise in a ground-to-ground configuration under a variety of weather conditions. Calculated losses from atmospheric absorption and spherical spreading have been subtracted from the attenuation measured in $1/3$ octave bands for distances of 110 m and 615 m. The numbers on the curves indicate the vector component of the wind velocity in the direction of propagation in m/s. All curves are for neutral conditions of temperature except for those marked L, which are for lapse. [Piercy et al., 1977]

It can be seen in Figure 2.11 that the refraction effect at a distance of 110 m starts at 400 Hz. The reason that sound enters the shadow zone is not fully understood, but one theory is that the shadow boundary wave is diffuse and therefore a significant amount of sound energy enters the shadow zone by turbulent air flow. In a non-turbulent atmosphere condition the SPL inside the shadow zone is attenuated well more than 30 dB SPL. Close to the ground, the atmosphere condition is always turbulent because of ground friction. The turbulence wind diffuses the sound wave and changes the direction of propagation. The wave that enters the shadow zone is considered as a creeping wave while turbulent air flow is present. The creeping wave will by them self also be refracted and therefore parallel to the other refraction waves. [Embleton, 1996]

Oblique- and crosswind The effect of oblique- and crosswind on acoustical wave propagation in inhomogeneous atmospheric conditions are rarely studied. The author in [Piercy et al., 1977] explain that the refraction is directly zero when only crosswind is present, and increase progressively as the direction of propagation deviate from the angle of crosswind. The author of [Crocker, 1998] support this theory for inhomogeneous atmospheric condition.

Since the effect of oblique wind on a line source array speaker is rarely studied, a measurement in windy condition is performed. The measurement is performed over mown grass in a large open area used for football. The used measurement technique is done according to [Gunness, 2001] where more than one impulse response is measured, and average by aligning the impulse response. The wind was considered as healthy for an outdoor concert. The wind speed was measured to 14 m/s during the full measurement. The measurement was done with a four element line source array 1.1 m above the ground. There were used two microphones, where both were situated 25 m from the speaker in the first measurements and 23 m from the speaker in the last measurements. While changing the distance, the angle to the speaker was changed. The frontal direction of the speaker was placed orthogonal to the wind direction, and the microphone was placed on both sides of the speaker as shown in Figure 2.12

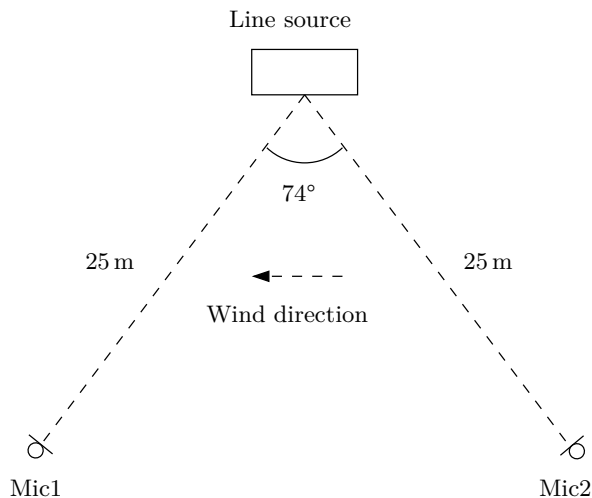


Figure 2.12: The figure shows the microphone position versus the position of the line source array angle of main lobe

The measurement was done with sine swept and according to the description in Appendix A. The measurement was performed with two microphone positions, two measurements where the microphone are within the speaker high frequency directional angle and three outside the speaker high frequency directional angle. The first measurement is shown in Figure 2.13. The other four measurement result can be seen in Appendix A. They show the same tendency, but the difference between the measurements are more drastically in the measurement where the microphone are situated outside the high frequency directional angle.

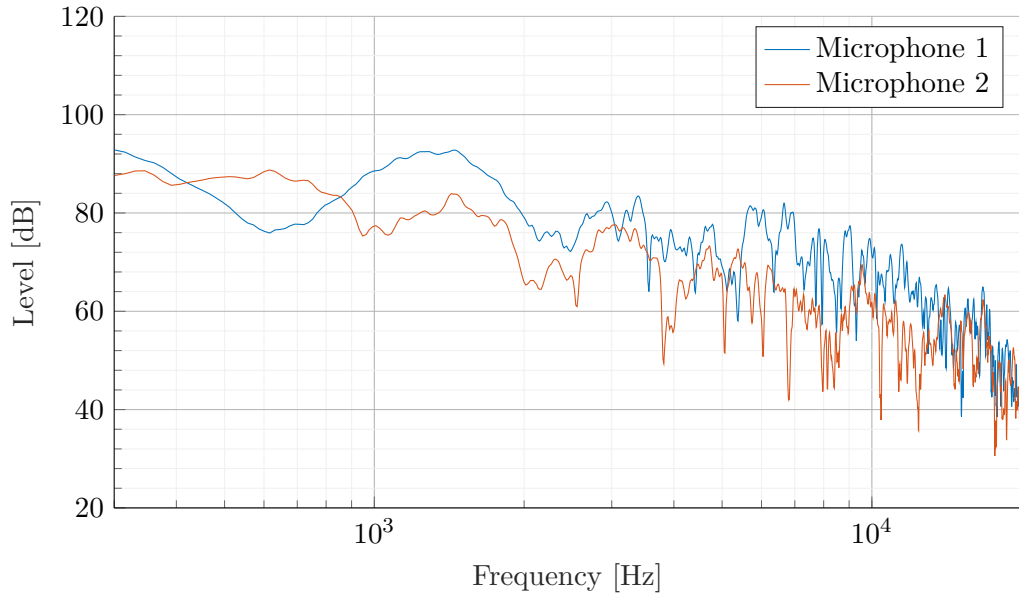


Figure 2.13: The graph shows the first transfer function measurement within the high frequency directional angle. The $L_{eq,5}$ SPL difference between the microphones is 4.41 dB SPL (IR_3)

It can be seen in Figure 2.13 that the general SPL is higher for microphone 1. Furthermore, microphone 1 also shows the typical downwards refraction ground reflection interference in the frequency response which is very similar to the calculated ground reflection interference in [Piercy et al., 1977]. Microphone 2 does not have the same strong interference in the low frequency and the general SPL is lower than microphone 1. This difference indicates upwards refraction in the direction of microphone 2 with only a small amount of ground reflection. The resulting $L_{eq,5}$ SPL difference for all measurement is shown in Table 2.1.

Table 2.1: The table shows the measured $L_{eq,5}$ SPL for all measurement and the difference between the microphone

Measurement number	Mic 1 $L_{eq,5}$	Mic 2 $L_{eq,5}$	Difference
Measurement 1 Figure A.4	71.82 dB SPL	66.33 dB SPL	5.49 dB SPL
Measurement 2 Figure A.5	69.09 dB SPL	64.69 dB SPL	4.40 dB SPL
Measurement 3 Figure A.6	67.67 dB SPL	63.44 dB SPL	4.23 dB SPL
Measurement 4 Figure A.7	68.10 dB SPL	63.69 dB SPL	4.41 dB SPL
Measurement 5 Figure A.8	68.44 dB SPL	63.62 dB SPL	4.81 dB SPL
Average	69.02 dB SPL	64.35 dB SPL	4.67 dB SPL

As it is shown in Table 2.1, the $L_{eq,5}$ SPL is higher for microphone 1 in all measurement. Moreover the average $L_{eq,5}$ SPL difference is 4.67 dB SPL while for A-weighted $L_{Aeq,5}$ SPL the average difference is 6.17 dB SPL.

With respect to the intelligibility frequency range, a weighting filter is designed to observe the SPL differences in the critical intelligibility frequency range. The filter is based on the founded intelligibility frequency range in [Letowski and Scharine, 2017]. It is shown in [Letowski and Scharine, 2017] that the critical intelligibility frequency range lays between 1.0 kHz and 4.0 kHz. The designed intelligibility weighting filter is an 8th order bandpass filter with lower crossover frequency at 1.0 kHz and higher crossover frequency at 4.0 kHz. The resulting average difference is 7.88 dB SPL and the maximum difference is 9.95 dB SPL.

Turbulent Turbulence is an atmospheric condition where the wind eddies. It often starts with large eddies and progressively brakes down like a cascade effect to smaller and smaller eddies which only depend on the local region. When the eddies are as small as 1 mm the energy disappears in viscosity and thermal conduction. A statistical distribution of the eddies is defined as turbulence. The turbulence wind flow is, therefore, a chaotic and stochastic process by nature and is present all the time. It can occur because of change in landscape, stage and blockage, but can also be a process of flow speed increase in the wind, which make the wind to refract on itself. Turbulence is often high on a windy afternoon day and low under the inverse of lapse. Turbulence also often occurs near the ground because the ground surface slows down the speed of wind by the friction to the ground. The effect of turbulence on sound is known to make phase and amplitude fluctuation of pure tone. The fluctuation increases with distance until the standard deviation of the phase fluctuation is comparable to 90° [Piercey et al., 1977]. At this point the phase correlation for each sound path is uncorrelated

2.4 sound pressure level doing a concert

In Denmark there is no law limiting the SPL doing a concert. The only restriction there might be of SPL is area dependent. In a city the local komunity has limited the total SPL average over 15 min of any event. Out on the countryside, the sound engineer can decide by himself and the often used limit is A-weighted 102 dB SPL average over 15 min.

The standard ?? for long term exposior of high SPL limits the SPL for A-weighted 94 dB SPL average over maximum of 1 h, then the ear needs to have a brake to ensure no damage the the hering. A concert i often more than 1 h with A-weighted 102 dB SPL average. This is at least 8 dB SPL A-waighed more than the regulation recommend. It shall here be clearly understood that the SPL measurement is done in the Front Of House (FOH) and the actian exposed SPL is higher for the audience close the the stage.

Chapter 3

Summary of Problem Analysis

The analysis started addressing the generally used method for a live concert. It is founded that live concert today use line source array system to cover the audience area with sound. The line source array is flown above the audience at the main stage, and the delay speaker covers the back audience at a large concert. The line source array is constructed of many identical speakers attached to each other in a vertical line. Moreover, the distance from the speaker to the individual audience depends on the audience position. The analysis founded that a homogeneous SPL among all audience might not possible but the SPL among all audience can be optimised by knowledge of the condition of the atmosphere and gain up for the spreading lose. The author observes that the wind does have a frequency and distance-dependent effect on sound propagation, for example at high frequency the high frequency attenuate audibly in the crosswind. The high frequency blows away for periods and comes back again. The analysis of sound from a line source array started by the ideal geometric spreading loss. Here it is founded that the sound propagation of the line source array highly depends on the hight of the source. The line source array propagates differently with respect to frequency. At a certain hight of the line source array the propagation is a cylindrical propagation until a certain distance from the source where it starts propagating as a spherical source. In the cylindrical propagation, the sound field is defined as near-field while in the spherical propagation the sound field is defined as far-field. In the non-ideal scenario, the line source array propagates in inhomogeneous atmospherical condition. To cover the inhomogeneous atmospherical condition, the local homogeneous atmospherical condition is analysed. In the homogeneous atmospherical condition, it is founded that the temperature, humidity, pressure and wind influence the sound field. The effect of temperature and humidity is close coupled on sound propagation. When the temperature is high, and the humidity is low the air has a significant high frequency absorption whereas when the temperature and humidity follow each other, the absorption is less. The second effect the temperature and humidity have on sound propagation is the speed of sound. The higher the temperature is, the higher the sound of speed. The humidity affects the speed of sound the same way as the temparature, but the increase is negligible

compared to the temperature. The effect of wind seems to have a sparse effect on the sound propagation when and only when the wind is homogeneous. It is founded that the speed of wind affects the speed of sound. If the wind moves in the direction of the sound propagation the wind speed is an addition to the speed of sound. In the opposite wind case, the speed of sound is lowered. In the case of oblique- or crosswind, the effect seems to be unclear for high frequencies. One author has simulated a low frequency spherical source and founded that the only effect is the time of arrival to the audience. The impact of the atmospheric pressure is small, and the pressure close to the ground is so high that other limitations of wave propagation limit the SPL before the negative amplitude riches vacuum in the condensation. When the wave compresses the air, the wave travels faster such that the received wave at the audience is a sawtooth wave. The effect produces harmonic distortion where some of the harmonic energy is attuned by the viscous losses. The harmonic distortion is present in SPL lower than 120 dB SPL but is not as critical as the distortion created by the construction of the speaker enclosure. The audience area is assumed to have high absorption in frequency above 1.0 kHz, while frequency in octave band 31.5 Hz is assumed to have low absorption of the audience.

In the inhomogeneous atmospherical condition, it is founded that refraction of the sound wave is one of the biggest challenges for an outside sound concert. The refraction occurs because of inhomogeneous speed which is present in both inhomogeneous wind and temperature. It is further founded that the refraction is frequency dependent and distance dependent. The effect, however, is low at a distance lower than 50 m with a wind speed of 5 m/s. Depending on the atmospheric condition two kinds of refraction was founded, upwards and downwards. Upwards refraction produces a shadow zone where turbulent atmospheric condition makes creeping wave into the shadow zone. For the case of oblique and crosswind the effect of high frequency, the refraction might be zero at direct crosswind but increases progressively as the direction of propagation deviate from crosswind. One measurement was done to research the effect of crosswind on a line source array. It was founded that the average $L_{Aeq,5}$ SPL at microphone 1 was 6.17 dB SPL higher than microphone 2. Therefore it can be concluded that the crosswind with respect to the speaker coverage area does affect.

Chapter 4

Problem statement

Based on the knowledge founded in chapter 2 and the conclusion drawn in chapter 3 a problem statement can be made. For the rest of this theses, the following will be the focus.

Is it possible to control the speaker directivity such that the average SPL over the speaker coverage area is more homogeneous in cross- and obliquewind condition

4.1 Delimitation

The following delimitations are made for the rest of the project:

- It is chosen to work with mono line source array since the number of line source array element is limited to six pieces.
- Due to the amount of needed audience to the research, the homogeneous SPL is searched over mown grass without the audience.

Part II

Test Design

Chapter 5

Preknowledge of outside measurement

5.1 Measuring in inhomogeneous atmosphere

The aim of this section is to gain pre knowledge about outdoor measurement, such that effecting condition doing measurement is controlled.

5.2 Ground reflection

5.3 Wind noise

Chapter 6

Proposal solution

6.1 proposal of solution to the wind problem

This section aims to propose a solution to the problem founded in the crosswind measurement section 2.3.1 and the problem statement in chapter 4. To be able to find a solution to the problem, the optimal condition is defined in section 6.2. Then a proposed solution to the crosswind is defined in section 6.3 and lastly a proposed solution to the parallel wind is defined in section 6.4

6.2 Optimality condition

To be able to search for a solution and design a test to research if the proposed solution has the which effect on the coverage area, the optimal condition is defined in this section. The optimal condition is as simple as the SPL coverage in the coverage area of the speaker without wind. In other words, the line source array has a frontal horizontal directional angle defined as the -6 dB SPL limit of the main pressure lobe. The line source array main lobe is given in the horizontal degree as an addition of the main lobe from the frontal direction to both side and can both be symmetric and asymmetric, depending on the line source array element. The following Figure 6.1 shows an illustration of the main lobe.

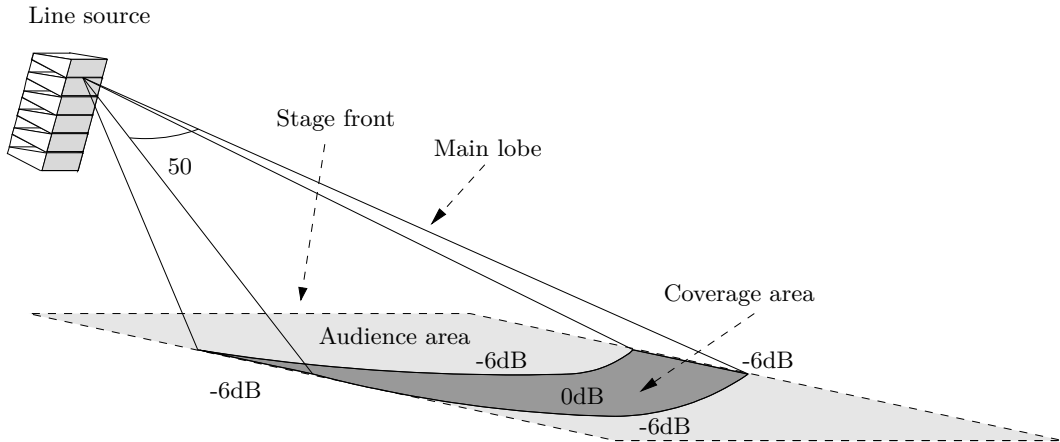


Figure 6.1: The figure shows the pressure limit which defined the main lobe of the line source array and the coverage area without wind

As illustrated in Figure 6.1 the coverage area is a parabolic surface which is limited as the -6 dB SPL coverage limit of the line source array. This is the coverage area with no wind effect and is the coverage area which is defined as the optimal condition. The solution to the crosswind and the parallel wind, therefore, is a way to be able to adjust the coverage area such that the line source array can eliminate the effect of the wind and cover the area as without wind. To be able to eliminate the wind effect at the audience area, audience area have to be defined. To define the audience area, a questioner is made among the large sound rental company in Denmark which ask for audience area to a concert. The questioner is founded in Appendix P. The goal of the questioner is to find the highest coverage distance from the line source array. The founded maximum distances before delay tower is approximate 60 m, and furthermore, the wind might be stronger than 5 m/s to a concert but wind above 10 m/s to 12 m/s will stops the concert. Therefore the defined coverage area as shown in Figure 6.1 is 60 m from the stage front.

6.3 Proposal solution to crosswind

The crosswind problem is shown in section 2.3.1 to highly modified the coverage area. Agents the wind the upwards refraction is shown to attenuate the sound more than 6 dB SPL A-weighted at a distance of only 25 m and a mean wind strange of 14 m/s. Furthermore, it is founded that the shadow zone SPL depends on the SPL in the sound path, because the wind eddies, eddies the sound into the shadow zone. It is then researched if adding more power into the upwards refraction direction also adds more power into the shadow zone by the wind eddies. The following Figure 6.2 illustrate the eddies theory in upwards refraction.

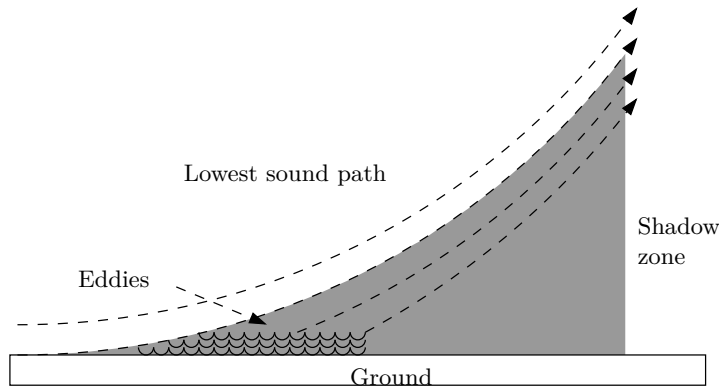


Figure 6.2: The figure shows the sound path above the shadow zone and inside the shadow zone produced by the eddies

The proposed solution is then to steer more power into the direction of upwards refraction and less power into the front and in the direction of downwards refraction to research the eddies theory shown in Figure 6.2. The following Figure 6.3 shows a graphical illustration of the proposed solution to archive a more homogeneous SPL in the coverage area of the line source array with the wind.

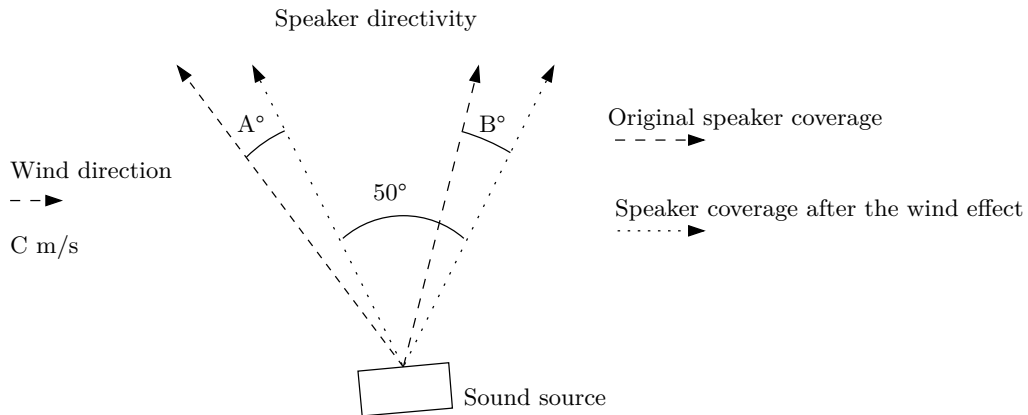


Figure 6.3: The figure shows the wanted direction of the sound coverage area after the effect of crosswind. C is the speed of wind in cross direction of the frontal direction of the speaker. A and B is the main lobe angle that needs to be founded. On the figure the angle are equal but that might not be true

The goal is then to search A° and B° based on wind speed $C \text{ m/s}$ and the optimal coverage area as shown in Figure 6.3 such that the SPL coverage differences is optimized. As founded in section 2.3.1 the refraction is frequency dependent, therefore, finding the optimal A° and B° might not be possible for all frequency. Furthermore the refraction in the low frequency is nearly zero for the distance present at the concert.

6.4 Proposal solution to parallel wind

The above proposal solution deals with the crosswind problem. When the wind direction change such that the wind comes from the back audiences to the stage, or in other words, is parallel with the frontal direction of the speaker, another theory is research than the eddies theory. The resand to search for another solution is that using the eddies theory in parallel wind require that the power from the line source array is raised. The proposed solution is then to move the shadow zone instead of raising the power in the shadow. To be able to move the shadow zone, the idea is to change the vertical angle of the main lobe, such that the upper speaker either point more downwards or upwards for upwards refraction or downwards refraction respectively. Therefore if the upper speaker points more downwards the energy from the speaker might arrive at the ground where else if the line source element is pointing parallel to the ground, the energy never enters the ground surface. The following Figure 6.4 shows the proposal solution to parallel wind refraction.

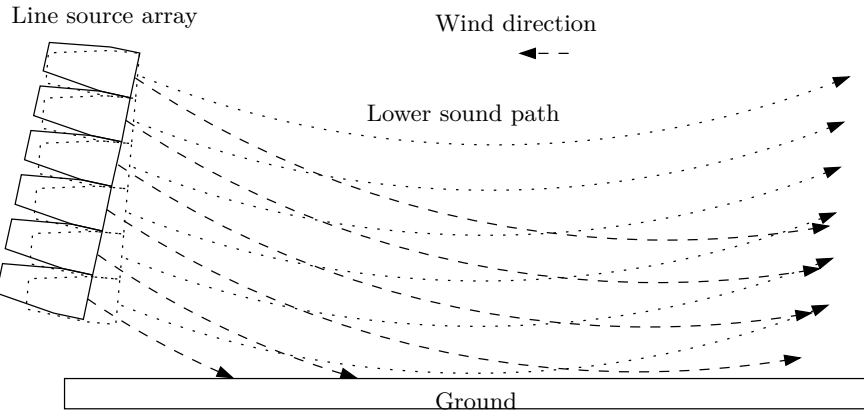


Figure 6.4: The figure shows the proposal solution to the upwards refraction. The non tilted line source array figure shows the lower vertical main lobe ray while the array is orthogonal to the ground where the tilted line source array shows the lower vertical main lobe ray while the line array is angled more downwards

The shadow zone distance is depending on the hight of the line source array from the ground within the limited hight of flying points on the stage. As higher the line source array is flown, as higher the distance is before the shadow zone is present while the vertical angle is optimised to the audience area.

Chapter 7

Test of Proposal Solution

7.1 Test of proposal solution

This chapter aims to design the measurement for the proposed solution. The measurement is based on an L-acoustics KUDO line source array, which is described as the first part of this chapter. Afterwards, the measuring setup for both crosswind and parallel wind is designed based on the used line source array and concert conditions. The second part of this chapter deals with the wind noise challenge in outdoor measurement. The end of this chapter design the measurement software and the needed sensors.

7.2 Description of the used line source array

The description of the used line source array starts with an introduction to the line source element, where the frequency response of the single element is measured as well as the directional characteristics. In the end, the horizontal directionally control, and the vertical directionally control is explained.

The line source elements which is used to test the proposed solution is an L-Acoustics KUDO line source array. This line source array is a legacy long throw variable curvature speaker. This speaker is today renewed and renamed to L-acoustics K2. The line source array can be flown as a vertical line with a maximum of 21 elements. The maximum number of an element is due to the safety limit on the flying tools. One single element have a frequency response from 50 Hz to 18 kHz with a approximatly deviation of ± 3 dB SPL and have a maximum SPL of 140 dB SPL at 1 m. The following Figure 7.1 shows a frequency response measurement of a single KUDO line source element in 50° horizontal angle.

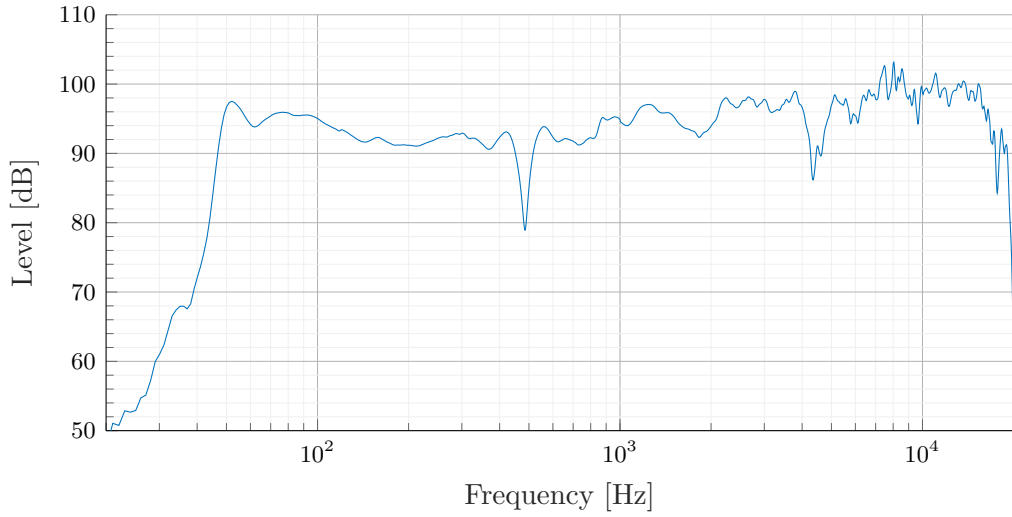


Figure 7.1: The graph shows the frontal frequency response in 50° horizontal angle

This measurement in Figure 7.1 is done in the anechoic chamber at Aalborg University as well as the following measurement in this section. The measurement is explained in Appendix J. The horizontal coverage angle of the L-Acoustics KUDO can be controlled individually on every line source element. The line source element allows both symmetric horizontal coverage and asymmetric coverage. The angle from the frontal direction to the outer main lobe -6 dB SPL is either 25° or 55° . By this two angle for both sides, four coverage angle of the speaker is possible, 110° , 50° and 80° ether to the left or the right. To obtain a better resolution that only the -6 dB SPL the directionality characteristics is measured in all settings. The measurement can be founded in Appendix J . The interesting settings while rotating the line source array is $25^\circ / 25^\circ$ and $25^\circ / 55^\circ$ which is shown in Figure 7.2 and Figure 7.3 respectively.

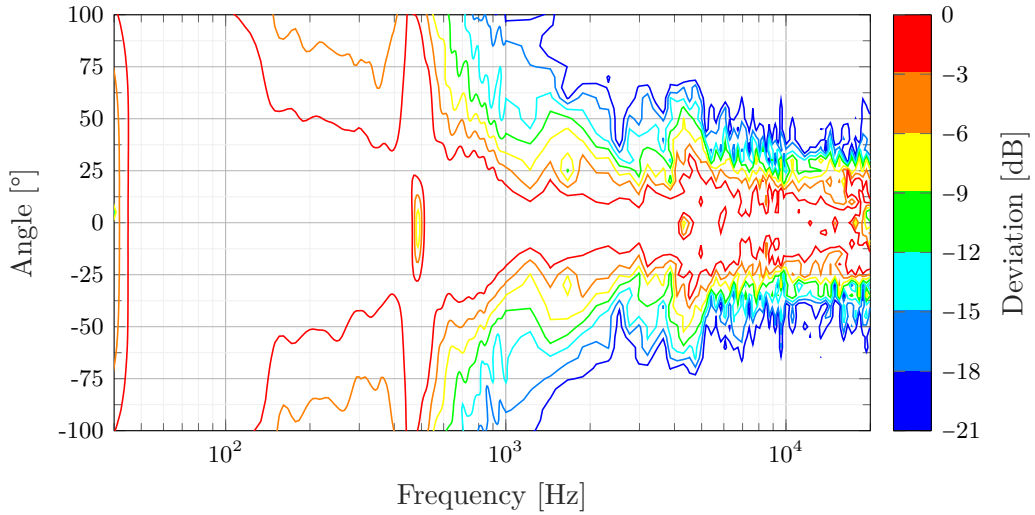


Figure 7.2: The graph shows a contour plot with 3dB SPL step of the directionality of the L-acoustics KUDO with $25^\circ / 25^\circ$ settings. The lower black contour line indicate the dBdirectionality for the maximum rotation of the speaker

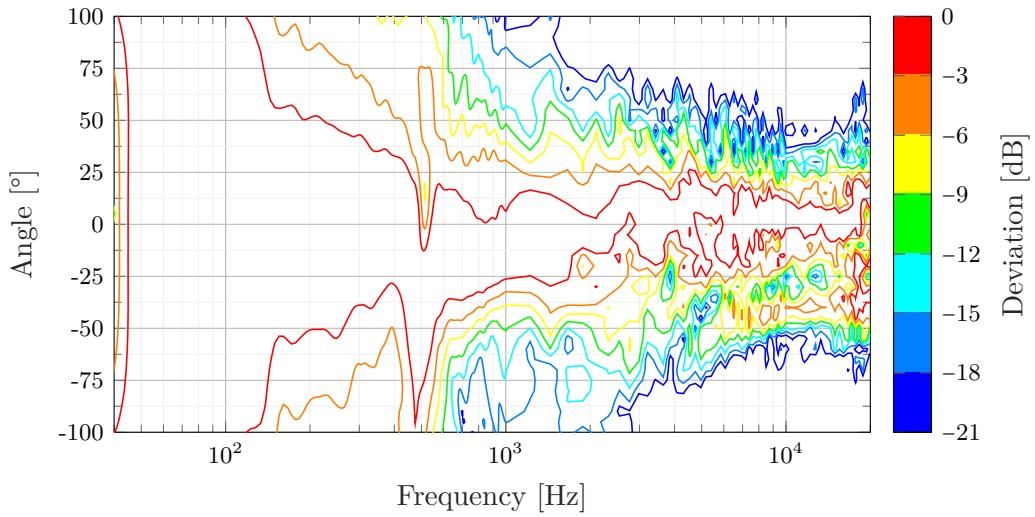


Figure 7.3: The graph shows a contour plot with 3dB SPL step of the directionality of the L-acoustics KUDO with $25^\circ / 55^\circ$ settings. The lower black contour line indicate the dBdirectionality for the maximum rotation of the speaker

The mechanical directional characteristics solution in the L-acoustics KUDO as well as other line source array element is not made for wind challenge but for neighbouring disruptions and higher SPL in the main lobe of the high frequency. All

solution used today is only possible to be changed by hand and is not electrically controlled. The method for changing the horizontal directivity in the L-Acoustics KUDO line source element is two plexiglass plate fixed to the front grill. The fixing mechanism can be adjusted sidewise by realising two splits on both plexiglass plates. The plate can then be slid along the grill to change the mouth of the speaker output. The following Figure 7.4 illustrate the principle.

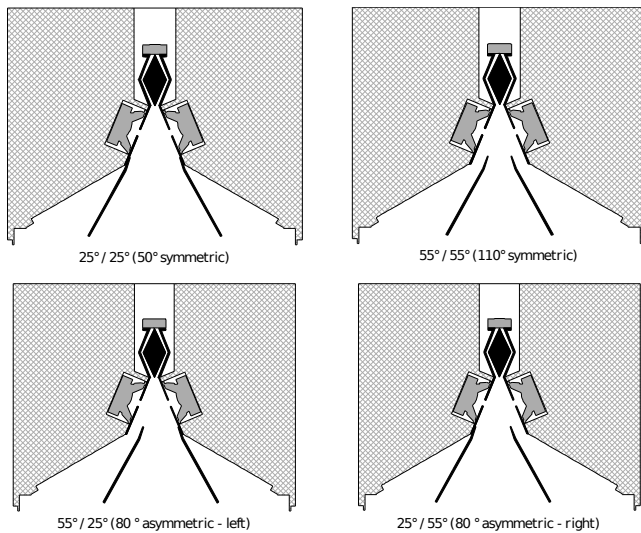


Figure 7.4: The figure shows how the horizontal directivity is controlled on a L-Acoustics KUDO line source array element [L-Acoustics, a].

While the plexiglass plates are in 55° mode as shown in Figure 7.4, the wider directionality is obtained by soundwave reflection on the plexiglass plate.

The line source array vertically coverage area can be controlled from 0° to 10° with 1° step size. To be able to control the vertical main lobe of the line source array, the mechanical solution is the angle between the line source element. This means that the vertical coverage control cannot be controlled on the individual line source element as the horizontal coverage. To be able to control the vertical coverage, the speaker is trapeze designed such that the high frequency horn throat stays together while the angle between the elements is adjusted in the back of the element. The following Figure 7.5 shows how the line source element are angled vertically.

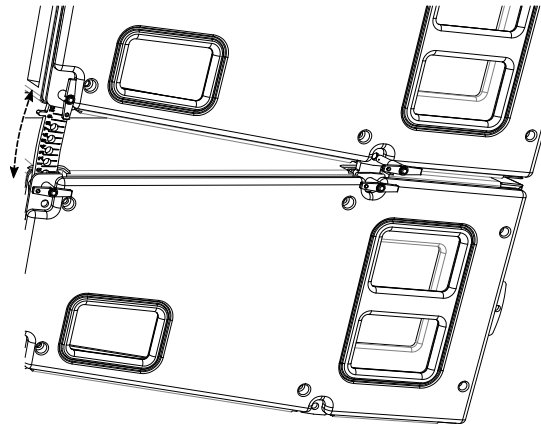


Figure 7.5: The figure shows how the vertical directivity is controlled on a L-Acoustics KUDO line source array element [L-Acoustics, b].

To be able to fix the vertical coverage on the L-acoustics KUDO, the upper left rigging pin shall only be placed into the line source element rig when the angle shown on the metal plate shows the desired vertical coverage angle between two line source element.

7.3 Designing the measurement

This section aims to design a measurement based on the proposed solution section 6.1 and the properties of the used line source array founded in the previous section. The first part of this section gives a general overview of the measuring setup. Afterwards, the independent measurement structure is designed for the crosswind and the parallel wind, respectively.

7.3.1 General measuring setup

The line source measurement setup is designed such that the proposed solution can be tested without mechanical change of the line source array. The test setup, therefore, do not change the speaker directionality along with the measurement. Furthermore, the amount of available line source array for the measurement is limited to six line source element. The following Figure 7.6 shows the line source speaker setup and start vertical angling for both the crosswind and side wind measurement.

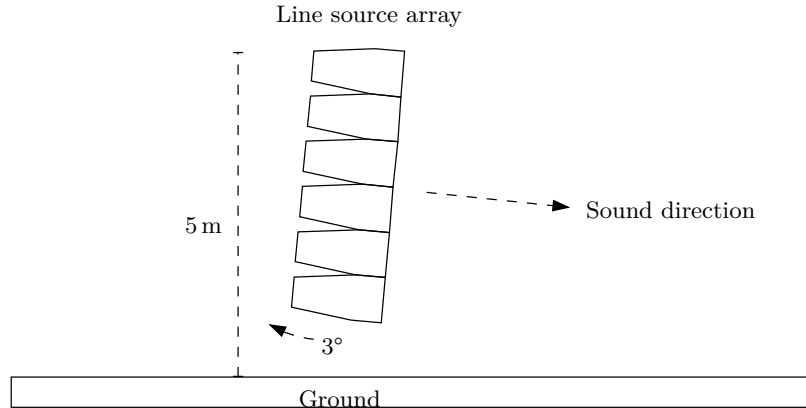


Figure 7.6: The figure shows test setup for both measurement

The vertical angle between the line source elements is 0° between all element for both the crosswind and parallel wind.

7.3.2 Crosswind line array settings

The idea is to measure the SPL coverage while playing in the frontal direction, and then measure the SPL coverage while the line source array is rotated against the wind. The search is then for the least SPL differences in the coverage area. To be able to ensure that the rotation of the line source array keeps the SPL in the downwards refraction direction as much as possible, this section designs the directional characteristics settings of the line source array doing the crosswind measurement.

It is founded in section 2.3.1 that downwards refraction raises the SPL by downwards reflection but the amplification is much less than the attenuation in upwards refraction and is therefore assumed negligible for directionally chose. Therefore, to decide on the horizontal directionally settings is compared in different settings. The comparison uses the founded characteristics directionally of the line source array in section 7.2 and the crosswind measurement in section 2.3.1

As seen in Figure 7.2, when the speaker is rotated 25° up against the wind, which is the rotation where the maximum SPL is pointed into the outer -6 dB SPL coverage angle of the line source array, the downwards direction is lowered from approximately -6 dB SPL to approximately -18 dB SPL. This rotation occurs an attenuation of 12 dB SPL, which might be too high. While comparing with Figure 7.3 instead, the line source array rotation of 25° only attenuation the SPL in the downwards direction with 6 dB SPL.

To decide on a mechanical solution an example is calculated based on the directionality measurement in section 7.2 and the crosswind measurement in section 2.3.1. The example is based on the optimal rotation for both directionality characteristics, where the difference between the upwards side and the downwards side is smallest. The following paragraph explains and shows the example.

Example The example shows four cases of the L-Acoustics KUDO line source array. One case where the data from the datasheet is used, one case where the measurement in section 2.3.1 is used. Then two examples where the differences in SPL is calculated from an rotation of 20° for 25° / 55° settings and a rotation of 10° for 25° / 25° settings and added to the measurement. The following Figure 7.7 shows the example.

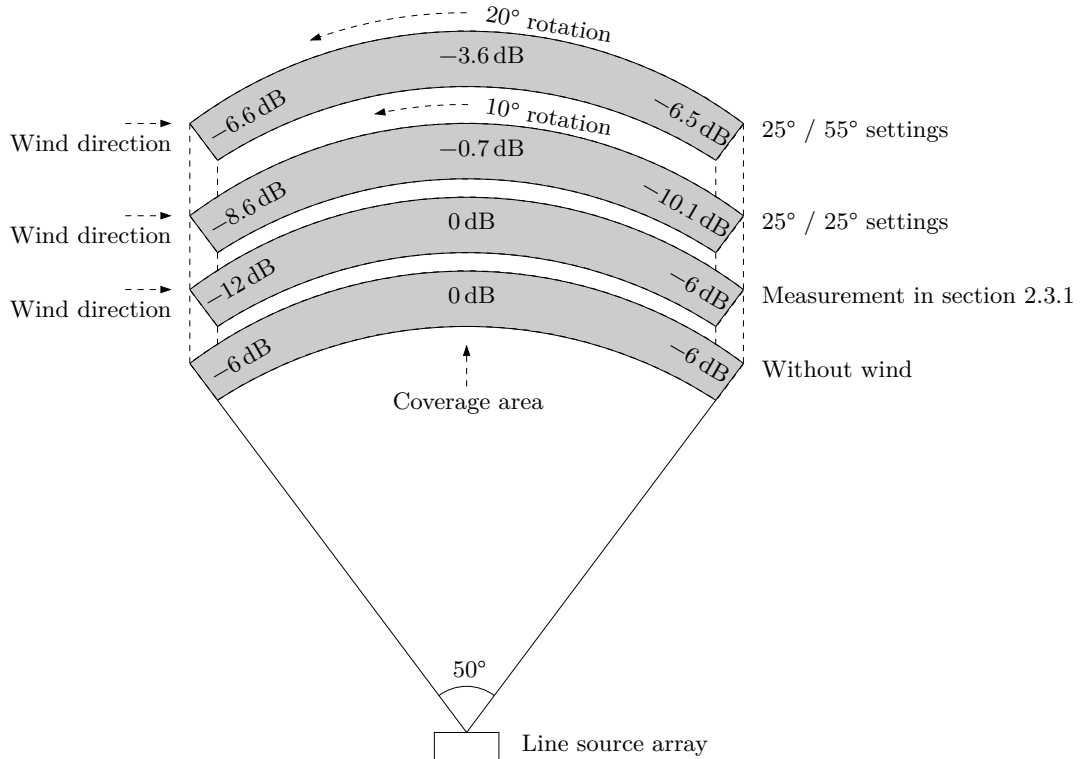


Figure 7.7: The figure shows the main lobe coverage area without rotation in the two lower and with rotation in the two upper

The centre SPL in the measurement in Figure 7.7 was not measured doing the measurement, the stated value is a prediction based on [Piercy et al., 1977] which indicate that the energy addition at short distances because of downwards refraction is small compared to the energy loss with upwards refraction.

As seen in Figure 7.7, a rotational of 20° gives a more homogenous SPL while the line source array is in 25° / 55° settings compare the the symmetric settings. The deviation from the frontal direction is approximately 3 dB SPL. In the other case while the rotation is only 10° and the settings is 25° / 25° the SPL is also approximately evenly spread but the deviation to the frontal direction is much higher. Based on the calculated example, the chosen directionally settings is 25° / 55° for the measurement. The following Figure 7.8 shows the speaker angle settings for the crosswind measurement as a top view.

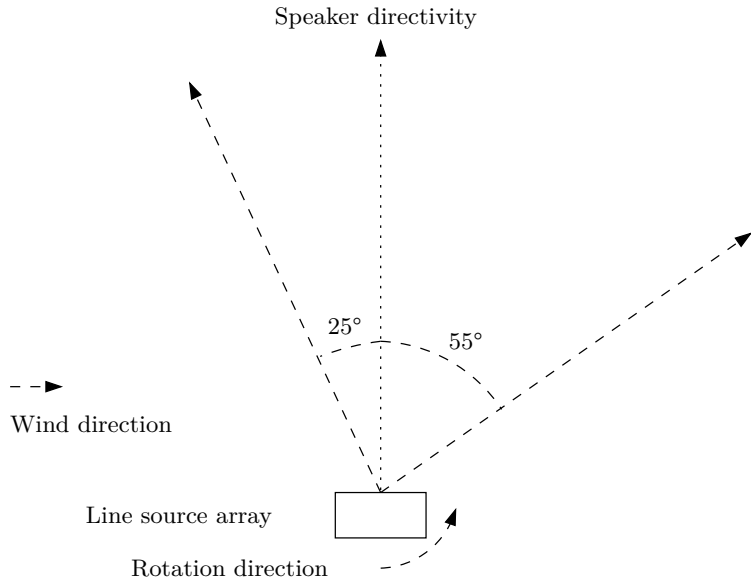


Figure 7.8: The figure shows the line source array setup for the measurement.

The Figure 7.8 shows the speaker settings versus the wind direction.

7.3.3 Parallel wind line array settings

The idea is to have horizontal symmetric coverage while changing the vertical angle for every measurement. The array is tilted some degree until the optimal angle is measured. The optimal angle is the angle where the shadow zone is pushed as far back as possible concerning the wind speed and the hight of the speaker array.

7.3.4 Microphone position at crosswind

The microphone position highly depends on the coverage area of the line source element. The line source element which is flown highest covers the back audience, while the line source element which is closest to the ground cover the frontal audience. Therefore, the distance from the speaker to the microphone has to be found based on the knowledge of coverage distance and the minimum distance before refraction. The distances from the stage to the back audience depends on the size of the concert. For a small concert, the main stage covers the full area where for large concert delay tower helps the coverage. Delay tower is often used for a concert where the distances from the stage to the audience is above 50 m and sometimes up to 73 m as Roskilde festival Appendix P. The general founded maximum distances from the main stage to the first delay tower is founded to be 73 m for a huge concert, 50 m for a large concert and 30 m for small concert Appendix P. Concerning the refraction distances it is shown in Table 2.1 that refraction occur at a distance of 25 m with 13 m/s. Base on the knowledge of the maximum distances founded in Appendix P and the

refraction distance, the coverage distances are chosen to be 50 m for the test, since the used line array flying tools is not able to fly the line array as high as the asked companies, and Roskilde festival is an extreme case concerning the size. The flying height of the line source array in the questioner is about 12 m to 16 m where the flying height of the used test setup is only up to 5 m. The hight of the microphone has to be decided based on the audience experience to a concert. To be able to simulate an audience packed area doing the measurement, the following describes the predicted ground reflection characteristics at a concert and how to be able to reproduce it in a measurement.

Along with a concert, the audience head is assumed to be the new ground plane for high frequency. This assumption is based on the high frequency absorption of the audience founded in section 2.2.4. Moreover, it is assumed that reflection occurs at low frequency since the audience absorption drops below 250 Hz. Based on the assumed audience sound reflecting experience, the microphone hight shall optimally be approximately 1.70 m above the ground with a mechanism which blocks for the high frequency reflection. In section 7.3.9 a windscreen is designed with high frequency reflection blockage and wind noise reduction. This method is tested before the final test to ensure that the reflection blockage work as described. Otherwise, the microphone is situated on the ground to eliminate the ground reflection at high frequency. The microphone is placed with an angle of $\pm 25^\circ$ from the frontal direction of the speaker as shown in Figure 7.9.

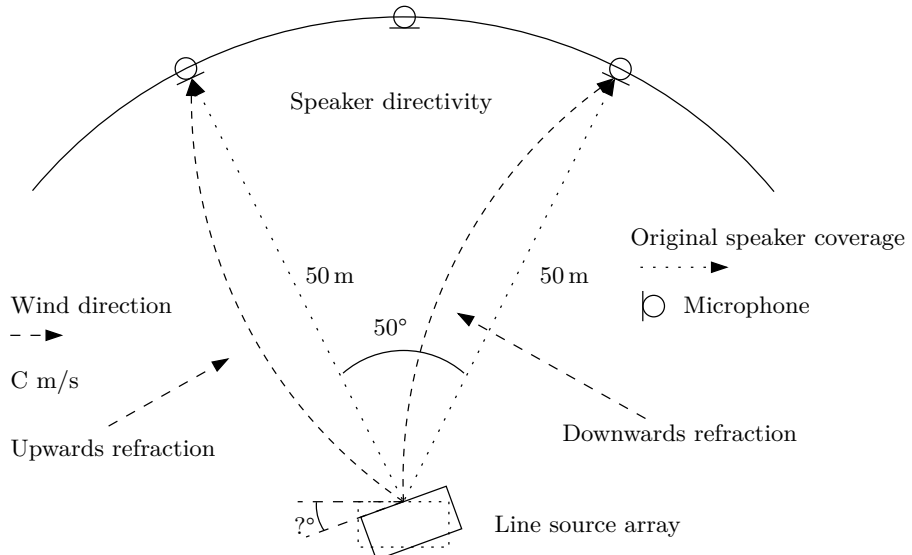


Figure 7.9: The figure shows the measurement setup

This angle is chosen such that the outer main lobe coverage area is measured and because it is the given directionality angle of the speaker at the narrow-angle settings.

7.3.5 Microphone position at parallel wind

The microphone position of the parallel wind measurement depends on the shadow zone position. It is wanted to measure in the shadow zone to explore if it is possible to move the shadow zone backwards by tilting the line array. Therefore, two measuring scenarios are designed. The first is based on a realistic tilt angle to a concert, where the coverage area of the line source array covers the microphone position. The second is based on a tilt angle where the coverage area of the line source array is in front of the microphone. The two scenarios are defined as scenarios one and scenarios two, respectively. By these two methods, the shadow zone is predicted to be present in scenarios one, while the line source array plays against the wind, and in scenarios two the wind refracts the sound wave to the microphone. The following Figure 7.11 shows scenario two.

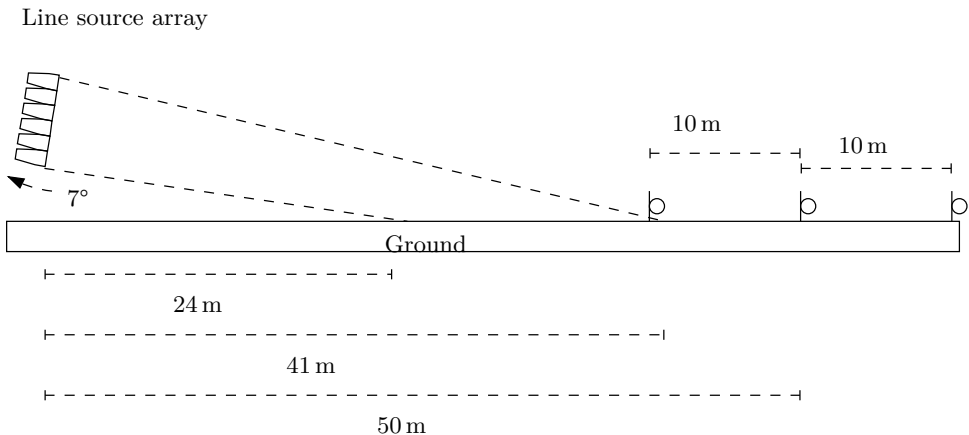


Figure 7.10: The figure shows the measurement setup while the line source array is tilted 7° forward

As seen in Figure 7.10, the main lobe of the line source array is assumed to be near-field, which only holds for high frequencies. At a distance of 40 m this illustration covers frequencies above 6.0 kHz, frequencies below will be wider as the frequency drops section 2.1. The illustration illustrates that the highest power of the line source array is within the centre of the main lobe in the frequency of interest due to the directionality characteristics of the line source array. In this case, the microphone should be outside the main lobe while no refraction is present, but as the wave refract, the microphone becomes inside the main lobe.

The following Figure 7.11 illustrate Scenario one.

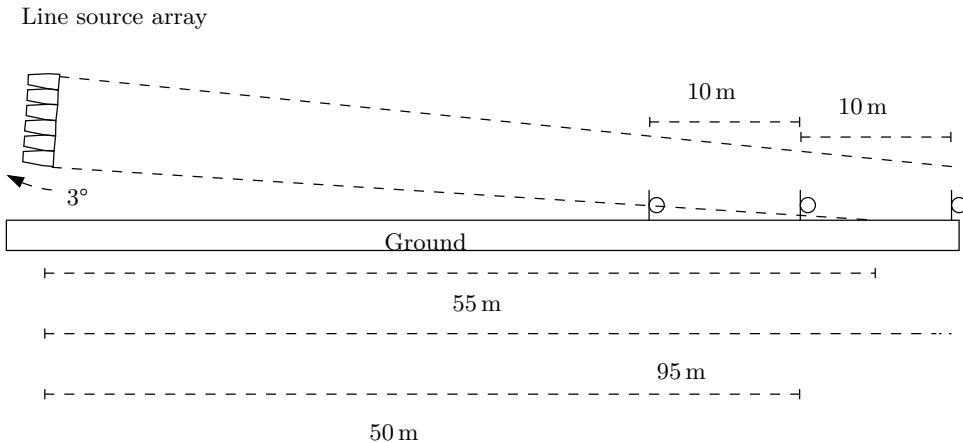


Figure 7.11: The figure shows the measurement setup while the line source array is tilted 3° forward

In the test case shown in Figure 7.11 more SPL is delivered to the centre and back microphone compare to the test case in Figure 7.10 while no refraction is present. While upwards refraction is present, the proposed solution in section 6.4 indicate that the refraction refracts the sound wave such as the SPL distribution is vice versa. The upwards refraction refract the sound wave in Figure 7.10 above the microphone and the refraction of the soundwave in Figure 7.11 refract the soundwave to the microphone. In this test case, the microphone is situated on the ground such that the microphone is as deep in the shadow zone as possible. In other words, as shown in Figure 6.2, while the microphone is positioned in the same distance from the line source array, while the microphone is on the ground compare to lifted above the ground, the shadow zone is most present at the ground. If more SPL is present in the Figure 7.10 compare to Figure 7.11 the shadow zone distance might be able to be optimised.

7.3.6 Sensors and its position

Doing the measurement, the temperature, the humidity and the wind direction and speed is measured. All measurement is done syncronised along with the impulse response measurement. The wind is measured into position since the wind condition is dynamic concerning the area. The wind measurement is done close to the speaker and at the centre microphone both in the crosswind measurement and in the parallel wind measurement. The temperature and humidity are only measured in one position near the line source array since the temperature and humidity are assumed to stable and identical at the measuring area.

Before the measuring system is built, the wind direction is measured to ensure a perfect angle of the speaker. To decide to set up the angle of the measuring system, the wind is measured visually by the directional fan on the anemometer. After the measuring system is built, the anemometer is positioned such that the output angle

is either 90° or 270° . A headroom of 90° before the anemometer goes to either 0° or 359° . The reason to have the headroom is that the cross point between 0° and 359° is a cross point of the measuring potentiometer where it jumps from maximum value to minimum value. The anemometer is further explained in section 7.4.2

7.3.7 Rotation of the line source array

This section aims to design the turning method for the line source array and ensure that the speaker point in the desired angle. A mechanical solution is chosen for both rotation of the line source array and measuring the rotational angle of the line source array. The mechanical solution to rotate the line source array with a long piece of truss connected to the back of the flying tools of the line source array. By this method, a person can move the other end of truss and stabilise the angle by placing the end of the truss on the ground. Moreover, to ensure that the rotation is as at the specified angle, two laser pointer is attached beneath the line source array — one in the vertical rotation axis and one behind the vertical rotational axis. The one on the vertical rotational axis is then the reference to the back laser pointer. The laser points onto a plate where a rotational angle is given. The following Figure 7.12 illustrate the solution.

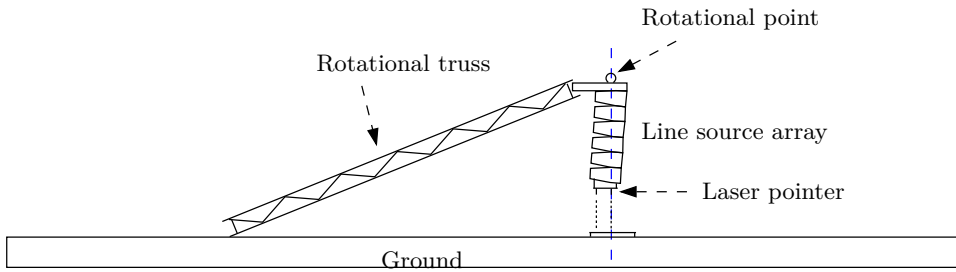


Figure 7.12: The figure shows the rotational mechanic where the blue dashed line illustrate the vertical rotational axis.

In Figure 7.12 the rotation is achieved by moving the ground position of the rotational truss towards the reader or away from the reader. The laser pointer holder and plate for measuring the angle is shown in the following Figure 7.13 and Figure 7.14.

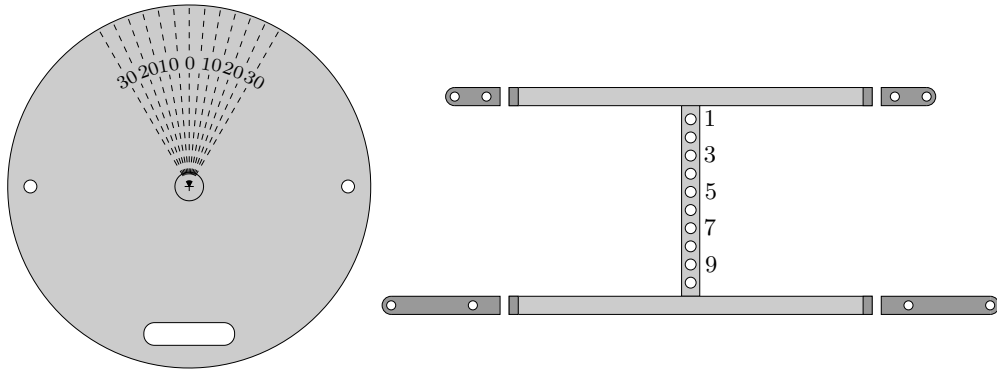


Figure 7.13: The figure shows the angle plate.

Figure 7.14: The figure shows the laser holder.

The reference laser is guided into hole 1 in Figure 7.14, which is at the rotational axis while the line source array is tilted 3° . The back laser is guided into hole 10 such that the highest distance between the laser is achieved. The measuring angle plate is then placed on the ground with the reference laser pointing at the centre and the back laser pointing at the 0° angle while the line source points directly forward. By rotating the line source array, the laser point in the back laser is rotated and gives the rotation of the line source array.

In the parallel wind measurement, the reference laser is used to measure the tilting angle. While the line source array is in the 3° general position, the laser pointer point directly down. The backwards movement of the laser point is calculated to be 44 cm from the general position to 7° downwards tilting.

7.3.8 Measuring area and condition

The measurement is achieved in a flat area with mown grass. The optimal area is without any building or trees, but this optimal area is not possible doing the measurement in this thesis. The second best measuring area is a flat area where only a few building is present, and with no forest but three is allowed in a small number of pieces. The mown grass area beside Tryvej 13, 9320 Hjallerup is chosen because it fits the second best description, and the author has a close relation to the owner of the area.

To keep the wind speed realistic for measurement at concert situation, while refraction is present, the wind speed doing the measurement is limited in the range for average 5 m/s to 10 m/s. Less average wind speed than 5 m/s is avoided to ensure the measurable effect of the wind on sound propagation. The higher limit of the 10 m/s is chosen to ensure that the speaker tower is safe at the height of 5 m. The limited size of the line source array tower setup, makes it wind sensitive. Moreover, no rain is allowed to be present in the measuring day.

7.3.9 Design of windscreen

It is founded in section 5.3 that wind effect the measurement by pink noise. This noise might not affect the measurement headroom in the refraction frequency range, but an overload of the microphone or preamp by the low frequency noise produces distortion which shall be avoided. Secondly, the signal to noise ratio shall be sufficiently high in the frequency range of refraction. Therefore, to be able to control the wind noise, this section design the preferable microphone windscreens configuration for the measurement based on the available equipment in the acoustics lab.

Only two outside measuring microphone system with two microphones in all is available in acoustics lab, and therefore a windscreens is designed such three identical windscreens can be made. A research of wind speed attenuation, wind noise and frequency effect is done on serval windscreens concept, which is founded in Appendix B. All windscreens is an addition to the original windscreen which always is present on the microphone.

Based on the finding in Appendix B, the final windscreens optimises the stability of the founded windscreens in Appendix B with a PVC foam mounted on a circular wood plate instead of the Rockwool bat. This configuration shows the best performance in lowering the wind speed near the microphone. Moreover, it is chosen that the microphone shall be at the height of the ear. Therefore, the wood plate is an additional ground plan added to the bottom of the windscreens to block for ground reflection. The following Figure 7.15 illustrate the windscreens

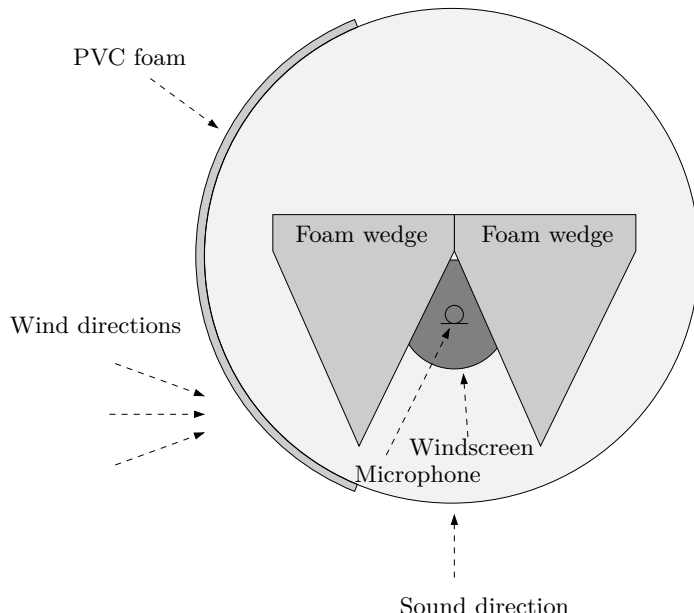


Figure 7.15: The figure shows the single rockwool concept

The change from Rockwool bat to PVC foam is made based on the better stability of PVC foam and that the foam wedge is assumed to cancel the reflection from the

PVC foam. While adding the wood plate the original windscreens to the microphone is lifted by 4.5 cm from the wood plate which might result in sound reflection from the wood plate. To eliminate the sound reflection from the wood plate, the technique from wind turbine measuring setup is used, where the windscreens are cut. In the wind turbine microphone setup, the cut is done such that half of the microphone is cut down into the wood plate. In the designed windscreens no hemispheres are available, therefore this cut is not suitable. The cut is therefore made 2 mm to 3 mm beneath the microphone opening of the original windscreens such that the original windscreens fully covers the microphone. The cut is illustrated in the following Figure 7.16.

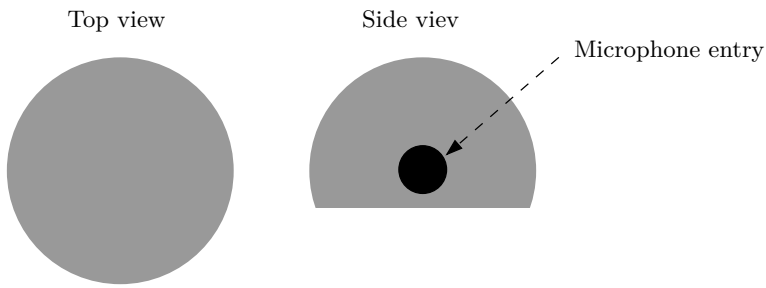


Figure 7.16: The figure shows the modified original windscreens

7.3.10 windscreens wind noise attenuation

This section aims to research the wind noise attenuation produced by the windscreens in real condition to ensure that the wind noise does not overload the microphone. The measurement is done both with and without the designed windscreens to decide if the windscreens work in a real scenario with high speed and directionality changing of the wind. The measurement is furthermore done both in the ear height and on the ground to research if one position has a better signal to noise ratio. The first performed measurement is a series of two measurements, one in the ear height and one on the ground. Both measurements are performed with the designed windscreens.

The measurement is done in the same vertical, and horizontal angle in two steps, first in ear height then at the ground with the same windscreens. The measurement is done 10 times at each position, such that the measurement with nearly the same wind speed can be compared. The windscreens are placed 90° against the wind, which means that the windscreens are placed in its optimal position where the wind blows directly onto the wide PVC foam plate. The following Figure 7.17 shows the result. Measurement, where the windscreens are rotated is also performed and can be found in Appendix N.

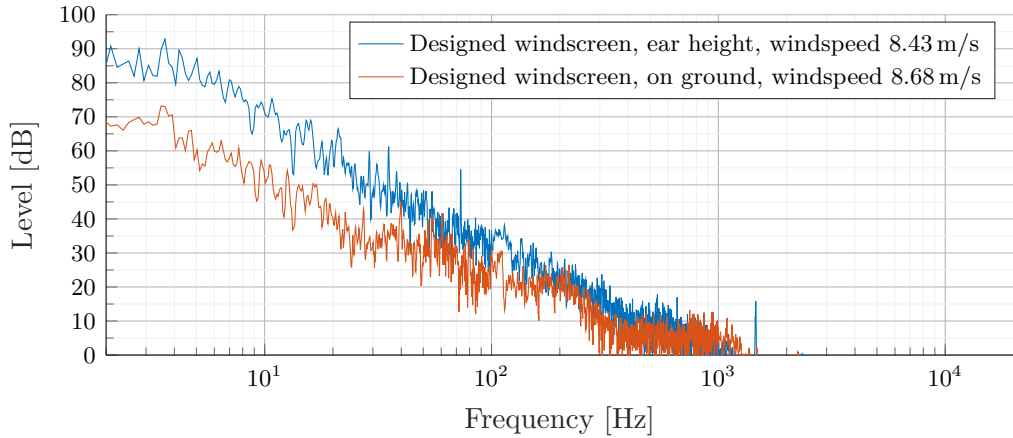


Figure 7.17: The graph shows the frequency content of the measurement with the windscreen in the hight of the ear and on the ground

As it is seen in Figure 7.17, the wind noise highly depends on the hight of the windscreen position. By lowering the windscreen from the ear hight, down to the ground surface, the wind noise is lowered with approximately 20 dB SPL in the low frequency range, which is the frequency area where the wind noise is highest. Furthermore, it is research if the designed windscreen has higher wind noise attenuation compared to only the modified original windscreen. The following Figure 7.18 shows the result.

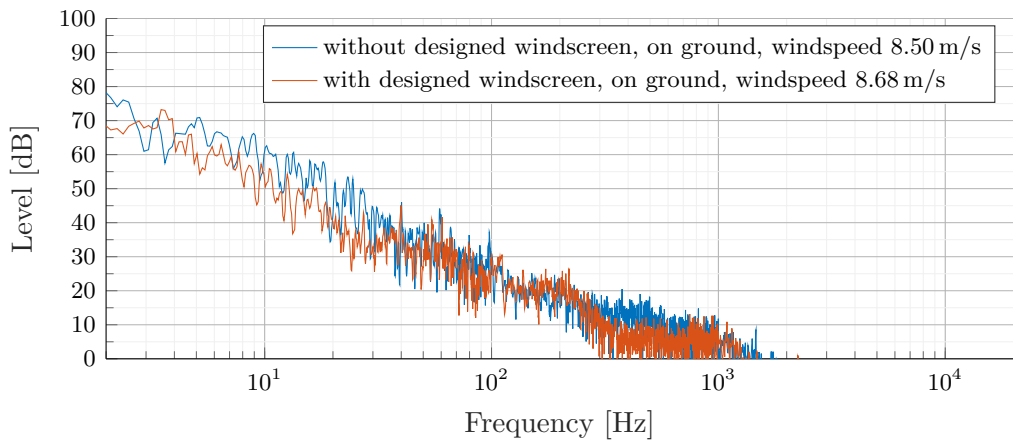


Figure 7.18: The graph shows the frequency content of the measurement with and without the windscreen

As seen in Figure 7.18, the windscreens have generally a 5 dB SPL to 10 dB SPL wind noise attenuation. The measurement description is founded in Appendix N.

7.4 Data logging system

This section aims to explain the measuring software and electronic hardware designed for the measurement. To be able to measure the weather condition, measuring hardware has to be chosen and designed. To be able to transfer data from the weather sensors to the measuring software, a small microprocessor is programmed to read sensor data and transfer the data to the measuring software. This section starts to explain the measuring software and its requirements to the weather data transfer protocol. Then the weather sensors are chosen and firmware is designed to a microprocessor. In the end, the hardware is designed.

7.4.1 Software

This section gives a short overview of the MATLAB®software used for the measurement. The overview does not include any code but only the method of measuring the impulse response and get nearly synchronised data from the serial bus. This section starts explaining the data transfer between the sound card and the computer and the weather hardware to the computer. Both part are connected via Universal Serial Bus (USB) connection. Afterwards, the impulse measuring method is explained.

The data transfer rate between the soundcard and weather hardware to the computer is decided by the buffer length of the audio signal. The audio signal is not allowed to lack while measuring the impulse response. MATLAB®transfer a buffer with audio to the sound card and gets a buffer back with measured signal. The played and recorded signal is syncronised. After the buffer is received MATLAB®have a short period to do calculations, but the calculation shall be finish, and the next audio buffer shall be sent between two samples. The chosen buffer size between MATLAB®and the soundcard is 4096 sample. The following Figure 7.19 illustrate the data transfer protocol.

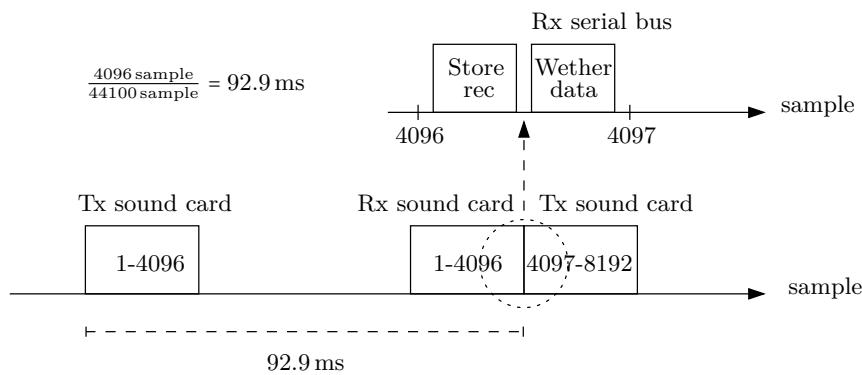


Figure 7.19: The figure shows the transferring samples between the sound card and computer and between the serial bus and the computer. The length of the buffer boxes is just an illustration, the actual length is not measured.

As seen in Figure 7.19, the length of the buffer size limits the amount of weather data. The sound sweep measurement which is explained next is chosen to be 5 s long. This gives 55 weather data measurement point doing the impulse response measurement. All weather information and sound information is stored into a mat file after every measurement such that the analysis can be done offline.

The impulse response is measured with sine sweep according to [Müller and Massarani, 2001]. The method is to deconvolute the measured signal by the reference signal which produces the impulse response of the speaker. In the measuring software, the deconvolution is done in the frequency domain, because it speeds up the calculation. A hanning window windows both the measured signal and the reference signal. To exclude the influence of the sound card, the reference signal is played through one output channel and measured by one of the microphone input. It is assumed that the characteristic of every output and input is equal. To be able to make calibrated impulse responses, the measured reference signal is related to the microphone sensitivity by the following Equation 7.1

$$\text{ref}_s = \text{ref}_m \cdot \frac{\text{mic}_{\text{sen}}}{\text{rms}(\text{ref}_m)} \quad (7.1)$$

Where:

- ref_s is the calibrated reference signal [1]
- ref_m is the measured reference signal [1]
- mic_{sen} is the rms sensitivity of the microphone in digital number [1]
at one pascal rms

After the reference signal is related to the measured signal, deconvolution is calculated by calculating the Fast Fourier Transform (FFT) for both signal, divide the measured signal by the reference signal and calculate the Inverse Fast Fourier Transform (IFFT). The result is an impulse response where the amplitude corresponds to a calibrated pascal value. By the impulse response both the octave SPL can be calculated and the frequency response.

The measuring software is founded in Appendix I

7.4.2 Sensor and microprocessor

The microprocessor for weather measurement is based on an Arduino UNO. The chose of an Arduino is made because code for both the temperature and humidity sensor and the used anemometer is available on the internet.

The chosen temperature and humidity sensor are an AM2302 because it is available as a component at Aalborg University and it covers relative humidity from 0 % to 100 % and a temperature range from -40°C to 80°C which is more than enough of the measurement. The data sheet of the sensor is founded in [AOSONG].

The chosen anemometer is a Davis Vantage Pro2 anemometer. This anemometer is chosen because the connection is direct to the wind speed sensor and the wind

direction sensor. The direction sensor is a $20\text{ k}\Omega$ 360° potentiometer, where the speed sensor is a contact which makes one short circuit to ground for every rotation. The directional sensor can, therefore, be connected to an analogue input port where the speed sensor is connected to a digital input. The data sheet for the anemometer is founded in [Davis]

7.4.3 Firmware

The firmware is designed to support two anemometers, one temperature sensor and one humidity sensor. The temperature and humidity sensor is one unit and communicates digitally to the Arduino. The communication is done through the dht.h Arduino library. The data is then called from a function of the library, and the author has not designed the digital connection. The anemometer both measure the wind direction and wind speed. The wind direction is an analogue voltage from 0 V to 5 V while the angle goes from 0° to 359° . The rotational angle from the direction sensor increases while the directional goes from south to west, therefore it works in the same direction like a compass. The analogue voltage is measured with the build in 10 bit Analog to Digital Converter (ADC) which gives a digital number from 0 to 1024. This measured number is transferred directly to the com bus without angle correction. The conversion to angle is done in MATLAB[®].

The wind speed measurement sensor gives a pulse for every rotation. According to the datasheet of the wind anemometer, one rotation of the wind speed sensor over a time period of 1 s correspond 1.0058 m/s. To be able to measure the wind speed in a higher resolution than 1.0058 m/s the pulses is time average over a defined period. To be able to measure over a period a First In First Out (FIFO) buffer is designed for the pulses as shown in the following Figure 7.20

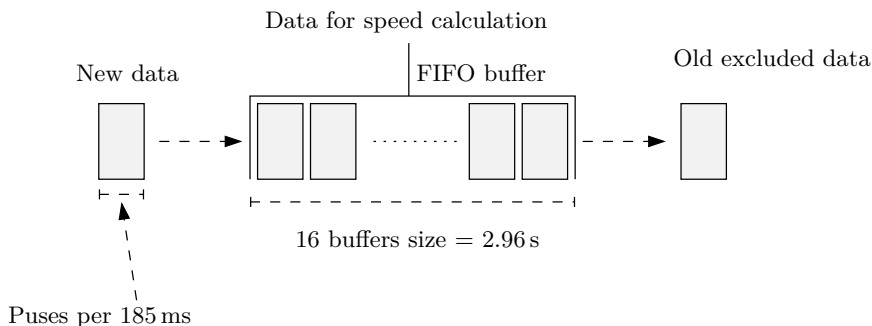


Figure 7.20: The figure shows the FIFO buffer system for wind speed measurement

As seen in Figure 7.20, the update time is for every 185 ms and the buffer contains 16 pieces of 185 ms which gives an average time over 2.96 s. This buffer size gives a wind speed resolution of 339.8 mm/s.

The update time is slower than the data transfer time interval between the Arduino and MATLAB®. This resolution is decided to be sufficient since the mechanic of the speed sensor by itself average the wind speed.

The firmware is synchronised with MATLAB® by adding a delay in the main loop and not tricking on a timer. Therefore, the program runtime is only stable down to ± 3 ms precision with a mean update time for the firmware of 92.3 ms. The mean update time is based on five time measurement with 80 samples in each. The negative shift of the firmware update doing the 55 weather update transferred to MATLAB® gives a lack of -38.8 ms after end measurement. The lack of -38.8 ms is much less than the update of -92.3 ms, which indicate that the time synchronisation lack is less than one sample and no time shift is present. Since the update sometimes is above 92.9 ms the weather updates sample to MATLAB® can be the same twice. This issue is only present in the first 5 samples. After those samples, the lack in synchronisation does that 96 ms is an update before the MATLAB® is ready to receive data from the serial bus.

Based on the above explanation, the following weather data is present in the impulse response measurement, where it shall be noted that within the first few samples, an repetition can occur. This repetition is considered as indifferent, since the first 500 ms is a starting silence period of the sine sweep and frequency below 40 Hz and, therefore, is removed from the data analysis.

- The wind direction is updated for every weather sample.
- The wind speed is updated for every second weather sample.
- The temperature and humidity are updated for every weather sample.
- The MATLAB® software ask in total for 55 weather samples doing one impulse response measurement.

The data transfer is done through the serial bus vis USB connection. The following Figure 7.21 shows a snapshot of the serial bus delivered by the Arduino.

Speed 1	Direc 1	Speed 2	Direc 2	Temp	Hum
5.44	790	6.12	884	21.90	68.90
5.44	791	6.12	882	21.90	68.90
4.42	790	5.78	863	21.90	68.90
4.42	791	5.78	832	21.90	68.90
3.74	790	5.44	820	21.90	68.90
3.74	790	5.44	827	21.90	68.90
3.40	791	5.10	831	21.90	68.90
3.40	790	5.10	832	21.90	68.90

Figure 7.21: The figure shows a snapshot of the serial bus. The first vertical line, which is the left vertical data line is the wind speed of the first anemometer. The second vertical line is the wind direction of the first anemometer. The third vertical line is the wind speed of the second anemometer. The fourth vertical line is the wind direction of the second anemometer. The fifth vertical line is the temperature and the last vertical line is the humidity.

The firmware is founded in Appendix H

7.4.4 Hardware

To be able to connect both the two anemometers and the temperature and humidity sensor to the Arduino UNO an Arduino shield is designed. The shield is designed such that it can be plugged directly onto the Arduino. The following Figure 7.22 shows the schematic of the shield and the Printed Circuit Board (PCB)

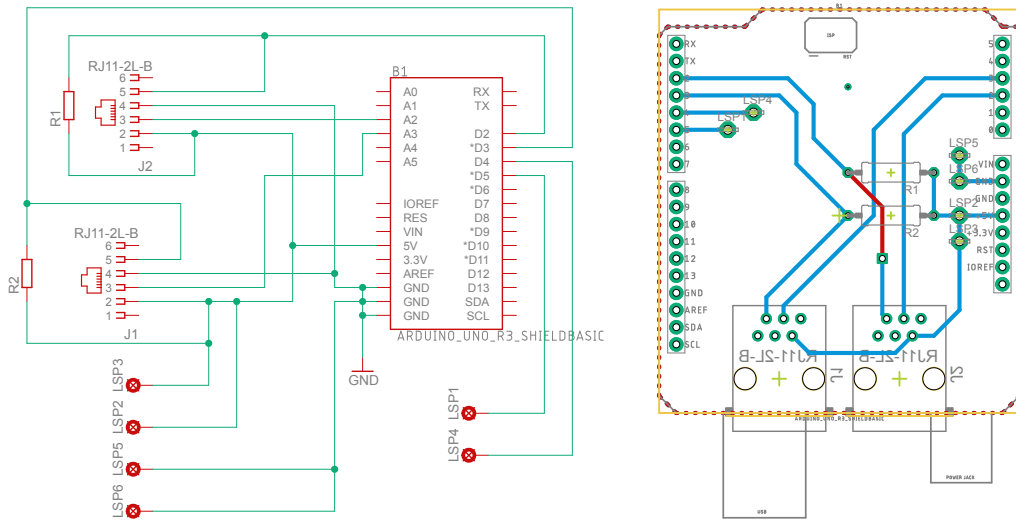


Figure 7.22: Ardouino shield design

The two resistors in Figure 7.22 R1 and R2 are pull-up resistors for the wind speed contact with a resistance of $4.7\text{ k}\Omega$. While the contact in the anemometer is not shorted, the voltage at the input pin on the Arduino is 5 V. While the contact is shorted the voltage is 0 V. The two RJ11 connectors are for the Anemometer connection. The six test points are soldering connection to the temperature and humidity sensor.

All hardware can be seen in Appendix O

Chapter 8

Test of measuring design

8.1 Test of measuring design

This section aims to test the design measurement in a windy day, to outsource problem and error in the measuring design. The test is done in full scale with all six line source array element and in the designed hight. The test is intended to both test the crosswind measuring design and the parallel wind measuring design, but the wind condition only allowed for crosswind test. After the crosswind measuring design was tested the wind speed dropped to beneath 1 m/s. In the crosswind measuring design, three problems and one code error are observed. The code error is a data save bug, where only the direction of the wind at the line source array tower is saved. The wind direction data at the microphone position is overwritten by the wind direction data at the line source array. The code bug is fixed for the final measurement. The following three section 8.1.1, section 8.1.2 and section 8.1.3 explain the observed difficulties or design failure and propose a solution to them. The first difficulty which is discovered is major ground reflections in the measurement. The second problem seems to be frequency response differences while using the windscreens, where the third error is the angle of the line source array while measuring in the hight of the ear. The explanations is based on the measurement as seen in Figure 8.1 which shows the frequency response on all three microphones at 0° rotation.

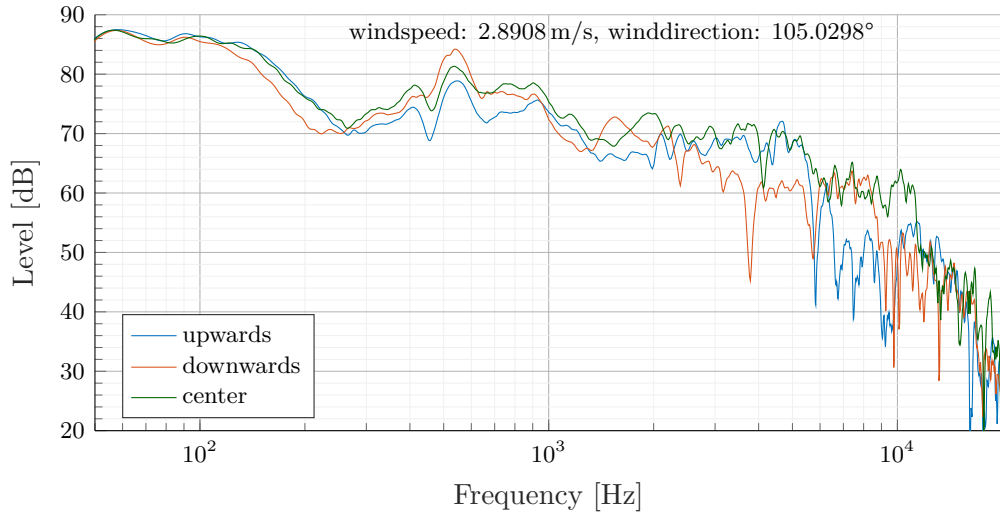


Figure 8.1: The graph shows the frequency response for all three microphone while the speaker is not rotated

All three microphone measurement in Figure 8.1 is the mean of 10 measurement. The mean is calculated in the time domain by aligning the impulse response with the help of cross-correlation. The wind speed and wind direction is also the mean of the 10 measurements.

To be able to differentiate between the microphone in the explanation, the microphone is named according to the position and the wind direction. In the upwards refraction direction, the microphone is named upwards microphone, in the downwards refraction direction the microphone is named downwards microphone, and the centre microphone is named centre microphone. The following ?? illustrate the microphone position versus the wind direction.

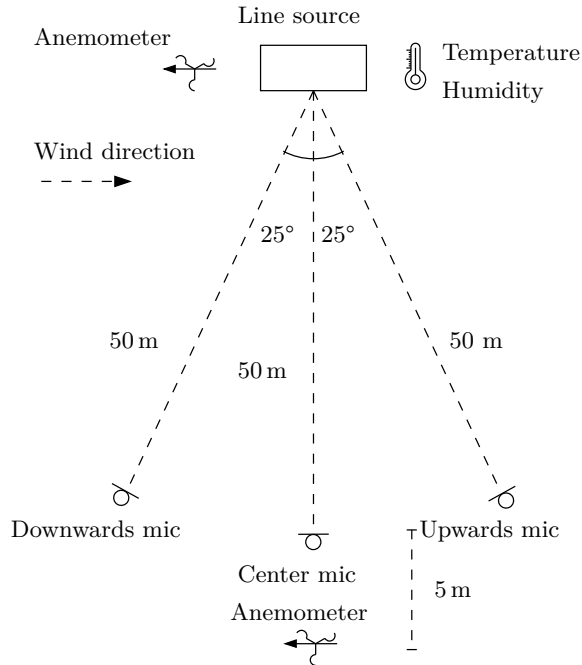


Figure 8.2: The figure shows the microphone position versus the position of the line source array, while the line source array is 0° rotated

As seen in Figure 8.2, the position of the anemometer temperature and humidity sensor is also given at its position doing the measurement. Ensure that the measurement is a measure of the transfer function and not the wind noise, a signal to noise measurement is performed as the first part. The signal to noise ratio is measured in two ways, one where the wind noise is measured and one where transfer function is measured at high SPL level wherafter the output level of the speaker is lowered by 10 dB SPL, and the transfer function is measured again. While the frequency response in the hole frequency range is lowered by 10 dB SPL, the headroom is at least 10 dB SPL. The noise floor is founded to be pink noise with 70 dB SPL as the maximum at 2 Hz at all microphone position and with a wind speed of 5 m/s. All measurement is done with sine sweep with constant amplitude and with a signal to noise ration of more than 10 dB SPL. The signal to noise ratio was visually checked by plotting the measuring result in MATLAB®. The signal to noise ratio measuring is not saved as a file in this test measurement but is saved and shown in the final measurement.

8.1.1 Ground reflections

One intended outcome of the windscreen is to block for the ground reflection by the circular wood plate, such that the measuring position can be in the hight of the ear, as explained in section 7.3.2. This part of the windscreen fails in blockage all ground reflections in the frequency above 250 Hz as seen in Figure 8.1, and as

the frequency grows the effect seems to be worse since higher peaks and depth are present in the measurement compare to the directionality measurement of the speaker in Figure 7.3. The centre microphone does not have that high peaks and deeps, but the upwards and downwards microphone seems to suffer from a ground reflection in the high frequency, which makes the refraction comparison between the microphone position difficult. One thing that might cause the reflection is the position different from 0° vertical of the windscreens with respect to the ground. If the plate is tilted forward, there might be some reflection reaching the microphone. A calculation of the reflection might have helped to justify the ground reflection theory, but since the source is a line source array and not a point source, the ground reflection is not as easy to calculate. There might be thousands of sound path from the line source to the microphone where the sound path length is half the wavelength longer or shorter. The following Figure 8.3 illustrate the path calculation difficulties and the forward tilting of the windscreens.

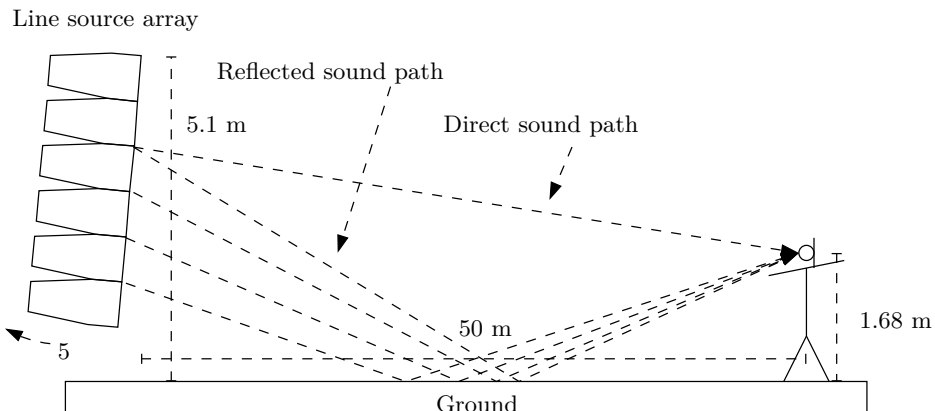


Figure 8.3: The figure shows an illustration of the measured setup and some soundpath

To be able to make a qualified considering to decide if the peaks and depth are due to ground reflection, the measurement is compared to a measurement where the microphone windscreens are situated on the ground and the frequency characteristics in the measuring direction in Figure 7.3. It has to be noted that the windscreens have a speaker stand connector mounted underneath, which lift the centre of the designed windscreens such that the windscreens cannot lay flat on the ground but is tilted forward. The windscreens were tilted forward by a maximum of 8° or less doing all measurement on the ground in all microphone position. The following Figure 8.4 shows a frequency response at all three microphones position of the line source array, where the windscreens are placed on the ground and with a non-tilted line source array.

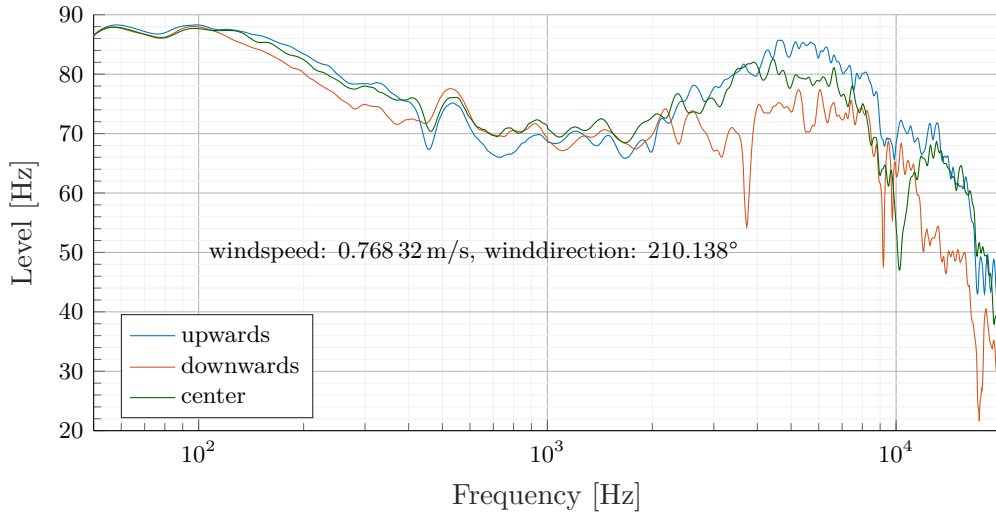


Figure 8.4: The graph shows the measuring result along with all three microphones, while the microphone is in the windscreen and the windscreen is on the ground. The graph is a mean of three measurements for the upwards and downwards microphone and one measurement for the centre microphone. The mean calculation is done in the time domain where all impulse responses are aligned with cross-correlation

The frequency depth seen at 3.7 kHz in the downwards direction is due to the directionality characteristics of the line source array and can also be seen in Figure 7.3. The same applies to 9.2 kHz and 10 kHz

Comparing the measurement where the windscreen is lifted 168 cm from the ground in Figure 8.1 and the measurement in Figure 8.4, it is seen that the first ground reflection comes around 250 Hz depending on the microphone. This ground reflection is dBwise even for all microphone position and might, therefore, be due to sound wave travels through the windscreen bottom plate. The following arriving ground reflection depends highly on the microphone position and then might be due to the vertical angle of the designed windscreen. For the upwards refraction microphone, there seems to be highly reflections in the frequency area from 5.5 kHz to 9.5 kHz where comb filtering is present. Comparing the line source array element frequency characteristics, it also shows depth in that frequency range, but not as many and not as low depth as present in the measurement.

Another common response on all microphone while the windscreen lays on the ground is depth around 10 kHz. This depth might be due to the lift of the microphone while it is within the modified original windscreen or that the windscreen is tilted forward.

Based on the finding in the measurement, ground reflection occurs in the measurement.

8.1.2 Frequency differences

Doing the measurement, a frequency differences between 2.0 kHz and 10 kHz is observed and is researched in this section. The frequency differences are observed while the microphone is laying on the ground with and without the windscreens. Furthermore, the wind doing the measurement is less than 1 m/s and therefore, refraction is assumed to be not present at a distance of 50 m. A comparison measurement is done, where the windscreens are removed from the centre microphone since the wind stopped at the end of the measurement. The following Figure 8.5 shows the measurement result for all three microphones with windscreens and one measurement where the windscreens are removed from the centre microphone. The original modified windscreens covering the microphone are also removed.

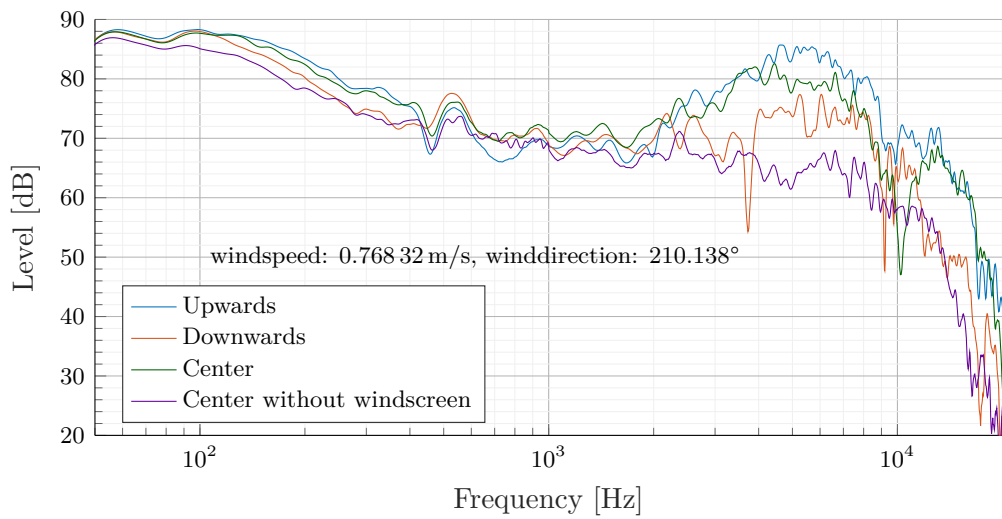


Figure 8.5: The graph shows the measuring result along all three microphones, where one of the measurements for the center microphone is done with designed windscreen setup and one measurement is done without the design windscreen setup but with only the modified original windscreen. While the microphone is in the designed windscreen, the designed windscreen is on the ground. While the microphone is outside the design windscreen, the microphone lays on a wood plate with the same size as the designed windscreen. The graph is a mean of three measurements for the upwards and downwards microphone and one measurement for the centre position for both centre measurement. The mean calculation is done in the time domain where all impulse responses are aligned with cross-correlation

It is seen in Figure 8.5 that the depth at 10 kHz is gone for the centre microphone without any windscreens, but either a 20 dB SPL attenuation of the center microphone or a 20 dB SPL amplification while the microphone is within the designed windscreen is measured. The amplification or attenuation is not a problem in itself, the arising problem is that the amplification might not be even along with the microphone position. The measurement is done with less than 1 m/s of wind speed, and therefore,

refraction is assumed to be excluded as a factor of differences. This means that the differences in the windscreens setup might influence the frequency response. Three mechanical differences are observed on the windscreens setup doing the measurement. The first is the vertical angle of the windscreens, which was different along with all designed windscreens doing the measurement because the ground is uneven. The ground unevenness is measured afterwards to a maximum of 8° . Secondly, the rotational angle of the designed windscreens was also different, along with all designed windscreens. The rotational angle is defined to be 0° to the line source array while the line source array points directly into the centre of the windscreens opening, as shown in Figure 8.6.

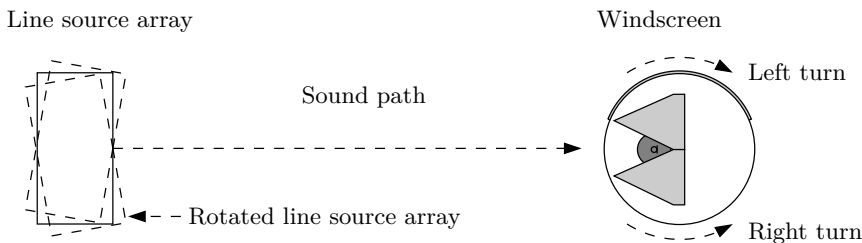


Figure 8.6: The figure shows an illustration the windscreen vertical 0° angle

As illustrated in Figure 8.6 no matter the tournament of the speaker, the opening shall point directly to the speaker. In the measurement, the opening was not pointing directly to the speaker. The vertical angle was adjusted with depends on the wind direction, this means that the windscreens at downwards direction is turned left, where the windscreens at upwards direction is turned right.

The last differences were the placement of the foam on the plate. In the downwards direction the foam is placed more inwards to the centre of the plate while the foam on the other two designed windscreens was placed as shown in Figure 8.6

8.1.3 Speaker angle

The angle of the line source array was calculated while the measurement setup was built. In the calculation, the wrong microphone reference point was used. The microphone position which was used in the calculation was while the microphone on the ground and not in the ear height and therefore, higher tilt angle was calculated. The measuring angle should have been the given angle in section 7.3.1 where the near-field covers both at the ground position and the ear height position in the distance of 50 m but the angle was calculated to 5.7° and the line source array was tilted to 5° . The following Figure 8.7 shows the microphone positions.

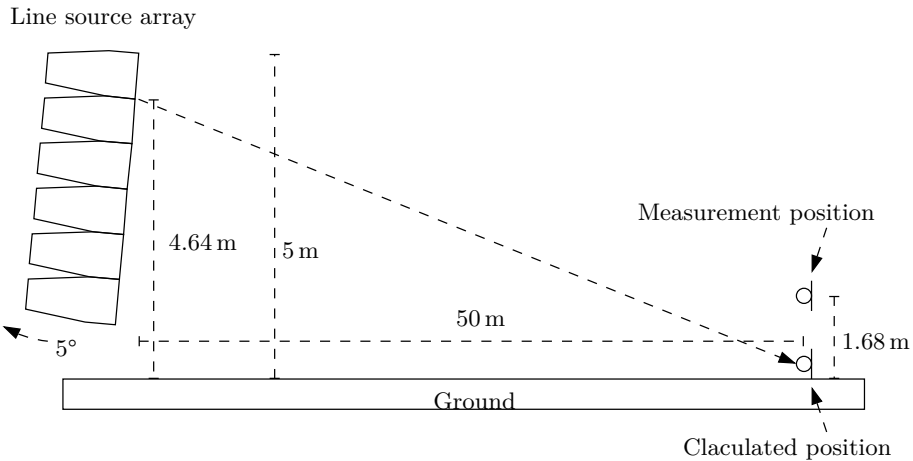


Figure 8.7: The figure shows the microphone position doing the calculation of the line source array tilting and the measurement

While using the 5° tilt angle doing the measurement, the height before the microphone exit above the near-field of the line source array coverage main lobe is calculated to be 63 cm. Therefore, since the microphone was placed 1.68 m above the ground, the microphone is far above the near-field. Comparing the Figure 8.1 and Figure 8.4 it is clearly seen that the microphone is outside the near-field of the high frequency. Above 2.0 kHz, the SPL is more than 10 dB SPL lower in the ear measuring height compare to the ground position with the same distances to the speaker.

8.1.4 Measuring result

While all error and difficulties are described and is known to disturb the measurement, the measurement indicates that raising the power in the upwards direction, also raising the power in the shadow zone. Comparing the microphone against each other is difficult since the differences in the frequency response between the microphone as described above. Therefore, to extract useful data, the frequency response on the same microphone is compared for 0° of tournament, 10° of tournament and 20° of tournament. The first microphone which is compared is the microphone in the upwards direction. The following Figure 8.8 shows the frequency response for every tournament.

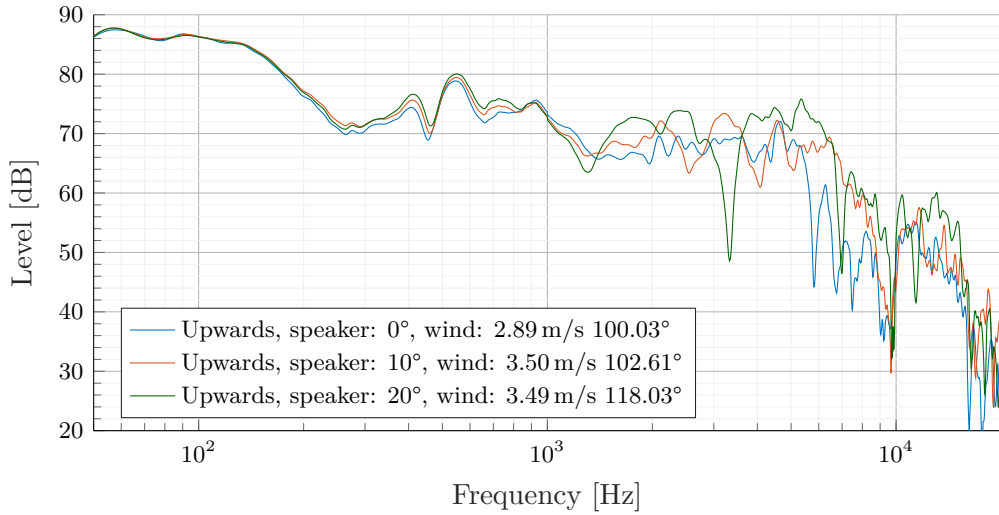


Figure 8.8: The graph shows the measuring result for the upwards microphone in three line source array rotation, while the microphone is in the windscreens and the windscreens are in the height of the ear. The graph is a mean of 10 measurements in all three angles. The mean calculation is done in the time domain where all impulse responses are aligned with cross-correlation

As seen in Figure 8.8, while the speaker is turned towards the upwards microphone, the SPL is raised. The peaks and depth are not at the same frequency, which makes the visually evaluation difficult, but it visually shows that turning the speaker raises the SPL in some frequency area, especially above 1.0 kHz. The following Table 8.1 shows the single number SPL both non weighted and A-weighted.

Table 8.1: The table shows the measured $L_{eq,5}$ and $L_{A_{eq,5}}$ SPL for the upwards microphone

Speaker angle	0°	10°	20°
$L_{eq,5}$	66.64 dB SPL	67.46 dB SPL	68.70 dB SPL
$L_{A_{eq,5}}$	63.90 dB SPL	65.19 dB SPL	67.27 dB SPL

The second microphone which is compared is the microphone in the downwards direction. The following Figure 8.9 shows the frequency response for every tournament.

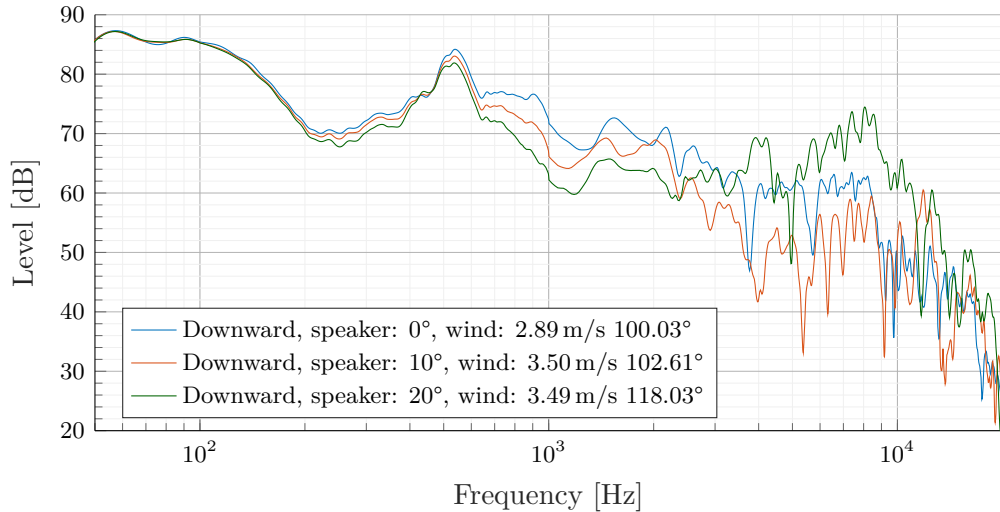


Figure 8.9: The graph shows the measuring result for the downwards microphone in three line source array rotation, while the microphone is in the windscreens and the windscreens are in the height of the ear. The graph is a mean of 10 measurements in all three angles. The mean calculation is done in the time domain where all impulse responses are aligned with cross-correlation

As seen in Figure 8.9, while the speaker is turned, the SPL is lowered unless the 20° above 2.5 kHz. The raise in power comes from the directionality characteristics of the line source array as seen in Figure 7.3. The peaks and depth is either not at the same frequency which make the visually justment difficult but it is observed generally that turning the speaker lower the SPL from 0° to 10° above 650 Hz. The following Table 8.2 shows the single number SPL both non weighted and A-weighted.

Table 8.2: The table shows the measured $L_{eq,5}$ and $L_{A_{eq,5}}$ SPL for the downwards microphone

Speaker angle	0°	10°	20°
$L_{eq,5}$	66.86 dB SPL	65.46 dB SPL	67.12 dB SPL
$L_{A_{eq,5}}$	64.24 dB SPL	61.59 dB SPL	64.36 dB SPL

The third microphone, which is compared, is the microphone in the centre direction. The following Figure 8.10 shows the frequency response for every tournament.

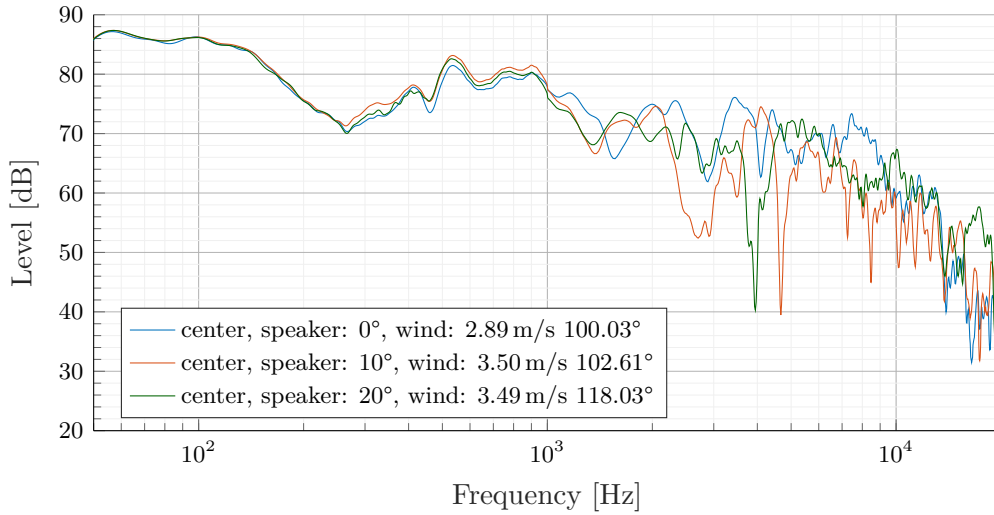


Figure 8.10: The graph shows the measuring result for the centre microphone in three line source array rotation, while the microphone is in the windscreen and the windscreen is in the hight of the ear. The graph is a mean of 10 measurements in all three angles. The mean calculation is done in the time domain where all impulse responses are aligned with cross-correlation

As seen in Figure 8.10, the frequency response does not ether raise or fall markebly while the speaker is turned. The large depth between 2.0 kHz and 5.0 kHz comes from the frequency characteristic of the line source array as seen in Figure 7.3. The following Table 8.3 shows the single number SPL both non weighted and A-weighted.

Table 8.3: The table shows the measured $L_{eq,5}$ and $L_{A_{eq,5}}$ SPL for the center microphone

Speaker angle	0°	10°	20°
$L_{eq,5}$	69.72 dB SPL	68.79 dB SPL	68.77 dB SPL
$L_{A_{eq,5}}$	68.64 dB SPL	67.07 dB SPL	67.00 dB SPL

8.2 research of the problems

To be able to decide the last few details of the final measurement based on the test and data analysis performed in section 8.1, the frequency response of the designed windscreen is founded in free field condition while rotating and tilting. Secondly, the final windscreen hight is decided. In section 8.2.1, the frequency response of the windscreen is founded where the windscreen is rotated and tilted.

8.2.1 windscreen frequency response

This section aims to research the frequency response of the designed windscreen. It is observed in section 8.1.2 that the measurement with the original windscreen have a

boost between 1.0 kHz and 10 kHz compare to one measurement without the designed windscreens. Therefore it have to be founded if the windscreens by itself makes high SPL boost in that frequency range or if the differences is an effect of other sources. To ensure that the windscreens does not have such boost in the measured positions, the windscreens are measured in the anechoic chamber both with tilting and with rotation to research the effect of differences of the windscreens. The measurement is founded in Appendix M. It is observed in the measurement that the windscreens does not have a boost as observed in the measurement in section 8.1.2. The windscreens does have a very small boost of 2 dB SPL beneath 1.0 kHz and above 4.0 kHz but not in the same level as the measurement in section 8.1.2. Furthermore small forward tilting upto 9° only have an attenuation effect above 10 kHz due to plate reflection. A rotation of 30° ether to the left or to the right does attenuate in the frequency range of 1.0 kHz to 4.0 kHz. The frequency response of the windscreens is also measured while removing the foam wedge but in this configuration many and high reflection occur and is not an option. generally the designed windscreens only change the frequency response upto 2 dB SPL while the designed windscreens points with 0° to the line source array and is non tilted. The following measurement Figure 8.11 shows the different while the microphone only is equipped with the original modified windscreens and with the designed windscreens

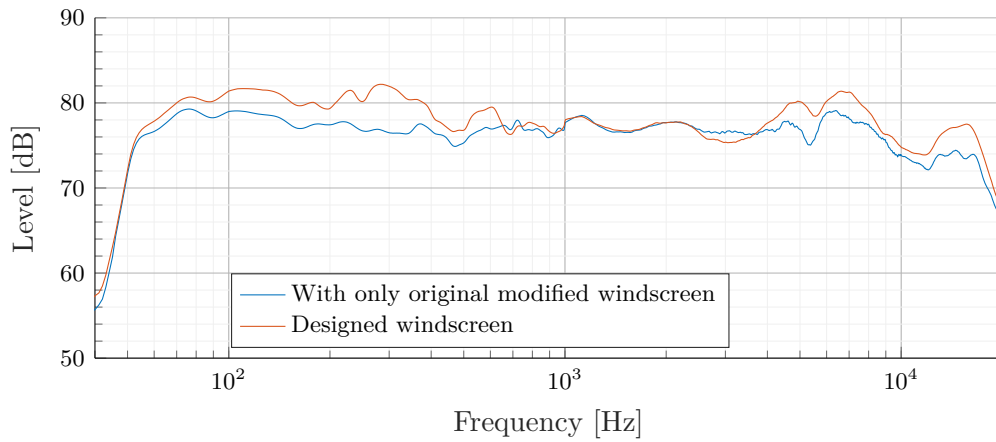


Figure 8.11: The graph shows frequency response of the speaker measured without windscreens and with the designed windscreens with no rotation and no tilting

8.3 Update to the final measurement

In the final measurement, the designed windscreens are used as it is designed. It is founded that the windscreens does not have any boost in the high frequency and small differences in position makes no difference. It is founded that high tilting and high rotation does have an effect of the frequency response and shall be avoided to the final

measurement. It is furthermore decided that the ground reflection shall be minimised as much as possible, such that it might be possible to compare between microphone. In the end the differences between the speaker characteristics with asymmetric makes it difficult to compare the side microphone since the high degree shows a boost in the higher frequency, as seen in Figure 7.3. Therefore the following points describe the update to the final measurement.

Update

The windscreen is positioned at the ground surface height and not in the ear height.

Argumentation

This requirement is made according to the founded ground reflection in section 8.1.1 and that the ground reflection shall be minimised such that the microphone might be able to be compared among each other. Secondly it is founded that the wind noise is up to 20 dB SPL lower near the ground section 7.3.10. finally it is assumed in ?? that the reflection is low while the area is full of audience which support that the ground reflection have to be minimised in the measuring point.

Update

The windscreen shall lay flat on the ground without tilting higher than 6° and point 0° to the line source array

Argumentation

This requirement is made according to the founded frequency response change in section 8.2.1 while the windscreen is tilted and rotated.

Update

The angle of the speaker shall be 3.5° downwards

Argumentation

This requirement is made according to the founded ground reflection in section 8.1.1, such that it is the lower speaker which have the direct sound path, and therefore ground reflection is minimised

Update

The speaker shall have symmetric directionality characteristics with beamwidth of 50°

Argumentation

This requirement is made according to the founded in the measuring result section 8.1.4, where the differences in directionality characteristics makes it difficult to compare since the characteristic have a SPL boost in the 55° directionality with an angle of 40°

Part III

Measurement

Chapter 9

Measurement

9.1 The measurement

The aim of this section is to show the measuring result from the final measurement, then try to find a relation between the wind direction, the wind speed and the angle of the line source array. The first section 9.2 deals with the wind noise in the measurement. The second section 9.3 covers the measurement done in crosswind. The third section 9.4 covers the measurement done in parallel wind. The third section ?? analyses the relation between the wind direction, the wind speed and the angle of the line source array.

9.2 Wind noise doing measurement

Doing the measurement, wind noise is present at the microphone. To ensure that the signal to wind noise level is high, a wind noise measurement is preformed as the first step. The following Figure 9.1 shows the wind noise at all three microphone position with a wind speed of

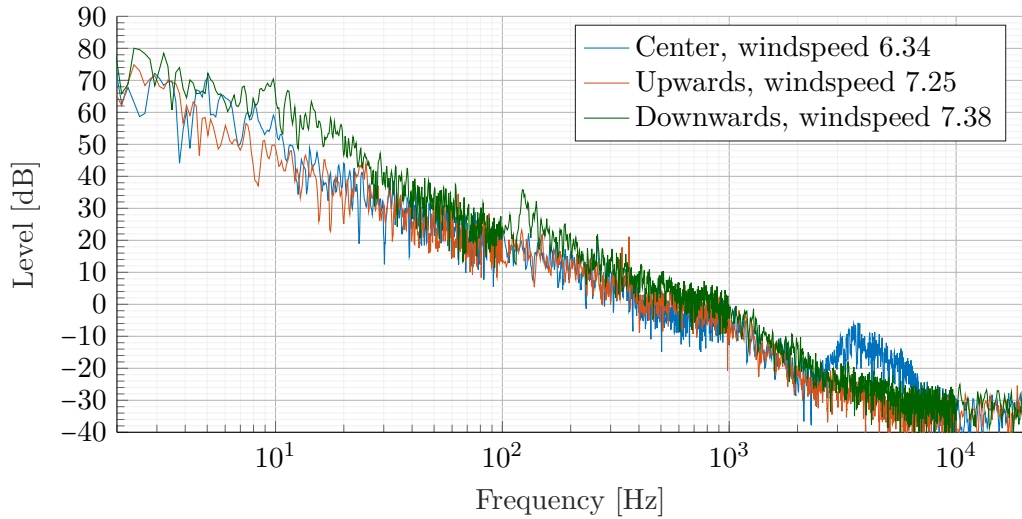


Figure 9.1: The graph shows the wind noise in all three measurement microphone at the exact position which is used for the crosswind measurement

The measurement Figure 9.1 shows that the wind noise is pink and therefore most present in the low frequency. To exclude the low frequency wind noise from the measurement, all impulse responses are filtered by a second order high pass filter at 40 Hz. The reason to filter the impulse response at 40 Hz is that the line source array by itself cannot go lower in frequency. The cut off is due to an internal filter in the Digital Signal Processor (DSP) settings of the speaker controller which cannot be turned off. Moreover, due to the way that the impulse response is calculated, wind noise is present along the impulse response. The impulse response is calculated according to ..., where the output signal is convoluted with the measured signal. Then if the noise signal component is present at another time than the signal, the wind noise in the impulse response is present as delayed signal. The following Figure 9.2 shows one impulse response measured during the measurement.

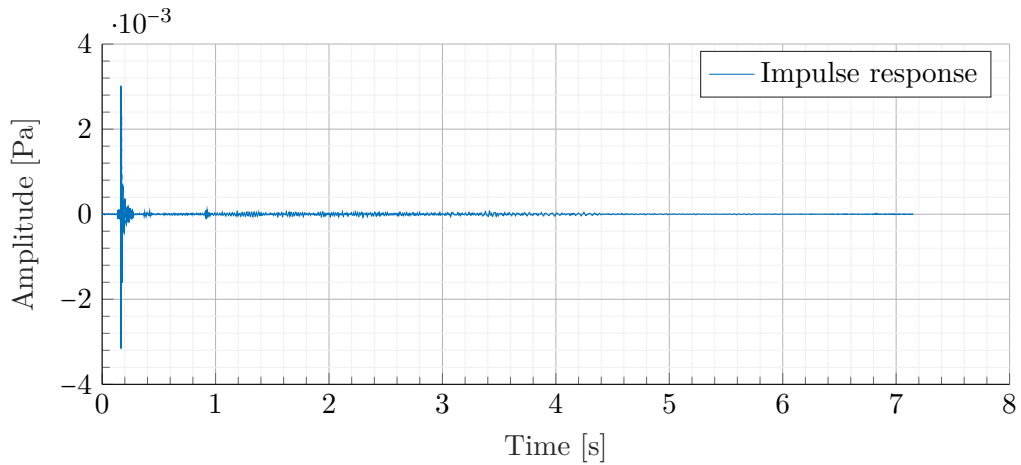


Figure 9.2: The graph shows one impulse response measurement of the upwards microphone where the line source array is non rotated

As seen in Figure 9.2, the noise is present along the impulse response time line. This wind noise is not interesting for the analysis and is therefore windowed by a custom made window.

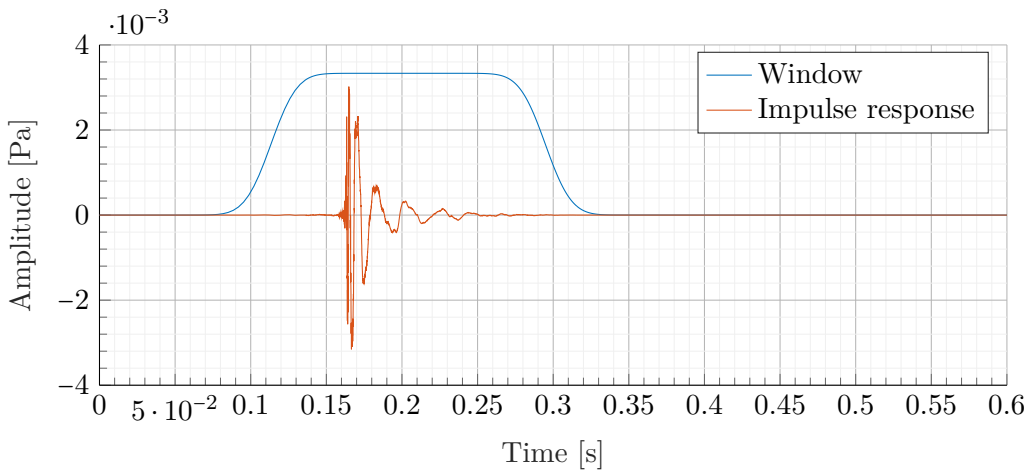


Figure 9.3: The graph shows one impulse response measurement of the upwards microphone where the line source array is non rotated

The window function in Figure 9.3 is amplitude wise scaled, such that both the impulse response and the window is visible. The window which is used in the calculation is non-scaled which means that the highest passing area have unity gain of 1 and not $3.3 \cdot 10^{-3}$. It is seen that the window passes the impulse response without change, while the noise is filtered.

9.3 Crosswind measurement

This section is presenting the final measurement which is done according to the crosswind measurement design description in chapter 7 including the update described in chapter 8. The measurement description is founded in ???. The measurement setup is nearly identical to the measurement in chapter 8 unless that the wind direction was turned 180° , the anemometer at the microphone position is placed 5 m to the right of the center microphone instead of 5 m to the back of the center microphone and the anemometer at the line source array is moved to the right side. The measurement setup is illustrated in Figure 9.4.

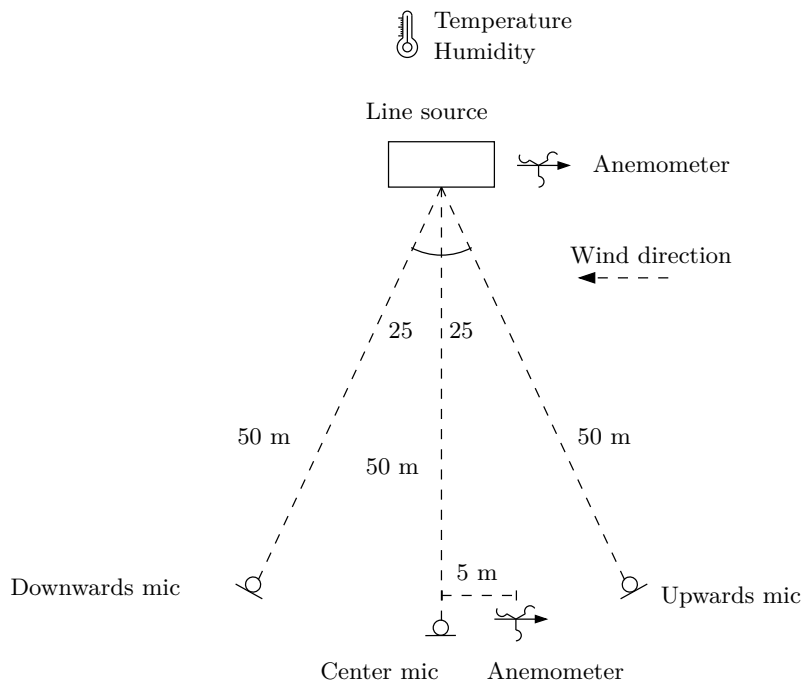


Figure 9.4: The figure shows the microphone position versus the position of the line source, while the array is 0° horizontal turned

while comparing the upwards refraction direction to the downwards direction, it is interesting to analyse at which frequency the refraction starts at the measured distance of 50 m and a wind speed between 5 m/s and 12 m/s. The refraction knowledge is used to generate a high pass filter such that it is only the part where refraction occurs which is compared during the data analysis. The frequency below the refraction is not interesting while comparing if turning the speaker makes more even SPL in the upwards direction compared to the downwards direction. While excluding this part in the one number SPL calculation the refraction part is more visible. To analyse where the refraction occurs, the frequency content is calculated for 3 measurements with high wind speed and compared. At the point where the upwards refraction,

downwards refraction and center microphone gets different is defined as the starting point of refraction at 50 m with the corresponding wind speed in this analysis. The following 3 ??, ?? and ?? shows the frequency response of all three microphone at three different measurement. All measurement is with 0° rotation of the speaker and is chosen since that have the most clear refraction separation and lowest refraction start point compare to the other measurement.

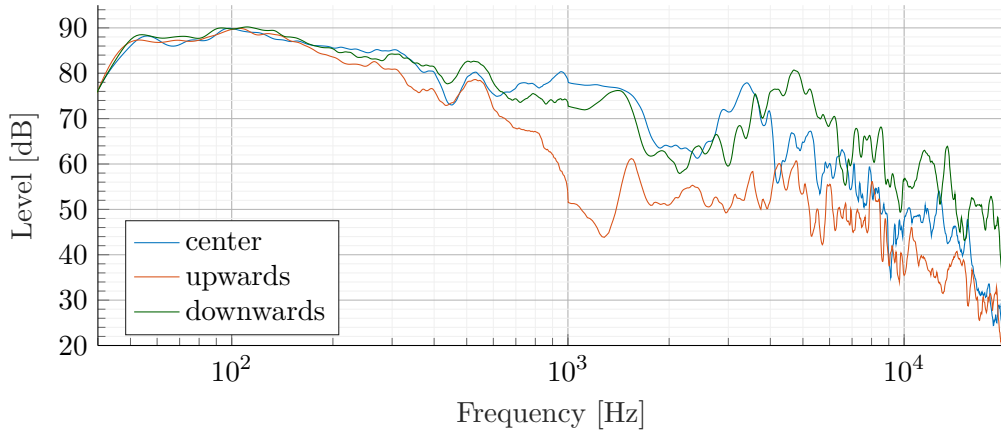


Figure 9.5: The graph shows

8.00 m/s

As seen in ... the refraction starts at 150 Hz, therefore all beneath 150 Hz have not interest for the further analysis.

The line source array in the test setup shown in Figure 9.4 is measured in four different angle where every angle above 0° is a rotation towards the upwards microphone. The resolution is with step of 10° with start as 0°, which is the angle shown in Figure 9.4 and up to 30°. The measurement is done at least 10 times for every angle and based on the amount of data, one graph for every angle will be shown where the rest of the result is shown in $L_{eq,5}$ octave separation above 150 Hz. The graph only includes the upwards measurement and the downwards measurement, the center microphone measurement is given in the $L_{eq,5}$ and in ?? to keep the plot visually manageable. The chosen graphs are measurements with high and identically with an average of approximately 8 m/s

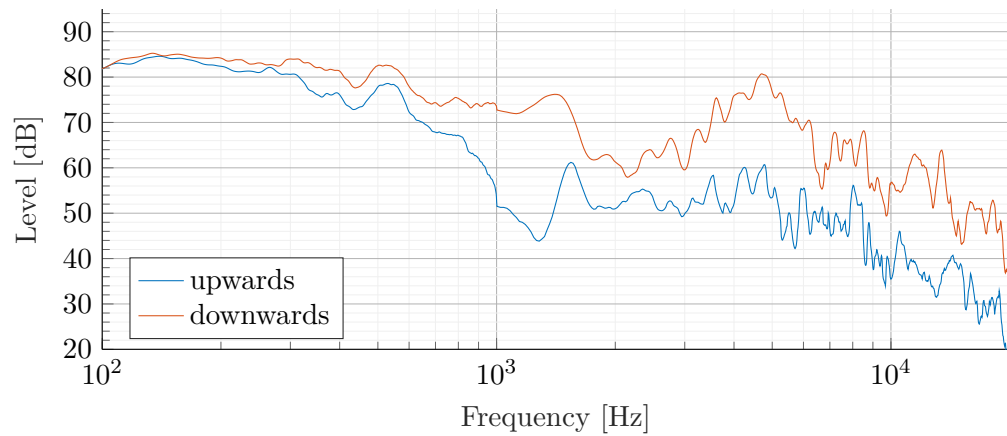


Figure 9.6: The graph shows 0°

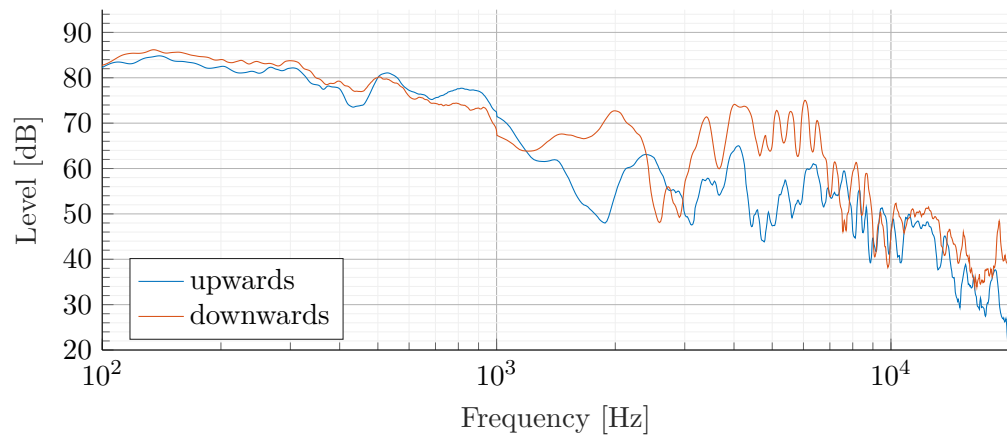
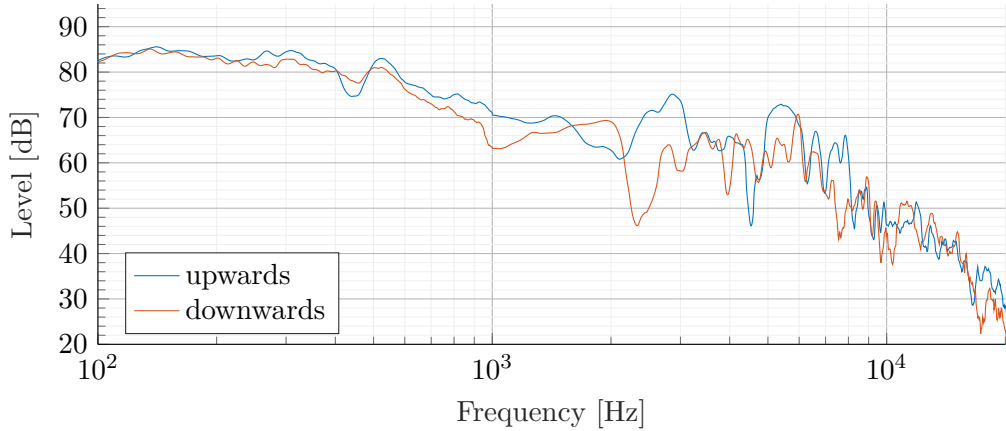
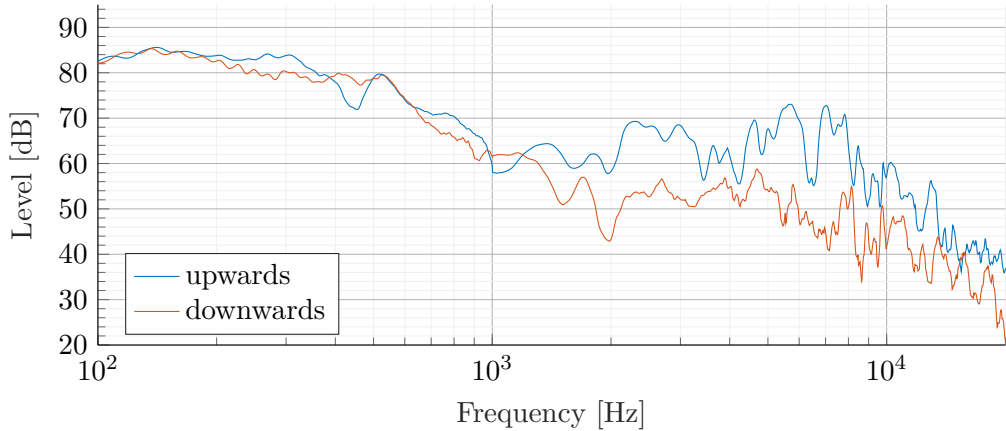


Figure 9.7: The graph shows 10°

**Figure 9.8:** The graph shows 20°**Figure 9.9:** The graph shows 30°

In the analysis the measurement is split into groups depending on the wind speed with a step of 1 m/s. Furthermore all measurement in the analysis is within $\pm 25^\circ$ from crosswind to the speaker. Crosswind to the speaker is defined as 90° and therefore 65° to 115° is the acceptable divience, all measurement deviate from this range is excluded. Moreover measurement with wind speed beneath 5 m/s is also excluded. From thoes limitation, the following Table 9.1 shows the amount of measurement for each wind speed step.

Table 9.1: The table shows the number of measurement which is between 65° to 115° in the given m/s interval

Speaker angle	0°	10°	20°	30°	Total
[5 m/s, 6 m/s[0	2	4	4	10
[6 m/s, 7 m/s[2	6	5	5	18
[7 m/s, 8 m/s[5	3	4	4	16
[8 m/s, 9 m/s[6	1	2	1	10
[9 m/s, 10 m/s[1	2	4	0	7
Total	14	14	19	14	61

It is seen in Table 9.1 that 62 measurement is available and the most fall within 6 m/s to 8 m/s.

Table 9.2: The table shows the measurement in octave band and within the interval [5 m/s, 6 m/s[with the given line source array angle

freq	1k			2k			4k			8k			16k		
Mic	U	C	D	U	C	D	U	C	D	U	C	D	U	C	D
10°															
m1	61	60	55	54	58	55	53	58	56	46	53	53	36	45	47
m13	54	50	55	48	51	50	55	65	57	50	61	54	42	49	47
avg	58	55	55	51	54	52	54	61	57	48	57	53	39	47	47
Dif	-2.50			1.41			3.10			5.28			7.93		
20°															
m4	64	60	56	64	58	56	57	61	59	50	57	58	40	46	46
m8	56	58	53	51	46	47	54	51	55	52	48	53	42	39	41
m15	52	52	54	50	48	49	59	51	48	56	53	45	43	44	39
m17	63	60	55	56	55	52	54	52	55	53	49	52	41	44	43
avg	59	58	55	55	52	51	56	54	54	52	52	52	42	43	42
Dif	-4.06			-4.39			-1.89			-0.29			0.39		
37°															
m3	50	53	46	44	41	37	49	47	42	48	42	39	42	33	33
m14	59	53	46	52	46	43	56	56	49	52	51	45	43	41	38
m15	56	55	48	50	43	39	56	48	44	55	43	39	47	33	32
m17	52	51	51	50	44	45	57	53	52	55	46	44	46	37	38
avg	54	53	48	49	44	41	55	51	47	53	46	42	45	36	35
Dif	-6.62			-7.95			-7.98			-10.93			-9.50		

Table 9.3: The table shows the measurement in octave band and within the interval [6 m/s, 7 m/s[with the given line source array angle

freq	1k			2k			4k			8k			16k		
Mic	U	C	D	U	C	D	U	C	D	U	C	D	U	C	D
0°															
m14	53	52	62	42	52	61	53	57	62	48	53	58	36	51	51
m17	49	59	59	40	52	56	49	54	59	45	53	56	35	44	46
avg	51	56	61	41	52	59	51	55	61	46	53	57	35	48	49
Dif	9.62			17.67			9.76			10.75			13.40		
10°															
m5	54	52	51	45	50	44	52	55	54	51	53	51	41	45	45
m6	56	60	58	47	64	64	53	67	66	51	66	65	43	54	53
m8	56	61	60	48	54	60	51	58	61	52	51	55	43	47	50
m9	55	60	57	54	52	49	52	54	53	49	57	51	40	51	43
m11	57	58	55	43	60	48	48	64	56	49	56	54	47	49	51
m12	63	59	58	58	60	58	56	66	63	51	61	59	44	48	48
avg	57	58	56	49	57	54	52	60	59	50	57	56	43	49	48
Dif	-0.39			4.82			6.77			5.38			5.44		
20°															
m2	66	58	57	53	53	51	56	55	58	52	48	50	45	41	42
m6	56	56	55	49	47	49	48	54	53	47	52	48	38	42	38
m9	53	52	54	47	49	48	54	52	54	51	45	51	49	36	38
m19	54	53	54	52	45	51	61	51	49	60	47	47	39	41	
m20	57	50	52	56	46	46	61	59	50	59	56	50	53	47	43
avg	55	54	55	51	48	49	56	54	53	54	50	49	46	41	40
Dif	-0.84			-2.32			-3.13			-4.67			-5.68		
37°															
m4	58	58	47	55	47	37	54	49	46	53	45	44	41	41	38
m6	48	47	48	50	43	44	55	55	46	58	48	40	50	41	33
m8	56	54	54	51	44	46	59	48	52	54	49	46	49	42	39
m13	56	53	47	54	45	42	61	50	45	59	47	38	49	37	32
m19	48	54	45	55	42	44	64	46	47	61	43	41	50	37	37
avg	53	53	48	53	44	43	59	50	47	57	46	42	48	39	36
Dif	-4.98			-10.22			-11.60			-14.99			-12.14		

Table 9.4: The table shows the measurement in octave band and within the interval [7 m/s, 8 m/s[with the given line source array angle

freq	1k			2k			4k			8k			16k		
Mic	U	C	D	U	C	D	U	C	D	U	C	D	U	C	D
0°															
m10	53	59	60	44	53	52	51	56	57	47	53	59	39	50	52
m15	53	60	58	39	59	51	46	67	56	44	64	57	37	51	47
m18	57	51	59	49	46	52	50	50	57	45	48	55	34	43	49
m20	47	47	58	42	48	55	47	55	58	46	54	56	39	47	49
m22	40	45	59	44	53	49	49	56	63	48	56	66	39	45	52
avg	50	53	59	44	52	52	49	57	58	46	55	59	38	47	50
Dif	8.74			8.19			9.24			12.66			12.39		
10°															
m2	46	59	54	42	56	51	46	65	62	45	56	59	38	51	50
m3	54	55	57	47	59	53	54	61	61	52	56	55	41	46	47
m15	58	59	56	47	56	56	49	56	61	48	60	59	40	53	45
avg	53	58	55	46	57	53	50	61	61	48	58	57	39	50	47
Dif	2.56			7.39			11.68			8.90			7.83		
20°															
m3	58	58	53	55	53	45	63	54	48	54	46	47	41	40	40
m5	53	60	56	45	51	53	53	55	56	53	54	51	41	44	41
m10	55	57	51	47	47	43	50	51	49	48	49	49	41	39	41
m14	53	55	52	47	49	48	55	53	48	51	53	42	41	48	36
avg	55	58	53	48	50	47	55	53	50	51	50	47	41	43	39
Dif	-1.96			-1.16			-4.91			-4.16			-1.52		
37°															
m9	51	51	49	54	46	43	58	53	46	60	48	43	49	38	38
m11	63	49	47	60	46	40	53	53	47	50	47	41	42	40	37
m12	54	58	55	54	48	41	58	52	49	58	46	44	48	37	41
m18	51	53	51	57	48	44	64	55	45	72	48	42	59	42	36
avg	55	53	50	56	47	44	58	53	47	60	47	43	49	39	38
Dif	-4.63			-12.21			-11.61			-17.48			-11.25		

Table 9.5: The table shows the measurement in octave band and within the interval [8 m/s, 9 m/s[with the given line source array angle

freq	1k			2k			4k			8k			16k		
Mic	U	C	D	U	C	D	U	C	D	U	C	D	U	C	D
0°															
m9	49	54	58	46	47	52	53	53	55	47	52	52	42	42	49
m11	52	58	60	49	58	54	50	62	59	44	67	54	35	56	49
m12	55	64	59	49	62	59	54	59	57	50	58	61	35	49	56
m13	49	56	61	42	51	63	45	54	63	45	53	58	34	50	50
m16	47	63	59	43	59	56	47	62	67	43	52	60	35	43	53
m19	48	57	57	38	58	51	47	62	59	45	58	62	34	53	52
avg	50	59	59	45	56	56	49	59	62	46	57	59	36	49	51
Dif	8.93			11.23			10.74			12.53			15.42		
10°															
m10	55	54	51	48	52	49	56	64	53	52	63	52	39	50	49
Dif	-3.77			1.11			-2.85			0.15			9.30		
20°															
m11	50	53	52	49	47	43	59	54	50	56	54	44	47	42	37
m16	57	59	54	57	57	54	60	56	55	57	50	53	43	44	41
avg	54	56	53	53	52	49	60	55	53	57	52	48	45	43	39
Dif	-0.18			-4.58			-6.80			-7.77			-5.76		
37°															
m7	53	56	48	59	48	46	65	55	50	61	52	45	47	46	35
Dif	-5.07			-13.06			-15.90			-15.60			-11.15		

Table 9.6: The table shows the measurement in octave band and within the interval [9 m/s, 10 m/s[with the given line source array angle

freq	1k			2k			4k			8k			16k		
Mic	U	C	D	U	C	D	U	C	D	U	C	D	U	C	D
0°															
m21	53	51	50	50	55	46	62	67	57	54	63	60	44	51	53
Dif	-2.57			-4.00			-5.10			5.98			8.46		
10°															
m4	44	54	54	47	51	52	47	52	55	41	50	54	37	40	49
m7	55	54	54	50	53	50	53	56	60	51	50	55	42	41	45
avg	49	54	54	48	52	51	50	54	57	46	50	55	40	41	47
Dif	4.94			3.10			7.69			8.55			7.64		
20°															
m1	53	57	49	50	51	49	54	51	55	53	50	48	44	45	40
m7	56	53	56	52	47	50	58	55	51	55	53	49	47	45	44
m12	55	57	55	53	49	59	59	58	56	55	53	51	43	43	42
m13	56	52	56	52	49	55	56	54	58	57	51	52	47	42	41
avg	55	55	54	52	49	53	57	54	55	55	52	50	45	44	42
Dif	-0.79			1.44			-1.93			-5.15			-3.73		

9.4 parallel wind measurement

This section is presenting the final measurement which is done according to the parallel wind measurement design description in chapter 7 including the update described in chapter 8. The measurement description is founded in ??.

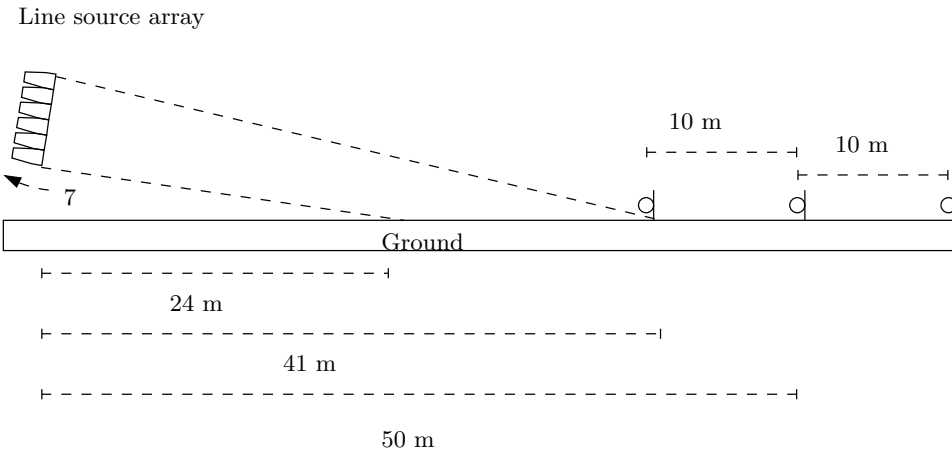


Figure 9.10: The figure shows the microphone position

The measurement setup is ... The measurement setup is illustrated in ??.

The line source array in the test setup shown in ?? is measured in three different tilt angle, one tilted 5° upwards, one with 0° tilting and one with 5° downwards tilting. The measurement is done at least 10 times for every angle and based on the amount of data, one graph for every angle will be shown where the rest of the result is shown in $L_{eq,5}$ octave separation above 150 Hz. The chosen graphs are measurement with high and identically with an average of approximately 8 m/s.

To be able to compare the result from each microphone, while the microphone is placed with different distance to the speaker the distance dependency of the microphones is removed. It is decided to norm the distance to 50 m which is the center microphone. Calculating the distance dependency loss is not as simple for a line source array as for a point source, since the SPL loss at doubling of distance depends on the wavelength, distance and height of the line source array section 2.1. Furthermore it also depends on the viscosity of the air section 2.2.1. To be able to remove this factor from the measurement, the frequency range for near field have to be founded. The graph in ?? shows the limiting distance where near field changes to far field for the used line source array. As seen ... All data measured under 5.799 99 kHz is propagating in far field at 40 m and above. This means that all data beneath 5.799 99 kHz is far-field calculation while normalising the frequency response. For the normalising from 40 m to 50 m all frequency above 7.2 kHz is propagating in near-field. Normalising from 60 m to 50 m all frequency above 8.7 kHz is propagating in near-field and frequency beneath 7.2 kHz radiate within far-field. The calculating rate is then as follows ??

	far-field	near-field
40 - 50	0 hz - 5800 hz	7200 hz - 20000 hz
60 - 40	0 hz - 7200 hz	8700 hz - 20000 hz

To calculate the far-field loss the following Equation 9.1 is used

$$L_2 = L_1 - \left| 20 \log_{10} \left(\frac{r_1}{r_2} \right) \right| \quad (9.1)$$

To calculate the near-field loss the following Equation 9.2 is used

$$L_2 = L_1 - \left| 10 \log_{10} \left(\frac{r_1}{r_2} \right) \right| \quad (9.2)$$

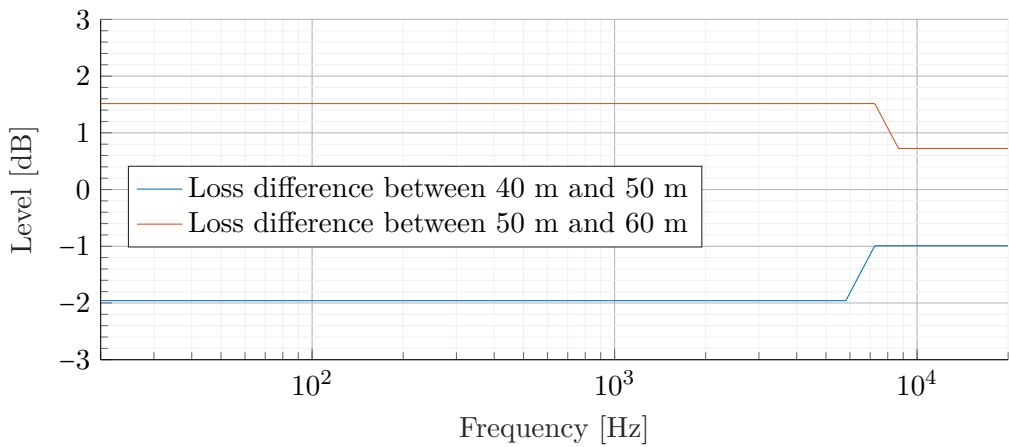


Figure 9.11: The graph shows

Absorption depending on humidity and temperature, to calculate the loss at 10 m of distances, the formula in standard [] is used with the measured data for every measurement. The atmospherical pressure is not measured doing the measurement, and therefore the reference 101.325 kPa is used as pressure. All 30 measurement is done with short time differences and therefore the temperature and humidity only change with fraction. One filter example is given in Figure 9.12 with 12 °C and 48 % humidity. The example temparature and humidity is from one of the measurement.

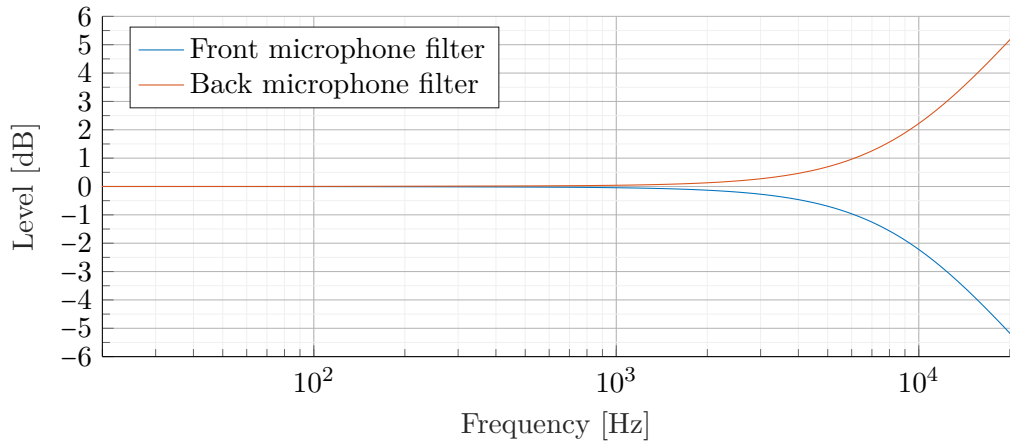


Figure 9.12: The graph shows

The frequency response in Figure 9.12 is used for compensate the viscosity in the air.

Both the filter in Figure 9.11 and Figure 9.12 is applied to the signal in frequency domain, while afterwards the result is transferred back to time domain for signal analysis.

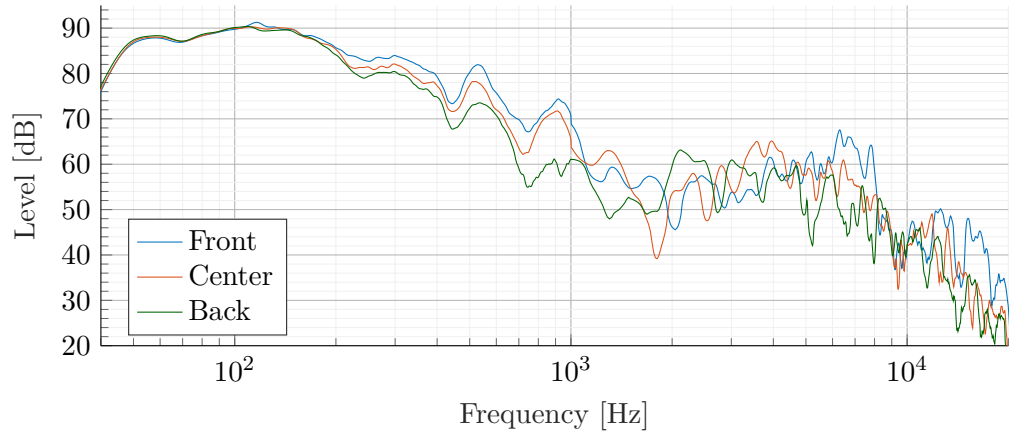


Figure 9.13: The graph shows 3°

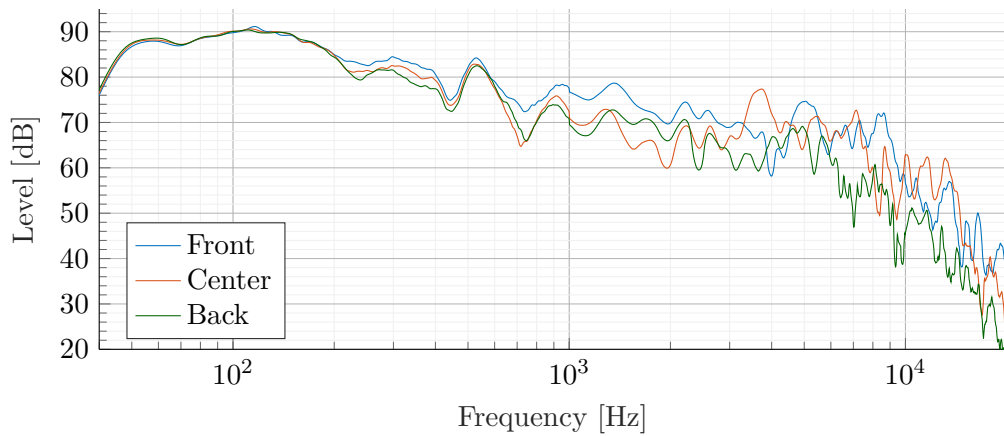


Figure 9.14: The graph shows 7°

Table 9.7: The table shows the number of measurement which is between -25° to 25° in the given m/s interval

Speaker angle	3°	7°	Total
$[5 \text{ m/s}, 7 \text{ m/s}[$	3	5	8

Table 9.8: The table shows the measurement in in octave band and within the interval [5 m/s, 7 m/s[with the given line source array angle

freq	132		327		570		1k		2k		4k		8k		16k	
deg	3°	7°	3°	7°	3°	7°	3°	7°	3°	7°	3°	7°	3°	7°	3°	7°
F																
m 1-3	66	66	64	64	63	63	57	59	53	55	54	54	58	53	48	45
m 5-4	67	66	65	63	64	61	60	57	58	54	57	55	58	58	51	49
m 6-6	66	66	63	63	60	62	54	62	44	61	60	61	54	61	42	51
m n-6	ND	66	ND	64	ND	64	ND	64	ND	68	ND	73	ND	68	ND	59
m n-10	ND	66	ND	64	ND	64	ND	61	ND	60	ND	63	ND	63	ND	49
avg	66	66	64	64	62	63	57	60	52	59	54	61	57	61	47	51
Dif	-0.6		-0.47		-0.55		3.31		7.57		7.59		4.25		3.39	
C																
m 1-3	66	66	63	63	61	61	57	58	53	61	58	67	53	58	45	44
m 5-4	67	65	64	62	60	60	59	58	56	58	59	62	56	55	44	44
m 6-6	66	66	62	62	57	61	52	57	44	56	52	63	48	60	38	52
m n-6	ND	65	ND	63	ND	62	ND	60	ND	62	ND	63	ND	60	ND	46
m n-10	ND	65	ND	63	ND	61	ND	57	ND	53	ND	57	ND	56	ND	51
avg	66	65	63	62	60	61	56	58	51	58	56	63	52	58	42	47
Dif	-0.64		-0.43		1.44		2.16		6.65		6.19		5.56		5.04	
B																
m1-3	66	66	63	63	61	61	60	58	58	58	55	63	55	54	43	42
m5-4	67	65	63	61	60	55	57	57	54	51	54	55	53	53	42	46
m6-6	65	65	61	61	54	60	44	57	47	57	48	57	44	52	35	41
m6	ND	65	ND	62	ND	60	ND	53	ND	46	ND	50	ND	52	ND	42
m10	ND	65	ND	63	ND	60	ND	53	ND	51	ND	62	ND	60	ND	49
avg	66	65	62	62	59	59	54	56	53	52	52	57	51	54	40	44
Dif	-0.79		-0.57		0.82		1.90		-0.66		4.66		3.73		3.76	

Part IV

Results

Chapter 10

Results

10.1 Result

This section aims to analyse the data obtained in the final measurement shown in chapter 9

10.2 Crosswind data analysis

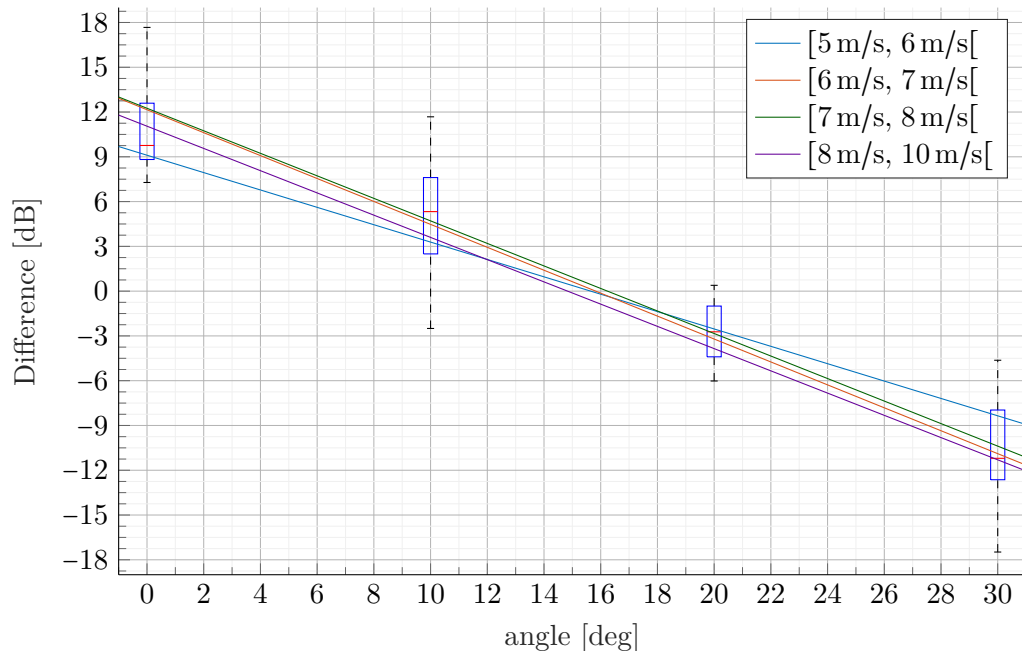


Figure 10.1: The graph shows

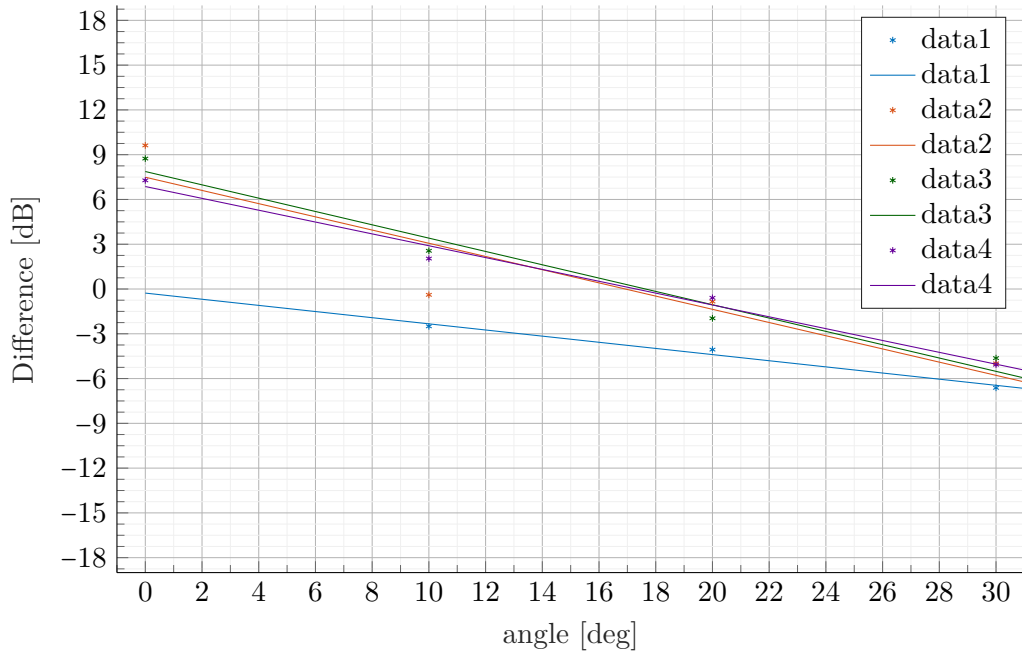


Figure 10.2: The graph shows [5 m/s, 5 m/s[

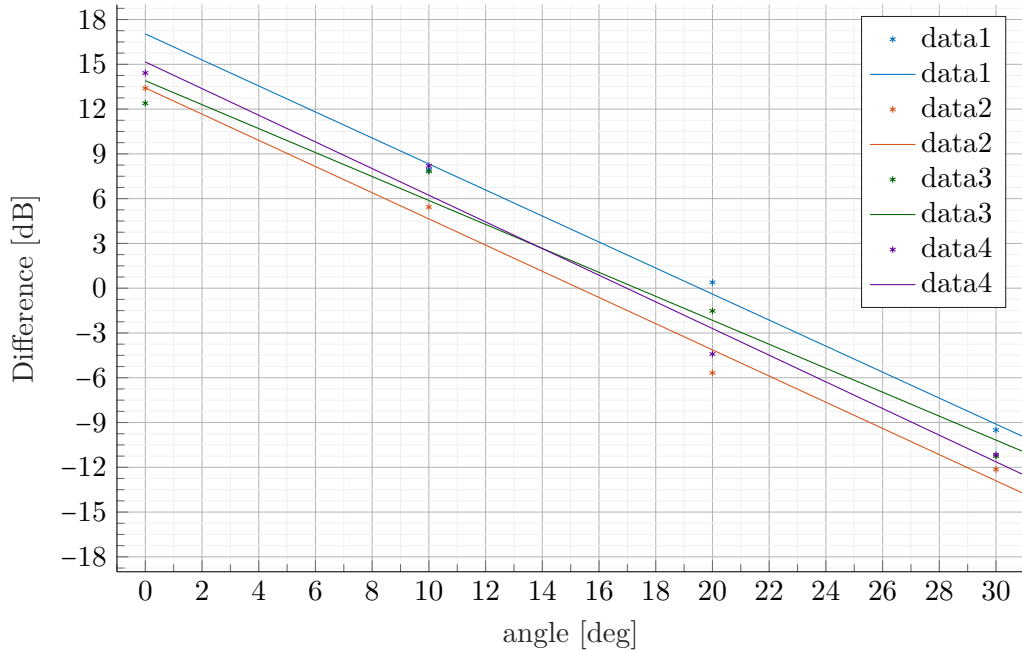


Figure 10.3: The graph shows [8 m/s, 10 m/s[

10.3 Parallel wind data analysis

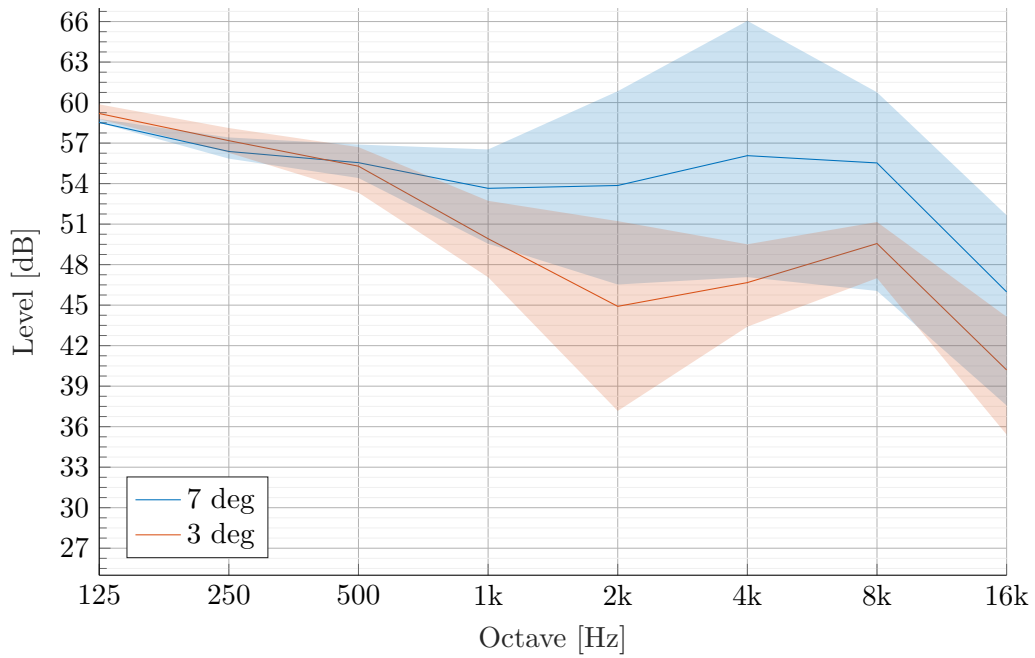


Figure 10.4: The graph shows the first microphone

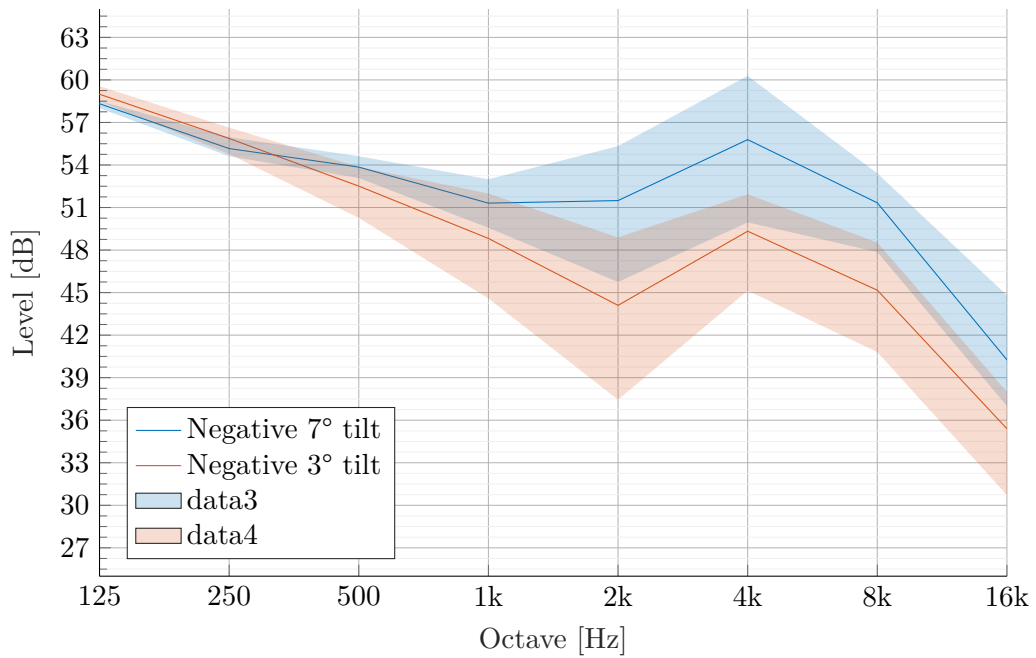


Figure 10.5: The graph shows the center microphone

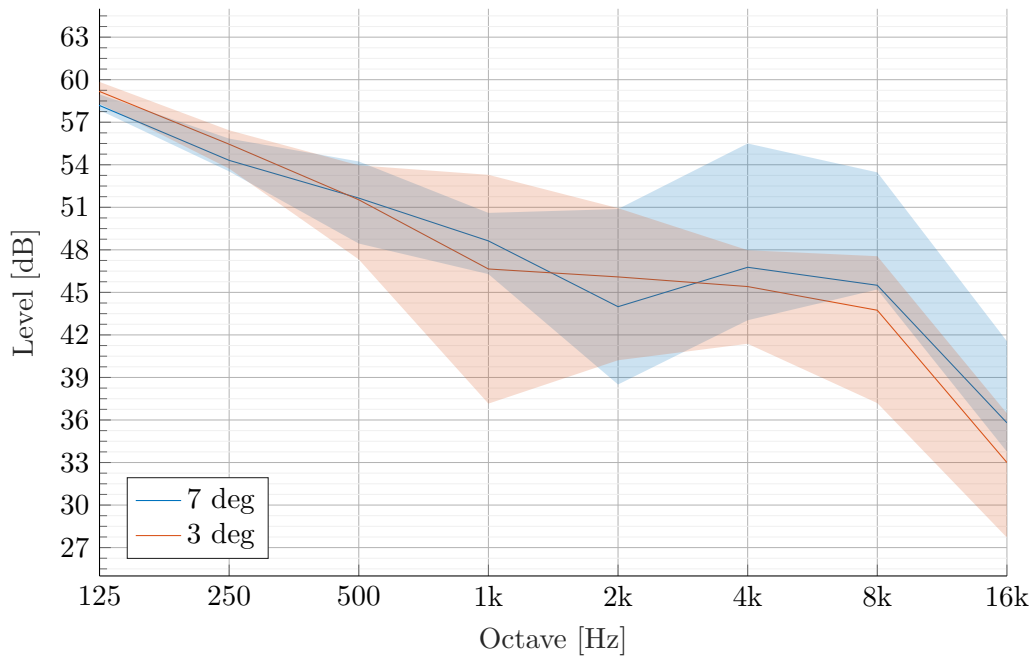


Figure 10.6: The graph shows the back microphone

Chapter 11

Discussion and conclusion

11.1 Conclusion

Part V

Appendix

Appendix A

cross wind effect on line source array

A measurement was made to measure the transfer function differences in two point in cross wind. The used speaker have a horizontal dispersion pattern of 100°.

Materials and setup

To measure the transfer function in a cross wind situation, the following materials are used:

Table A.1: Equipment list

Description	Model	Serial-no	AAU-no
PC	Macbook	W89242W966H	-
Audio interface	RME Fireface UCX	23811948	108230
Microphone	GRAS 26CC	78189	75583
Preamp	GRAS 40 AZ	100268	75551
Microphone	GRAS 26CC	78186	75582
Preamp	GRAS 40 AZ	100267	75550
dB technologies	DVA T4	-	-
Wind measurement tools	Drahtlose Wetterstation	-	2157-45
flying tools	-	-	-

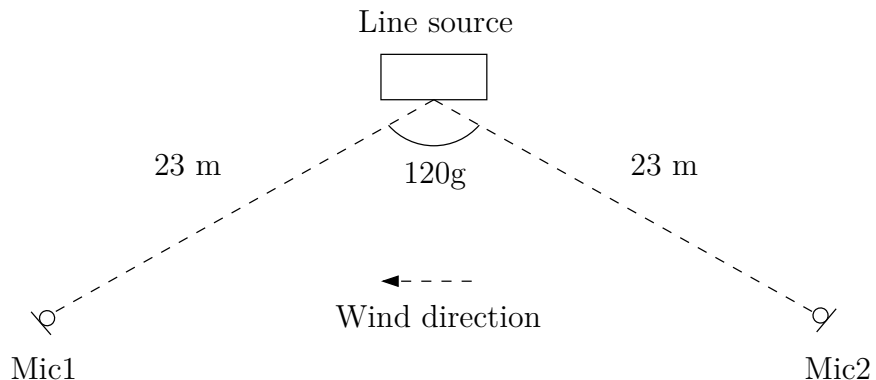


Figure A.1: The figure shows the microphone position versus the position of the line source



(a) The picture shows the speaker setup **(b)** The figure shows the wind direction

Figure A.2: The figures shows the measurement set up for Appendix A and ??

Test procedure

1. the microphone i calibrated.
2. The wind direction is measured.
3. The materials are set up as in Figure A.1 where the speaker is placed in cross wind direction, such that the frontal wave direction is orthogonal the the wind. The microphone and speaker is connected to the audio interface.
4. The speaker and microphone is placed 1.1 m above the ground
5. the wind direction goes from microphone 2 to microphone 1.
6. 10 sine sweep is performed with a length of 5 s each.
7. The impulse response is calculated and filtered with a 4th order highpass filter at 300 Hz to exclude wind noise.
8. The correlation is calculated for each impulse response to the first impulse response for time alignment [Gunness, 2001] of both microphone channel.

9. The mean impulse response is calculated for the 10 measurement of both microphone.
10. The transfer function is calculated with a 40 sample moving mean filter.
11. The measurement is repeated three times.
12. The measurement is repeated with an angle of 74° and a distance of 25 m for both microphone.

Measurement area

To be able to measure in a windy area, the football stadium at Fredrick Alfred Nobels Vej 7, 9220 Aalborg is used. The following Figure A.3 shows a picture of the area and the approximate position of the speaker and microphone.



Figure A.3: The picture illustrate the area, where the wind flow is measured

Results

The wind speed was 14 m/s for each measurement and the temperature was 5° . The humidity was not measured.

The following measurement shows the result for 120°

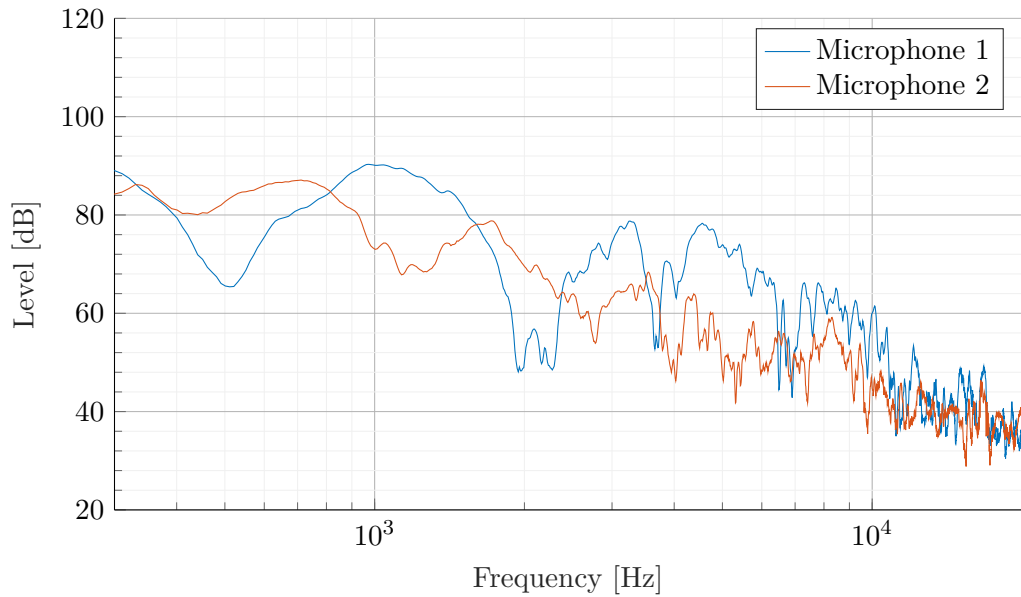


Figure A.4: The graph shows the first transfer function measurement. The $L_{eq,5}$ Sound Pressure Level (SPL) different between the microphones is 5.49 dB SPL (IR_6)

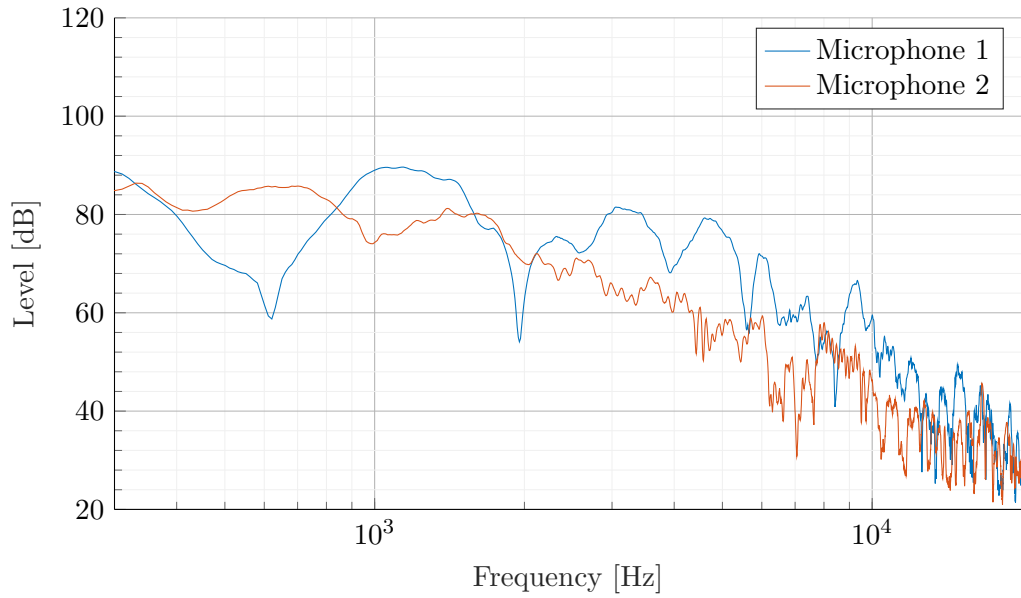


Figure A.5: The graph shows the second transfer function measurement. The $L_{eq,5}$ SPL different between the microphones is 4.40 dB SPL (IR_7)

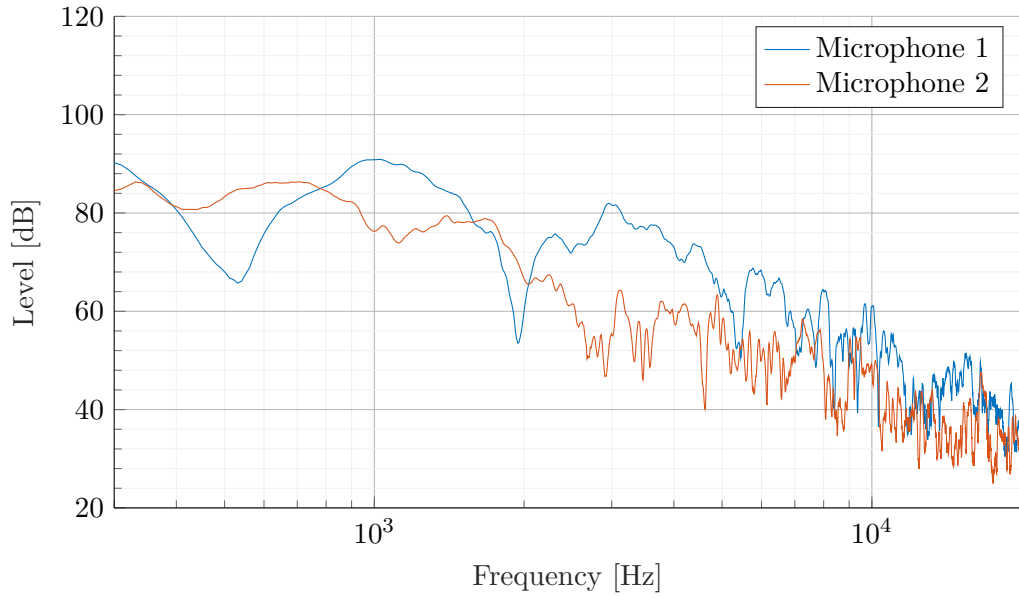


Figure A.6: The graph shows the third transfer function measurement. The $L_{eq,5}$ SPL different between the microphones is 4.23 dB SPL (IR_8)

On Figure A.4, Figure A.5 and Figure A.6 it is seen that the general pressure is higher for microphone 1. It is also seen that ground reflection effect is much higher on microphone 1 than microphone 2. This support the theory about upwards refraction of sound wave on microphone 2 and downwards refraction on microphone 1

The following measurement shows the result for 74°

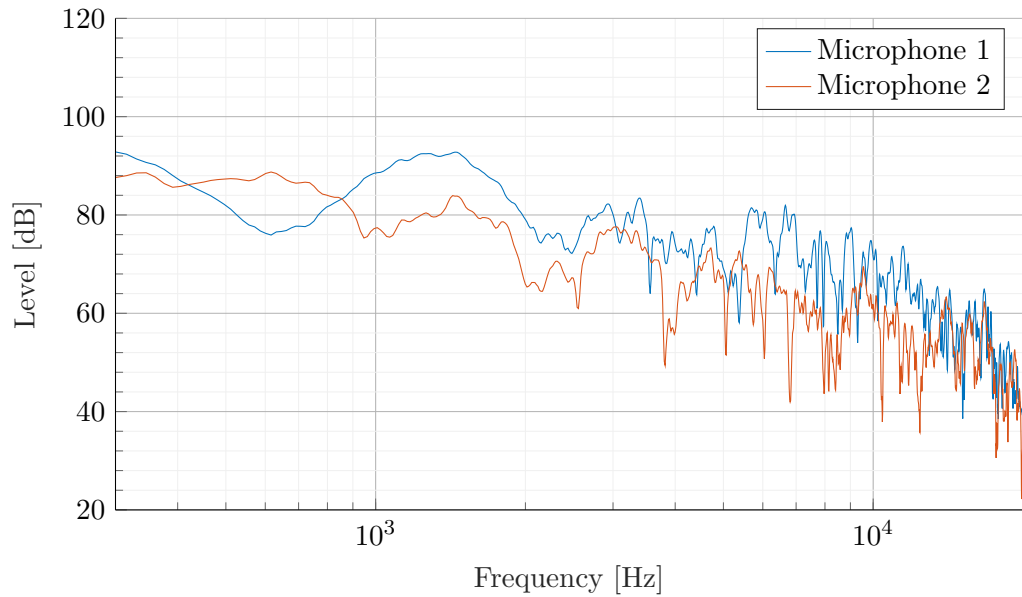


Figure A.7: The graph shows the first transfer function measurement. The $L_{eq,5}$ SPL different between the microphones is 4.41 dB SPL (IR_3)

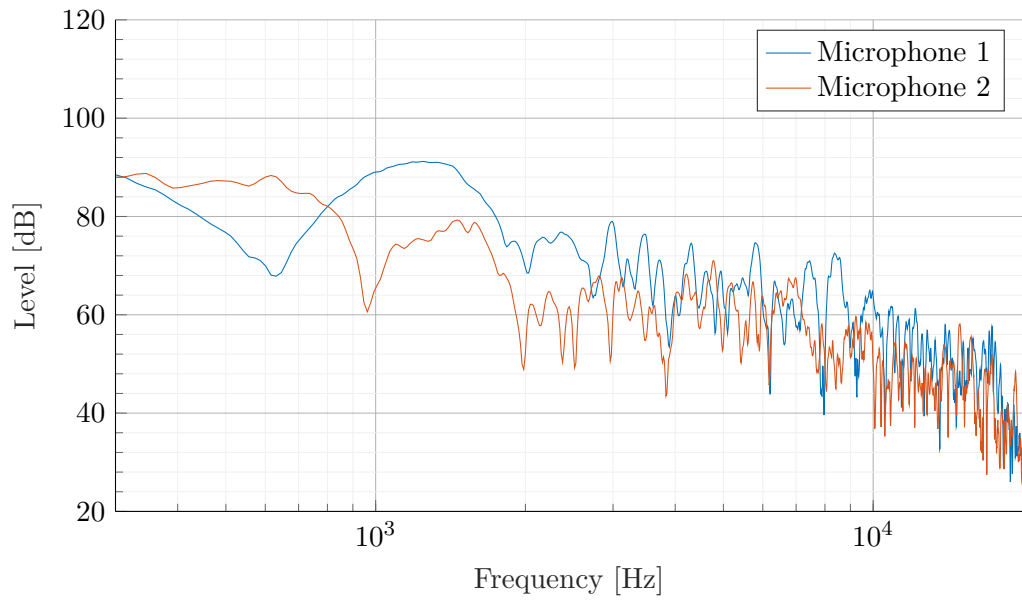


Figure A.8: The graph shows the second transfer function measurement. The $L_{eq,5}$ SPL different between the microphones is 4.81 dB SPL (IR_5)

On Figure A.7 and Figure A.8 it is seen that the general pressure is higher for microphone 1. It is also seen that ground reflection effect is much higher on microphone 1 than microphone 2. This support the theory about upwards refraction of sound wave on microphone 2 and downwards refraction on microphone 1

Summary

Appendix B

Design of windscreen

The idea of an additional wind screen is use the original windscreen to the microphone and then try to stop the wind in just at the microphone with a blocking surface. The surface shall therefore be able to lower the windspeed at the microphone and have as less reflection as possible. The original windscreen is kept on the microphone in the wind stop area to attenuate the wind noise that passes the blockage and attenuate the turbulence produced by the wind stopper.

The first two windscreen concept is very identical but just with difference size of material. The idea for the first windscreen is to seal the microphone with foam all around except at the frontal direction. The frontal direction include both 180° angle in the vertical direction and 90° in the horizontal direction. The reason to chose that high degree vertical opening is that no sound from ground reflection is effected and no sound from upwards is stopped by the foam. The reason to have a narrow horizontal opening is to be able to get sound inside the opening but still have a wind stopping effect. The following Figure B.1 illustrate both windscreen configuration one and windscreen configuration two, just with one size foam wedge.

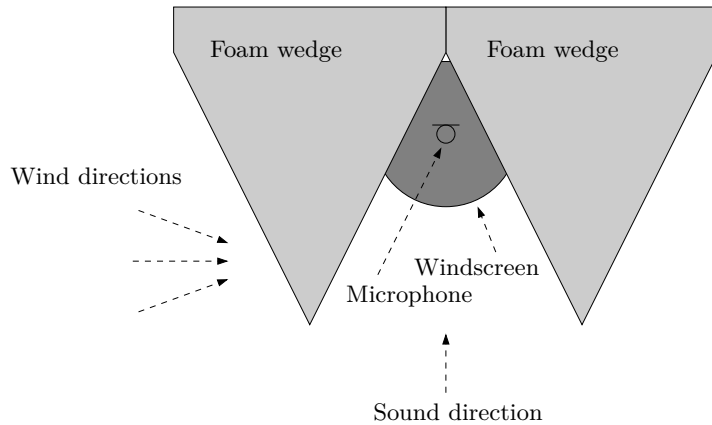


Figure B.1: The figure shows the foam wedge concept. The concept is covering over to different foam wedge, either two small or two large. The small concept is defined as windscreen configuration one, where the large concept is defined as windscreen configuration two.

The next concept build on the concept in Figure B.1 just with plan surfaces rockwool plates. The opening is also 180° angle in the vertical direction and 90° in the horizontal direction. The concept is defined as windscreen configuration three. The following Figure B.2 illustrate the concept.

The next concept build on minimizing the reflection from the additional windscreens by only placing the microphone close against one surface, which cover for the wind noise. The concept is defined as windscreen configuration four. The following Figure B.3 illustrate the concept.

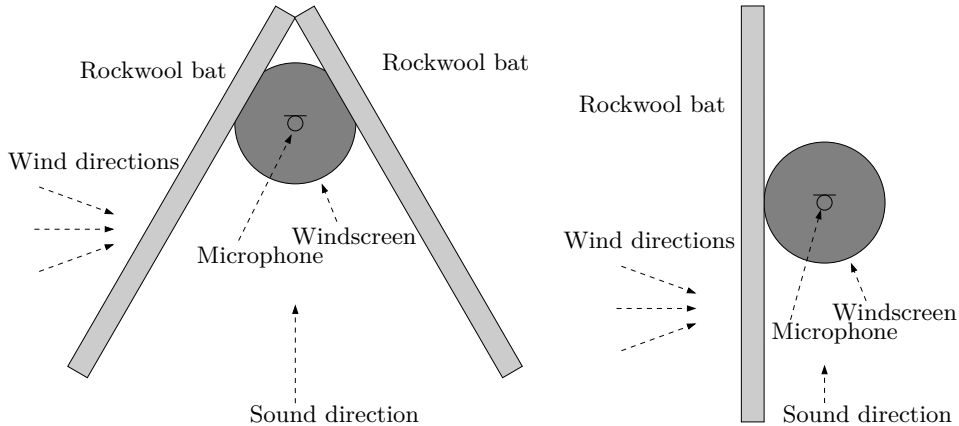


Figure B.2: The figure shows the rockwool concept. This concept is defined as windscreen configuration three.

Figure B.3: The figure shows the single rockwool concept. This concept is defined as windscreen configuration four.

Before the optimal windscreen configuration is founded, an optimality criteria is defined and a test is designed. The optimal criteria for the windscreens is as low wind noise as possible at the microphone position and low sound reflection. To find

the windscreen configuration which meets the criteria best, three tests are made on the windscreen configuration. First the wind speed attenuation of the windscreen configuration is measured to ensure that the windscreen configuration concept does have an effect on the wind speed. The measurement of the windspeed attenuation can be founded in ???. Secondly the frequency response of the windscreen have to be founded to ensure that the windscreen configuration does not have a large influence on the frequency measurement response of the speaker. To test this criteria, the frequency response of a speaker is measured in the anechoic chamber without any windscreen configuration and without the original windscreen. This measurement is compared with the frequency response of the speaker with the windscreen configuration. The measurement is founded in ???. Finally the wind noise is measured. To measure the wind noise two low speed and low noise fans are generating 2.5 m/s at the microphone position. The wind noise is measured without any windscreen configuration and the original windscreen and compared with the wind noise in the microphone position in the windscreen configuration. To ensure that the background noise is identically on the wind noise measurement with and without the windscreen configuration two microphones are used and recorded simultaneously. Both the time signal and the frequency content is analysed. The measurement is founded in ???. The result for all configuration is as following.

Configuration one is the one with the smallest foam wedge and size of the wedge is measured to have the worst wind attenuation. The wind attenuation shows that the wind speed is lowered from 8 m/s to 2 m/s. But the directional turbulence in the wind is more stable in this configuration compare the configuration three and above. The frequency response of the windscreen configuration is the one that have the lowest effect. At low frequency up to 100 Hz the windscreen does not effect the measurement. Frequency above the frequency response gets off with about 2 dB SPL compare with only the original windscreen. The measured wind noise attenuation is equal zero. In the measurement the wind noise is actually a bit worse compare to only the original windscreen. The attenuation is both approximately 10 dB SPL for both with only the original windscreen and the windscreen configuration in the low frequency below 10 Hz, but at some frequency the attenuation is lower than 5 dB SPL for the windscreen configuration. For frequency above 10 Hz the windscreen configuration have no effect.

Configuration two is the one with the largest foam wedge and size of the wedge is measured to have one of the best wind attenuation. The wind attenuation shows that the wind speed is lowered from 8 m/s to 1 m/s and have less peak in the wind speed compare to the windscreen with rockwool. The directional turbulence in the wind is more stable in this configuration compare the configuration three and above but little less stable compare to configuration one. The frequency response of the windscreen configuration have an amplification in the low frequency range from 80 Hz to 600 Hz of 2 dB SPL. From 1.0 kHz and above the frequency response is very similar compare

to only the original windscreen. At low frequency upto 80 Hz the windscreen does not effect the measurement much. The windscreen attenuate the wind noise 10 dB SPL more than only the original windscreen from 30 Hz and downwards to the measured limit at 2 Hz. The frequency range between 30 Hz and 600 Hz have the same attenuation as the original windscreen and the frequency above have further 10 dB SPL more attenuation than the original windscreen.

Configuration three is the one with two rockwool bat formed as an arrow and is measured to have wind attenuation between the small wedge and large wedge. The frequency response of the windscreen configuration is the worst. It alternate between ± 6 dB SPL. At the low frequency range from 80 Hz to 600 Hz the amplification goes from 2 dB SPL at 80 Hz to 6.2 dB SPL at 250 Hz and then back to 0 dB SPL at 700 Hz. At 1.0 kHz the attunuation is at 6 dB SPL and above the frequency response alternate around the frequency response of the original windscreen. The windscreen attenuate the wind noise 10 dB SPL more than only the original windscreen from 30 Hz and downwards to the measured limit at 2 Hz. The frequency range between 30 Hz and 600 Hz have the same attenuation as the original windscreen and the frequency above have further 5 dB SPL to 10 dB SPL more attenuation than the original windscreen. Based on that the frequency response and the wind wind noise attenuation is worse than configuration two, the configuration is excluded from the rest of the test and is not used.

Configuration four is the one with only one rockwool bat where the microphone is situated close to the side of the windscreen and is measured to have one of the best wind attenuation. The wind attenuation shows that the mean wind speed is lowered from 8 m/s to 1 m/s, but the directional and wind speed turbulence is less stabile compare to the configuration the windscreen with foam wedge. The wind speed turbulence circulate from 0 m/s to 2 m/s. The frequency response of the windscreen configuration is does not change more than ± 2 dB SPL in the low and high frequency range. At frequency from 600 Hz to 300 Hz the windscreen have an attenuation of 4 dB SPL. The noise attenuation is not measured in this configuration, since the mechanical stability is founded to be poor in wind speed above 5 m/s.

Based on the finding in Appendix B the final windscreen is designed. The design of the final windscreen combines configuration two to and and a updated version of configuration four where the stability problem is solved.

As the first test of the final windscreen solution an preliminary setup is done with the available material in acoustics lab. The preliminary setup is defined as windscreen configuration five. The following Figure B.4 illustrate the concept.

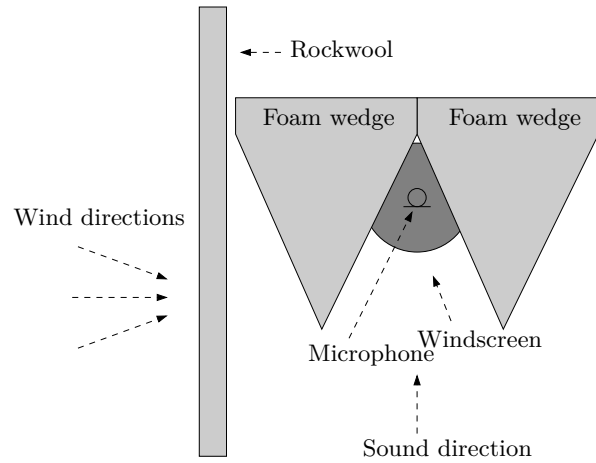


Figure B.4: The figure shows the single rockwool concept. This concept is defined as windscreen configuration five.

This configuration is measured to have more wind speed attenuation than this combination apart. The wind speed attenuation shows that the mean wind speed is lowered from 8 m/s to 0.8 m/s, but the directional turbulence is less stable compared to the configuration with only foam wedge. The frequency response of the windspeed configuration is as configuration two but with a closer fit to without windspeed in the high frequency.

Appendix C

Windscreen concept measurement

A measurement was made to measure the wind attenuation of difference windscreen configuration. All configuration include the GRAS AM0069 windscreen with an additionally wind stopper surface all around the microphone except of the frontal direction. The measurement is done as a preliminary test with low wind speed, to test the concept before a field test with wind speed as in the speaker measurement. The measurement is done to ensure that the measured wind does not overload the preamp of the microphone at the specified wind speed.

Materials and setup

To measure the wind attenuation of the windscreen configuration the following materials are used:

Table C.1: Equipment list

Description	Model	Serial-no	AAU-no
PC	Macbook	W89242W966H	-
Audio interface	RME Fireface UCX	23811948	108230
Microphone	GRAS 26CC	78189	75583
Preamp	GRAS 40 AZ	100268	75551
Microphone	GRAS 26CC	78186	75582
Preamp	GRAS 40 AZ	100267	75550

Table C.2: Equipment list

Description	Model	Serial-no	AAU-no
Fan	IMPEGA	-	-
Fan	IMPEGA	-	-
Windscreen	GRAS AM0069	-	-
Windscreen	GRAS AM0069	-	-
large foam wedge	-	-	-
Small foam wedge	-	-	-
Rockwool bat	-	-	-

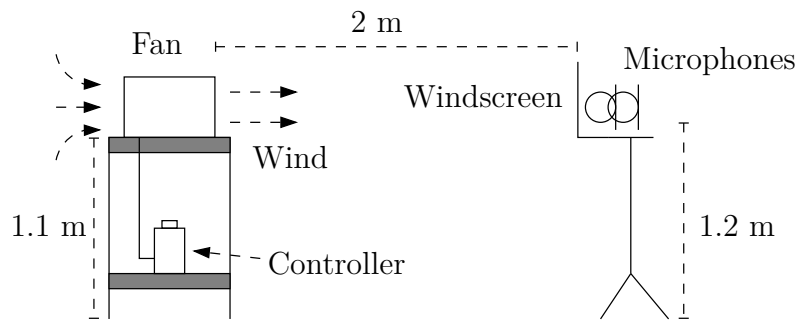


Figure C.1: The figure shows the measurement setup for the wind noise measurement in the microphone position and outside the windspeed. The two microphone seems to lay onto each other but it shall show that one is inside the windspeed and one is outside the windspeed



Figure C.2: The picture shows the measurement set up

Test procedure

1. The materials are set up as in Figure C.1 where the two microphone connected to the audio interface.

2. Both microphone is calibrated.
3. Both fan is activated
4. A 7s time signal is measured three times synchronise on both microphone.
5. The frequency content is calculated by **fft** on all six measured time signal.
6. The average of the frequency response for each microphone is calculated
7. The difference between the microphone is calculated to find the attenuation of the windscreens configuration
8. The procedure is done for all windscreens configuration and one where no additionally wind stopper is added around the microphone. This last configuration is defined as reference configuration.
9. A no wind measurement is measured the same way just without the fan activated and only with GRAS AM0069 windscreens in the end.
10. The wind speed is measured.

Measurement area

To be able to generate a controlled wind flow, the hall way in Fredrick Bajers vej 7B5, 9200 Aalborg is used. The following Figure C.3 shows a drawing of the area and the position of the fan and windscreens.

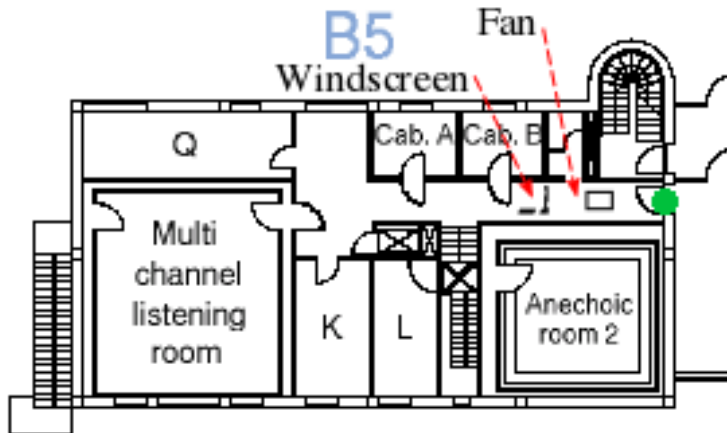


Figure C.3: The picture illustrate the area, where the wind flow is measured

Results

The following graphs shows the result of the measurement. The wind speed is measured to be 2.5 m/s.

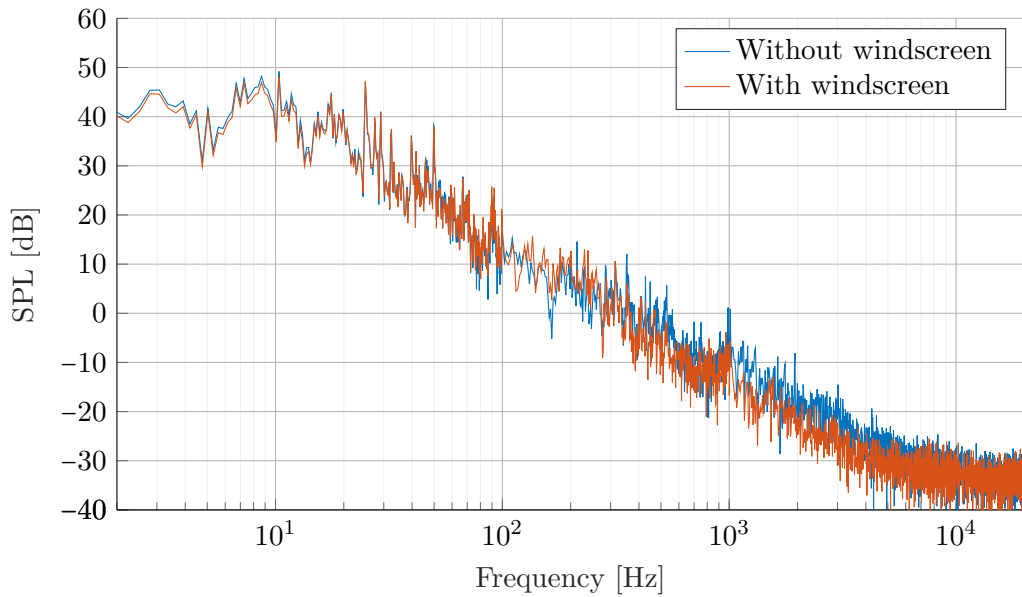


Figure C.4: The graph shows the frequency content without the fan activated

The Figure C.4 shows the frequency content in the measuring area without the fan activated for both microphone and the reference windscreen configuration.

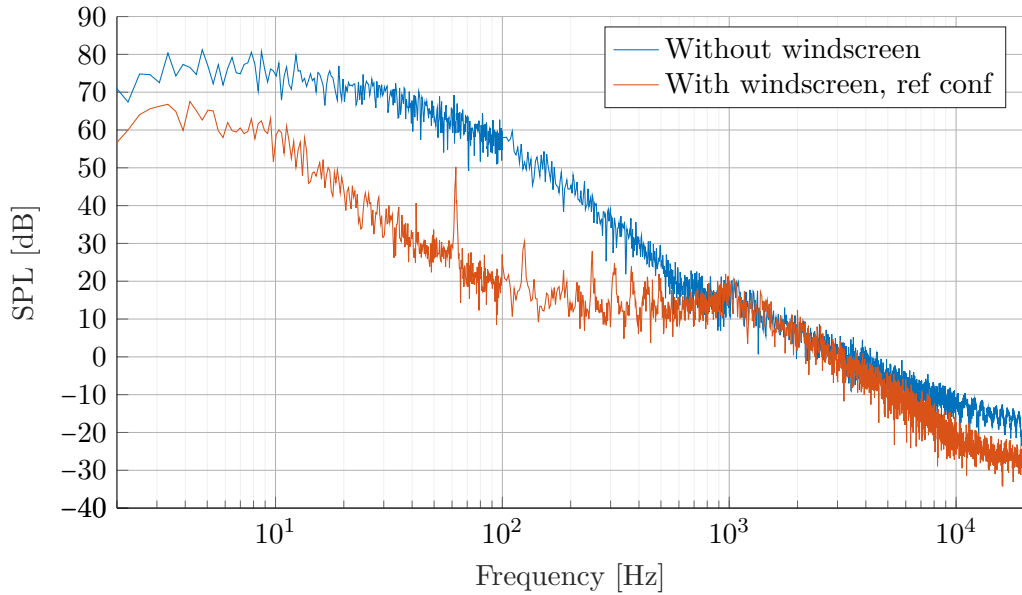


Figure C.5: The graph shows the frequency content with the fan activated

The Figure C.5 shows the frequency content in the measuring area with the fan activated for both microphone and the reference windscreens configuration. It is seen that the highest attenuation is at 900 Hz but the general attenuation is

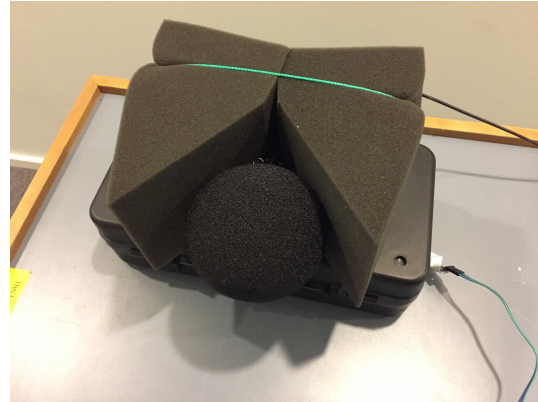


Figure C.6: The picture shows the microphone covered with windscreens and the Small foam wedge windscreen configuration. This configuration is defined as configuration one

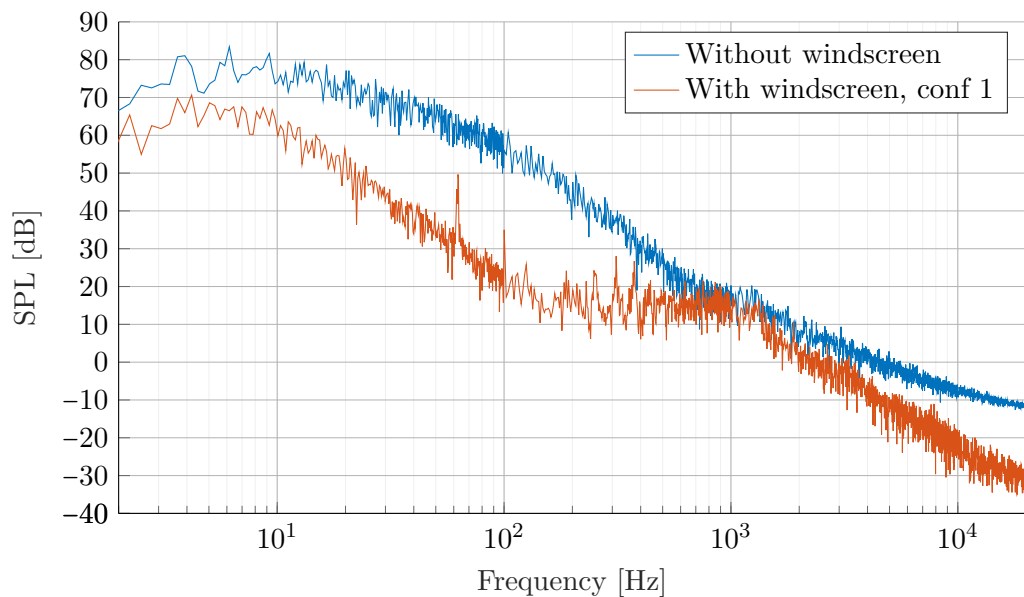


Figure C.7: The graph shows the frequency content of the measurement with configuration one

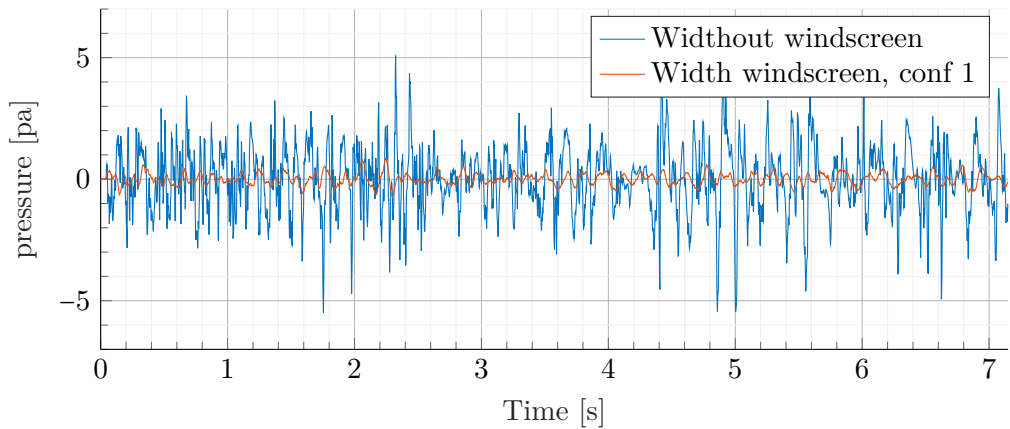


Figure C.8: The graph shows one of the time measurement with configuration one

The Figure C.7 and Figure C.8 shows the measurement with configuration one in frequency and time domain respectively. It can be seen that the general windscreen attenuation is not lowered compared to the reference windscreen measurement.

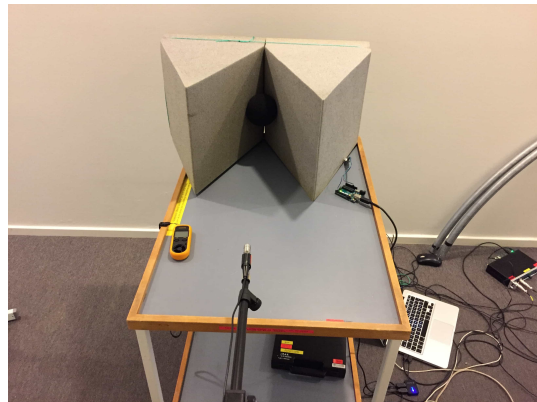


Figure C.9: The picture shows the microphone covered with windscreen and the large foam wedge windscreen. This configuration is defined as configuration two.

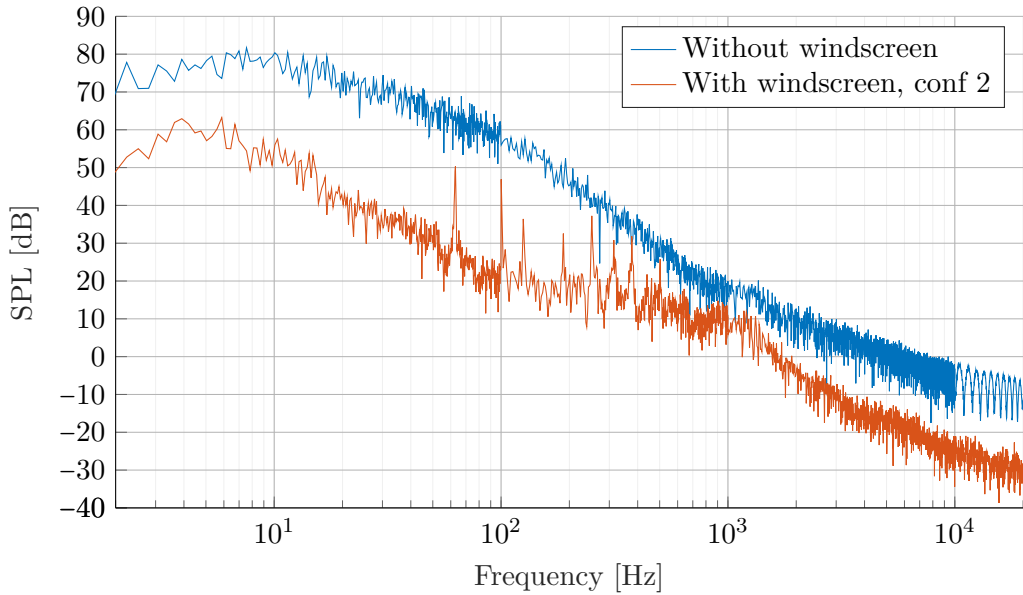


Figure C.10: The graph shows the frequency content of the measurement with configuration two

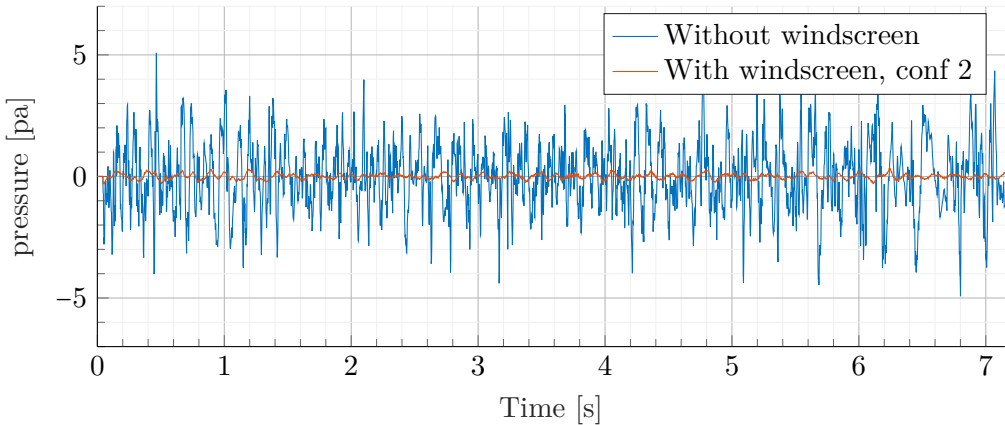


Figure C.11: The graph shows one of the time measurement with configuration two

The Figure C.10 and Figure C.11 shows the measurement with configuration two in frequency and time domain respectively. The measurement shows that the windscreens attenuation does have an effect compare to the reference windscreens measurement. The attenuation is nearly greater for all frequency especially in the low and high frequency range.

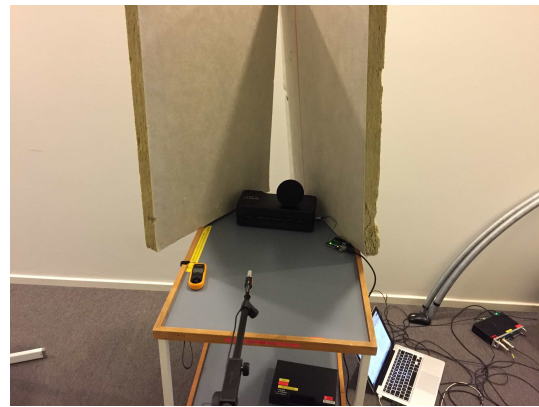


Figure C.12: The picture shows the microphone covered with windscreens and the rockwool wind stopper. This configuration is defined as configuration three.

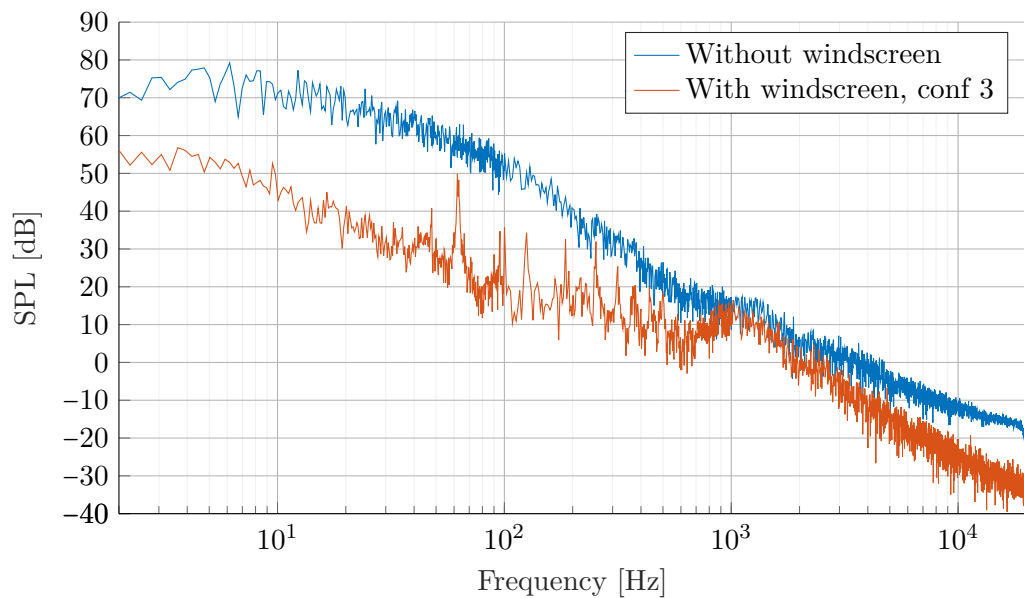


Figure C.13: The graph shows the frequency content of the measurement with configuration three

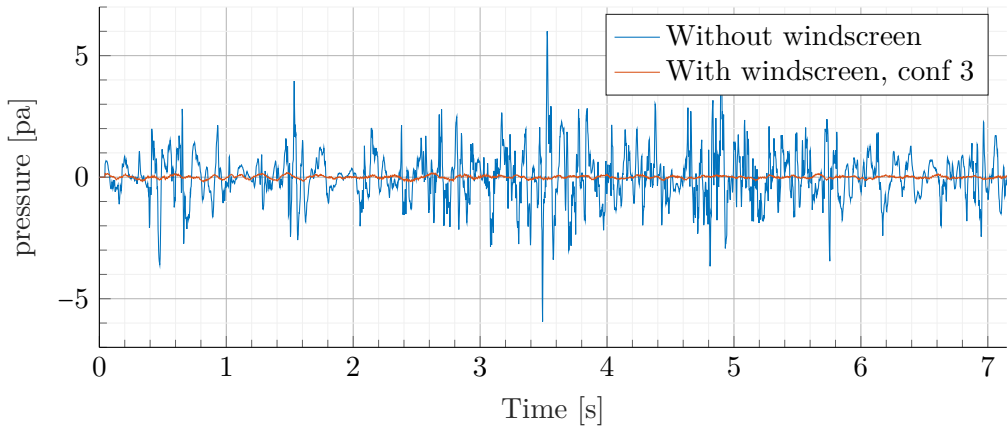


Figure C.14: The graph shows one of the time measurement with configuration three

The Figure C.13 and Figure C.14 shows the measurement with configuration three in frequency and time domain respectively. The measurement shows that the windscreen attenuation does have an effect compare to the reference windscreen measurement but the attenuation is not as good as in configuration two. There is better attenuation in the low frequency compare to the reference windscreen measurement but in the high frequency the attenuation is worse than the reference windscreen measurement, that might be due to reflection on the surface of the rockwool filter.

Summary

It is shown that the additionally wind stopper hypotheses does attenuate the wind noise at a wind speed of 2.5 m/s

Appendix D

Windscreen attenuation measurement

A measurement was made to measure the frequency attenuation of difference windscreen configuration. All configuration include the GRAS AM0069 windscreen with an additionally wind stopper surface all around the microphone except of the frontal direction. The measurement is done in the anechoic chamber. The measurement is done to analyse the effect of the windscreen in the frequency domain to ensure that the chosen windscreen do not add to much reflect to the measurement. The optimal criteria is therefore as low difference as possible.

Materials and setup

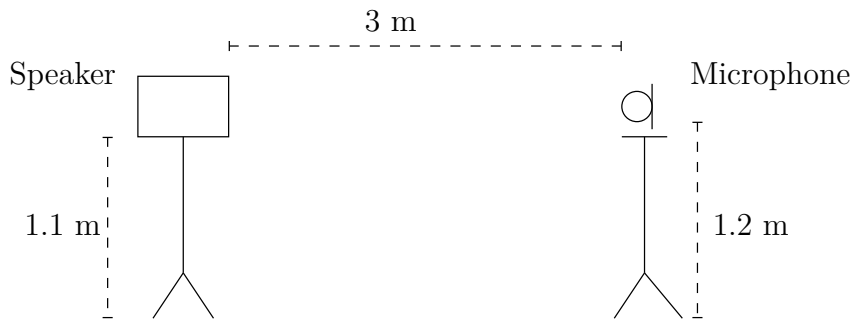
To measure the frequency response of the windscreen configuration the following materials are used:

Table D.1: Equipment list

Description	Model	Serial-no	AAU-no
PC	Macbook	W89242W966H	-
Audio interface	RME Fireface UCX	23811948	108230
Microphone	GRAS 26CC	78189	75583
Preamp	GRAS 40 AZ	100268	75551
Windscreen	GRAS AM0069	-	-
large foam wedge	-	-	-
Small foam wedge	-	-	-
Rockwool bat	-	-	-

Table D.2: Equipment list

Description	Model	Serial-no	AAU-no
Speaker stand	-	-	-
Speaker stand	-	-	-
Speaker	Dynaudio	03508438	1441-0

**Figure D.1:** The figure shows the measurement setup in the anechoic chamber

Test procedure

1. The materials are set up as in Figure D.1 where the microphone is connected to the audio interface.
2. The microphone is calibrated
3. The speaker is placed 3 m from the microphone and pointing in the direction of the microphone.
4. The windscreens configuration is placed such that the microphone have approximately the same position as without the windscreens.
5. The transfer function is measured
6. The procedure is started over until all windscreens are measured.
7. The transfer function is calculated and plotted versus the transfer function without windscreens MATLAB®.
8. The difference between the transfer function with and without windscreens is calculated and plotted in MATLAB®.

Measurement area

To be able to measure the windscreens frequency response, the anechoic chamber in Fredrick Bajers vej 7B4, 9220 Aalborg is used. The following Figure D.2 shows a drawing of the area and the position of the fan and windscreens.

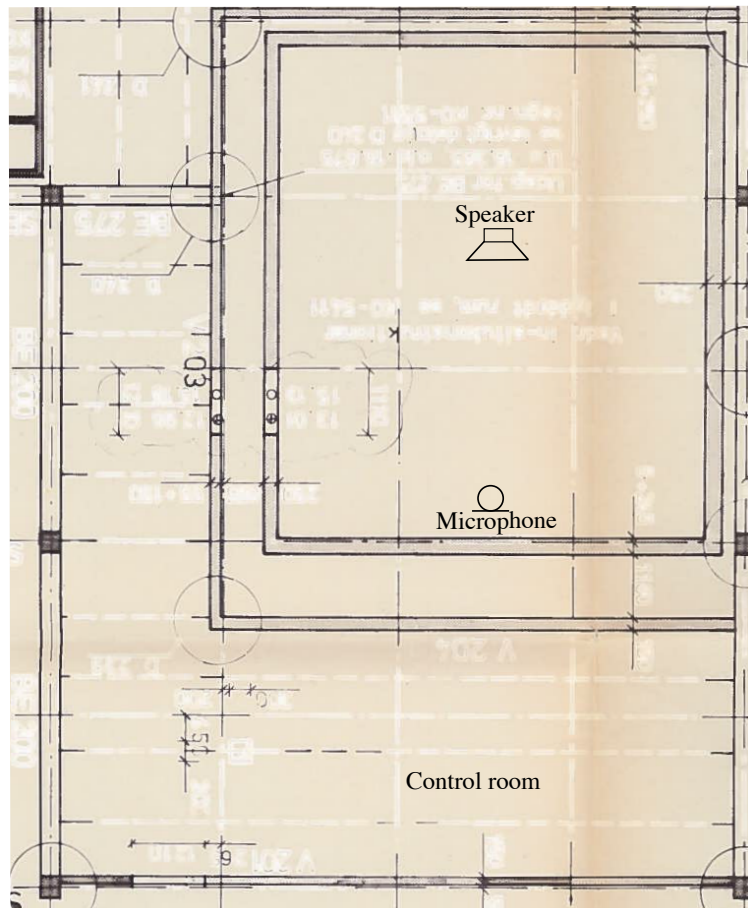


Figure D.2: The picture illustrate the area, where the wind flow is measured

Results

The following Figure D.3 shows the speaker.

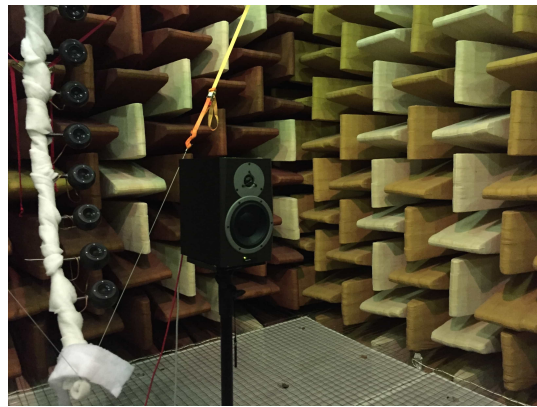


Figure D.3: The picture shows the used speaker

The following graphs shows the result of the measurement.



Figure D.4: The picture shows the measurement microphone with the original windscreen

The measurement shown in Figure D.5 shows frequency response of the speaker with and without the windscreens. The Figure D.4 shows the microphone position with the windscreens. The position is not changed for the measurement without windscreens.

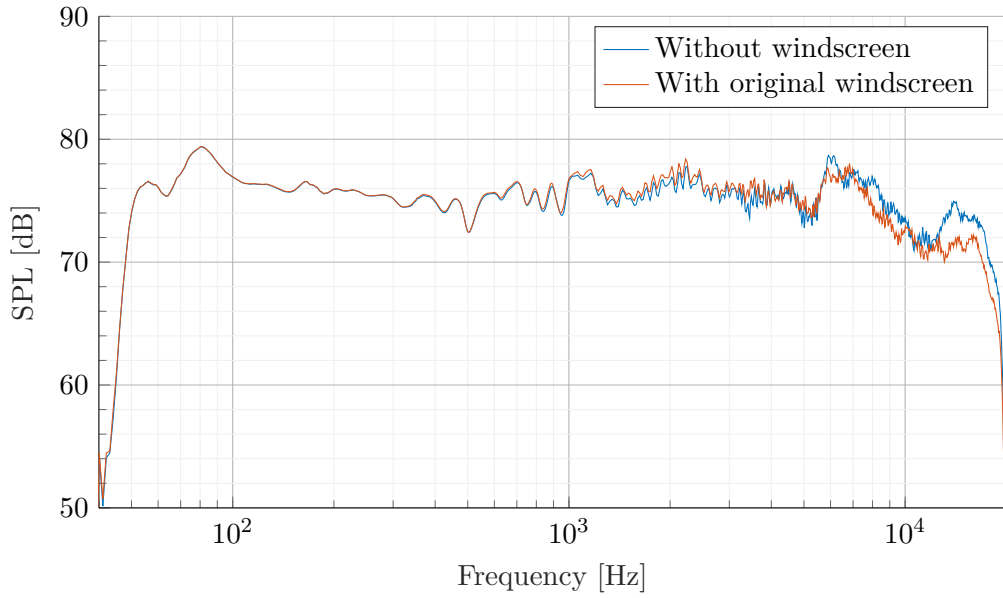


Figure D.5: The graph shows frequency response of the speaker measured without windscreen and with the original windscreen

The measurement shown in Figure D.6 shows the difference SPL between the measurement with and without original windscreen.

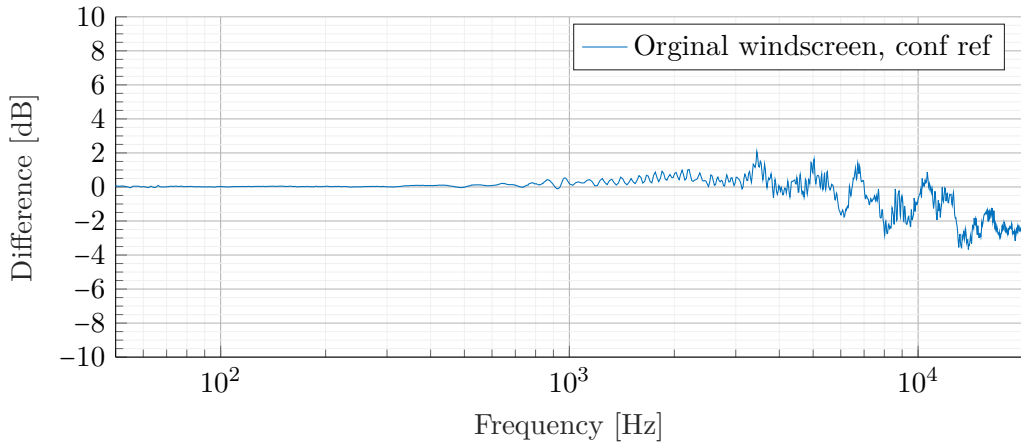


Figure D.6: The graph shows frequency response of the windscreen, where the frequency characteristic for the speaker is out calculated.



Figure D.7: The picture shows the measurement microphone with the large foam wedge configuration two

The measurement shown in Figure D.8 shows frequency response of the speaker without the windscreens and with the windscreens configuration one. The Figure D.7 shows the measured set up.

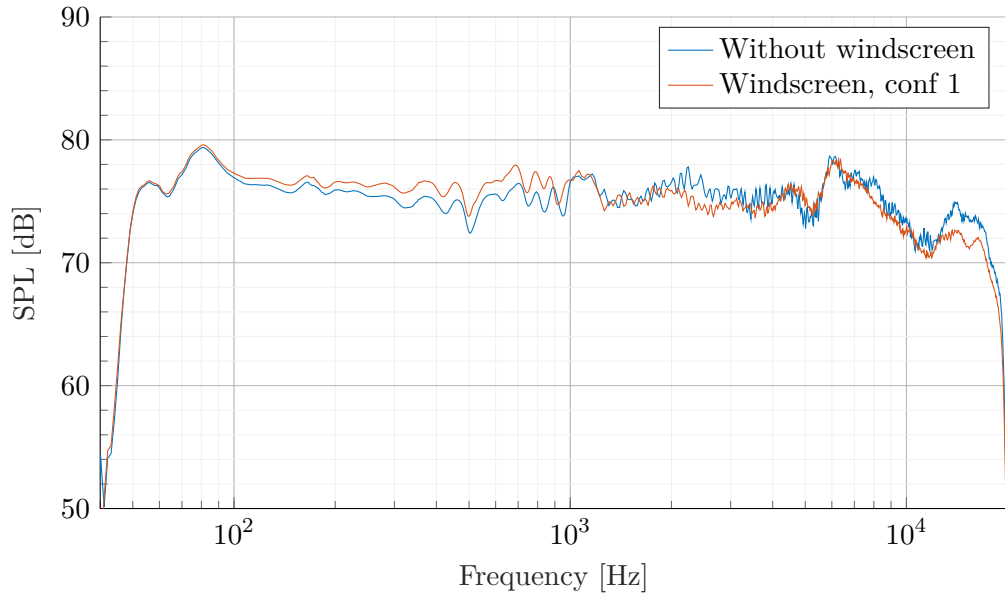


Figure D.8: The graph shows frequency response of the speaker measured without windscreens and with windscreens configuration one

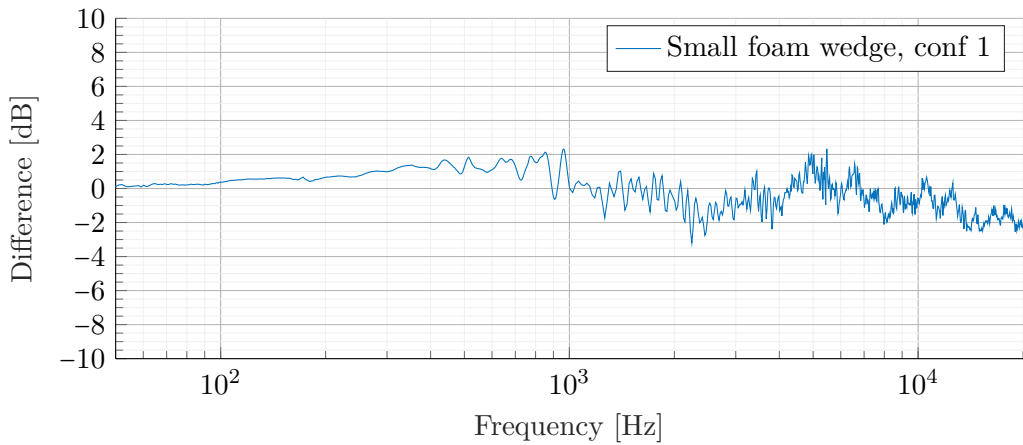


Figure D.9: The graph shows frequency response of the windscreen, where the frequency characteristic for the speaker is out calculated.

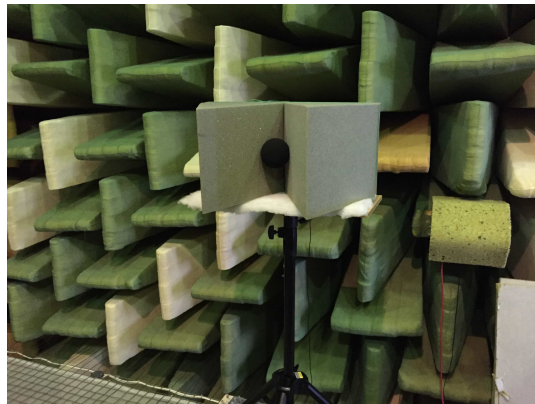


Figure D.10: The picture shows the measurement microphone with the large foam wedge configuration two

The measurement shown in Figure D.11 shows frequency response of the speaker without the windscreens and with the windscreens configuration two. The Figure D.10 shows the measured set up.

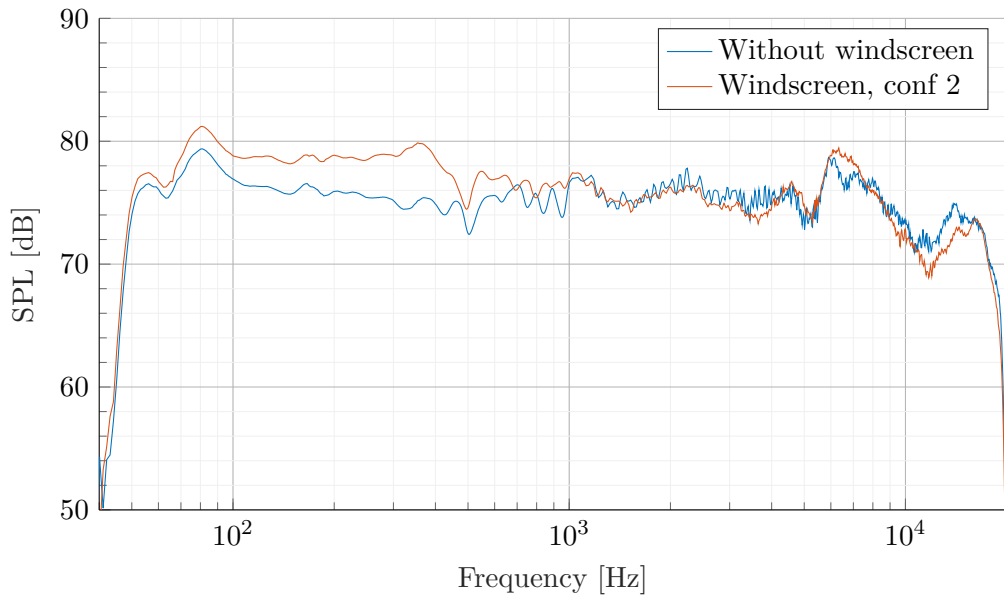


Figure D.11: The graph shows frequency response of the speaker measured without windscreen and with windscreen configuration two

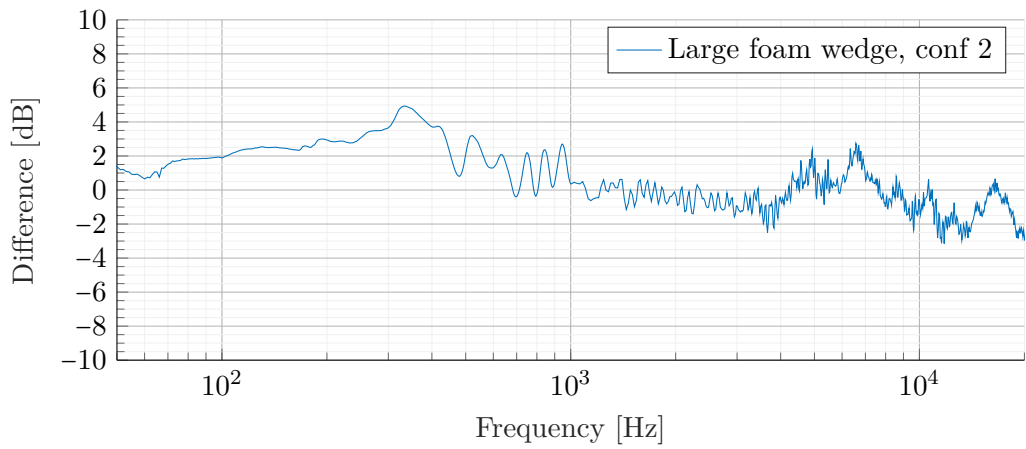


Figure D.12: The graph shows frequency response of the windscreen, where the frequency characteristic for the speaker is out calculated.

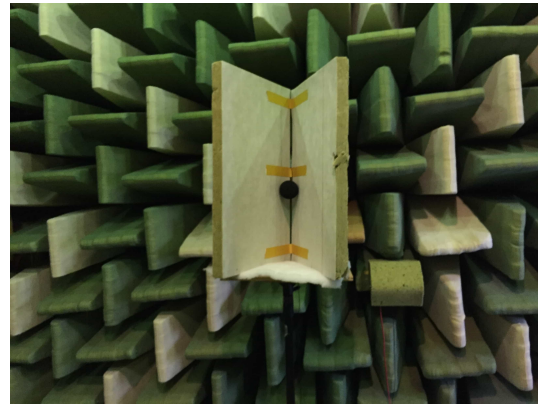


Figure D.13: The picture shows the measurement microphone with the rockwool bat configuration three

The measurement shown in Figure D.14 shows frequency response of the speaker without the windscreens and with the windscreens configuration three. The Figure D.13 shows the measured set up. In this measurement both the speaker and the microphone is lifted 20 cm

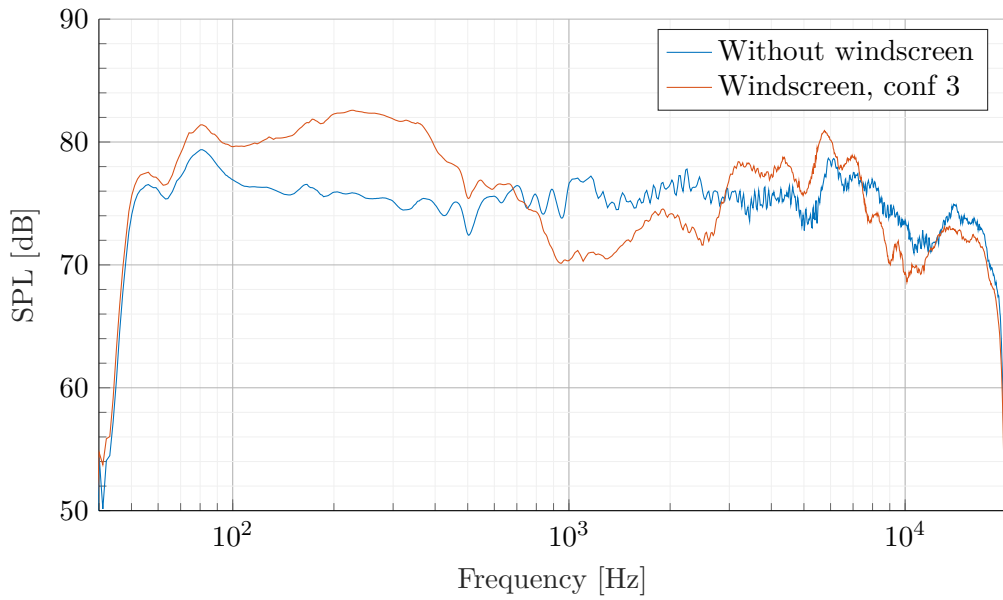


Figure D.14: The graph shows frequency response of the speaker measured without windscreens and with windscreens configuration three

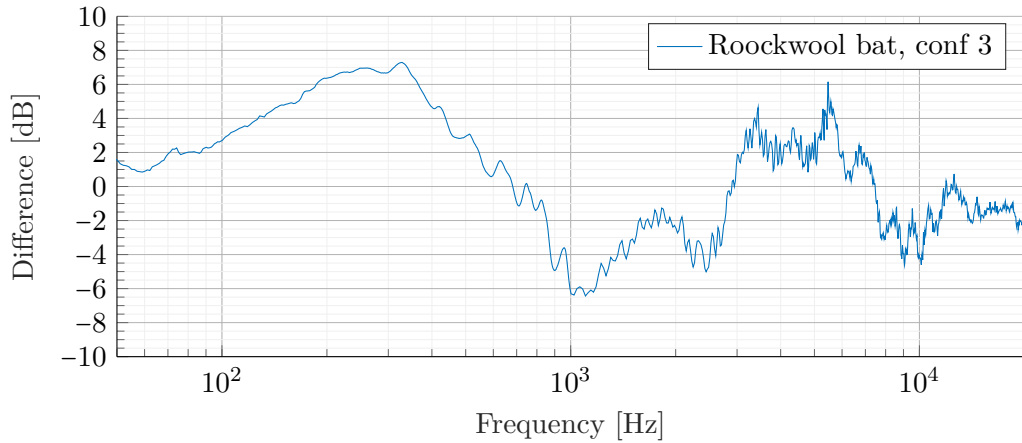


Figure D.15: The graph shows frequency response of the windscreens, where the frequency characteristic for the speaker is out calculated.



Figure D.16: The picture shows the measurement microphone with the rockwool bat configuration four

The measurement shown in Figure D.17 shows frequency response of the speaker without the windscreens and with the windscreens configuration four. The Figure D.16 shows the measured set up. In this measurement both the speaker and the microphone is lifted 30 cm

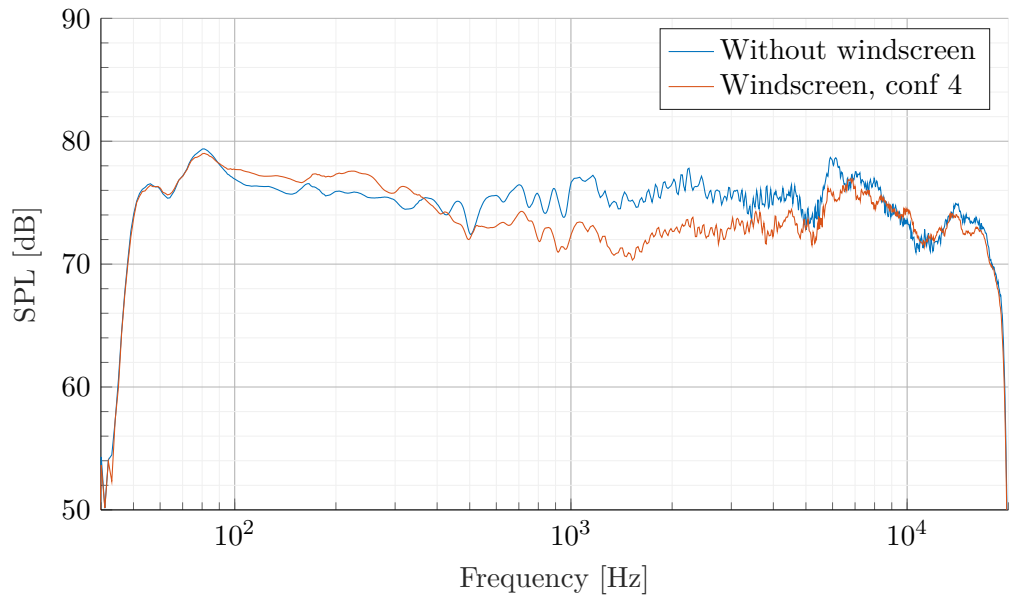


Figure D.17: The graph shows frequency response of the speaker measured without windscreen and with windscreen configuration four

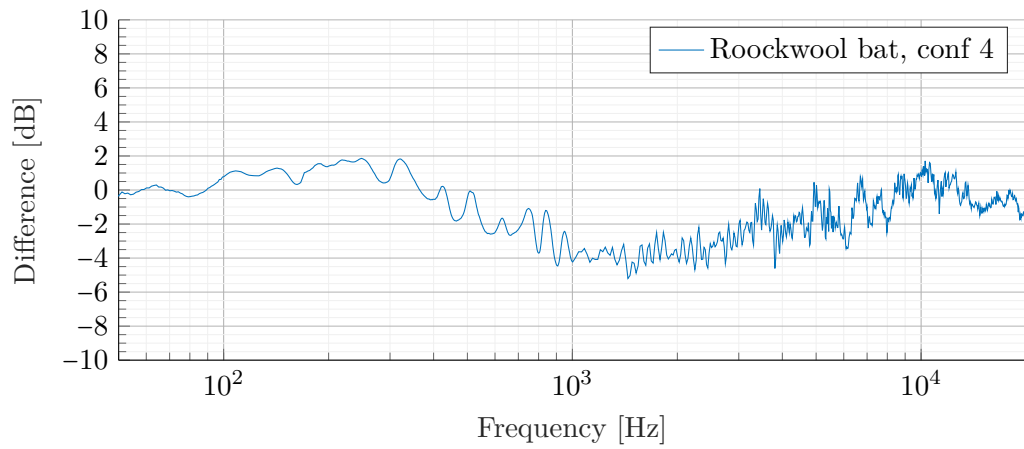


Figure D.18: The graph shows frequency response of the windscreen, where the frequency characteristic for the speaker is out calculated.

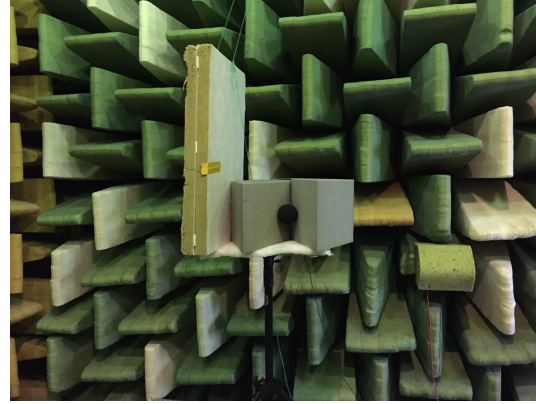


Figure D.19: The picture shows the measurement microphone with the rockwool bat configuration four

The measurement shown in Figure D.20 shows frequency response of the speaker without the windscreen and with the windscreen configuration four. The Figure D.19 shows the measured set up.

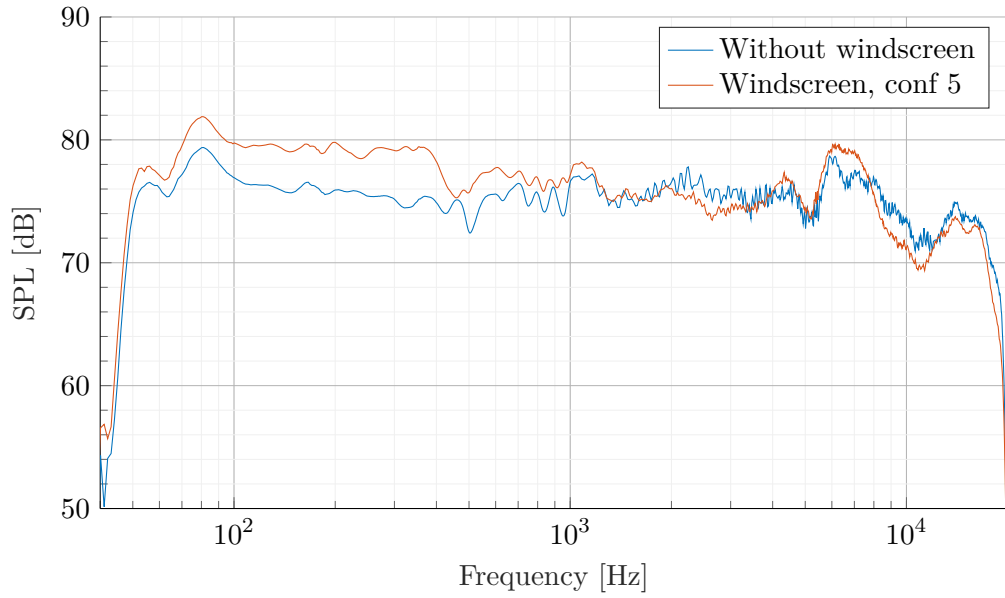


Figure D.20: The graph shows frequency response of the speaker measured without windscreen and with windscreen configuration five

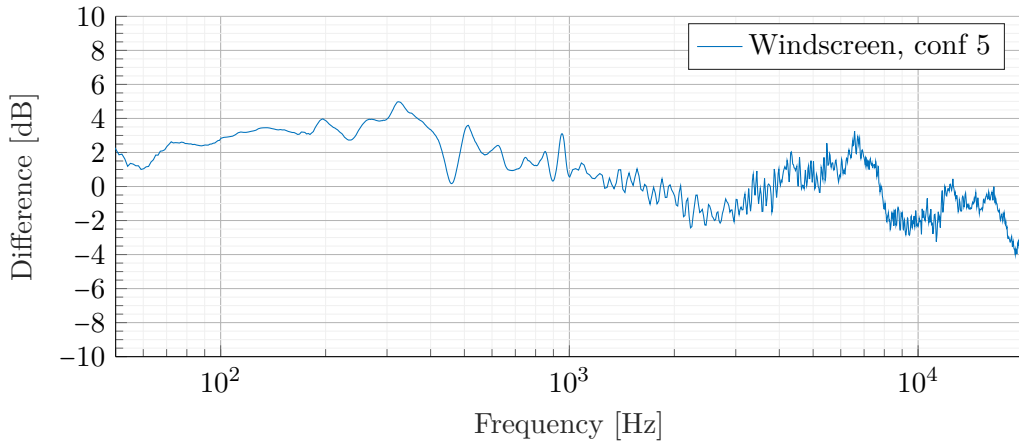


Figure D.21: The graph shows frequency response of the windscreen, where the frequency characteristic for the speaker is out calculated.

Summary

It is seen in the graph that all windscreen configuration change the frequency response of the microphone, even with only the original windscreen. Without taking the reference configuration intro account, the one with the lowest frequency change in the low frequency response is configuration one and four. The one with the lowest frequency change in the middle frequency is configuration one and two. The one with lowest frequency change in the high frequency is configuration four. The mix between configuration two and four shows a low frequency change in the middle and high frequency.

Appendix E

Windscreen attenuation measurement

A measurement was made to measure the wind attenuation in the microphone position with the difference windscreen configuration.

Materials and setup

To measure the wind attenuation of the windscreen configuration the following materials are used:

Table E.1: Equipment list

Description	Model	Serial-no	AAU-no
PC	Macbook	W89242W966H	-
large foam wedge	-	-	-
Small foam wedge	-	-	-
Rockwool bat	-	-	-
Fast fan	-	-	-
Fan control	transformator	-	60398
Windspeed tools	FT technologies FT742-D-SM	9002-922	105634

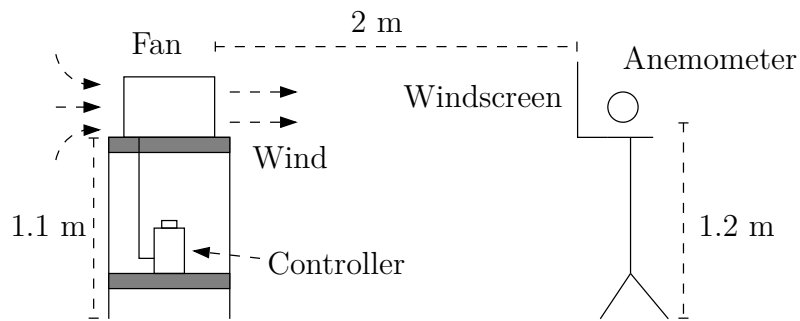


Figure E.1: The figure shows the measurement setup for the wind speed measurement in the microphone position

Test procedure

1. The materials are set up as in Figure E.1.
2. The fan is placed such that it produces crosswind.
3. The fan is activated.
4. The anemometer is activated to record.
5. The anemometer is placed in the wind for approximately 10 s.
6. Then the anemometer is moved into the microphone position for approximately 10 s.
7. Then the anemometer is moved back in the wind for approximately 10 s.
8. Then the anemometer is moved into the microphone position for approximately 10 s again.
9. The wind speed measurement is plotted in MATLAB® with a moving mean filter with 2 sample and as m/s versus s.
10. Next the wind direction measurement is plotted in MATLAB® with a moving mean filter with 2 sample and as ° versus s.
11. The measurement is done for all windscreen configuration the same way.

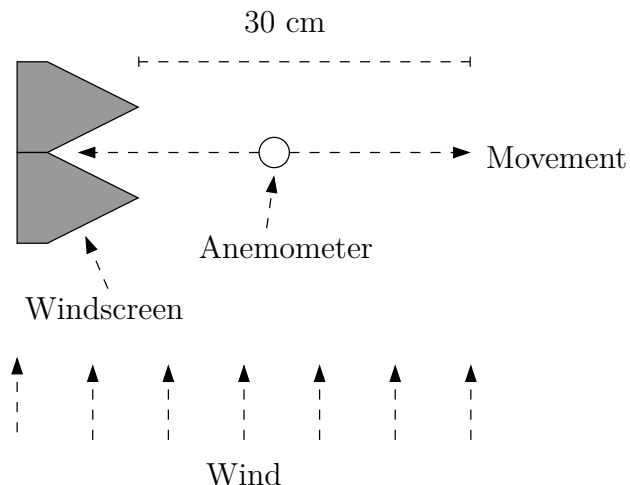


Figure E.2: The figure shows the movement of the anemometer doing the measurement

The following Figure E.3 shows the anemometer used for the measurement.



Figure E.3: The picture shows anemometer used for the measurement

Measurement area

To be able to generate a controlled wind flow, the hallway in Fredrick Bajers vej 7B5, 9220 Aalborg is used. The following Figure C.3 shows a drawing of the area and the position of the fan and windscreens.

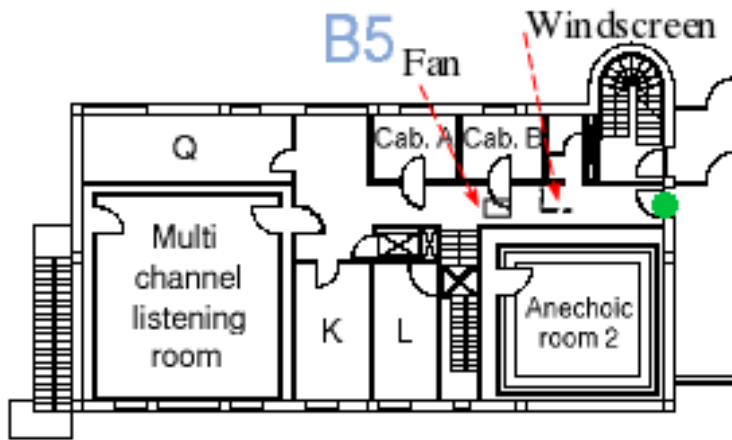


Figure E.4: The picture illustrate the area, where the wind flow is measured

Results

The following graphs shows the result of the measurement.

Figure E.5 shows the measurement setup of the foam wedge, where the Figure E.6 shows the result.



Figure E.5: The picture shows the measurement setup with the small wedge, configuration one

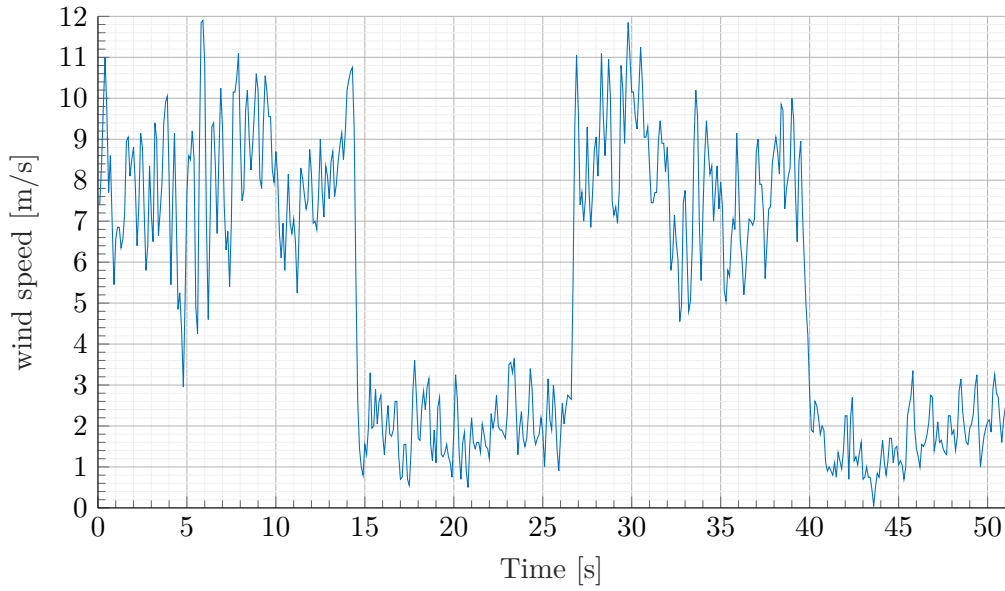


Figure E.6: The graph shows the wind speed versus time for configuration one. The grape have a high speed period and a low speed period, in the high speed period, the anemometer is in the wind approximately 30 cm from the windscreens where in the low speed period, the anemometer is inside the windscreens.

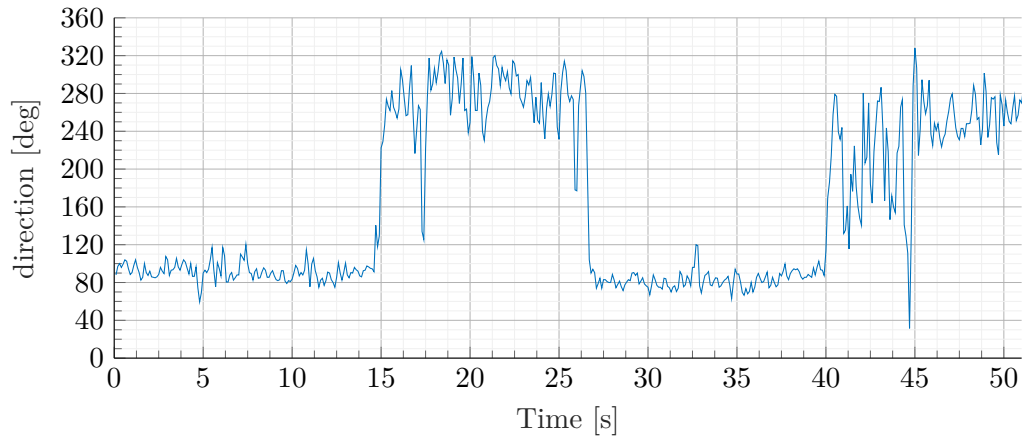


Figure E.7: The graph shows the synchronous direction of the wind with respect to the wind speed in Figure E.6

It is seen in Figure E.6 that the wind speed is lowered from approximately 8 m/s to 2 m/s. It is seen in Figure E.7 that the windscreens produce turbulence in the windscreens and the direction of the wind change approximately 180° .



Figure E.8: The picture shows the measurement setup for the large wedge, configuration two

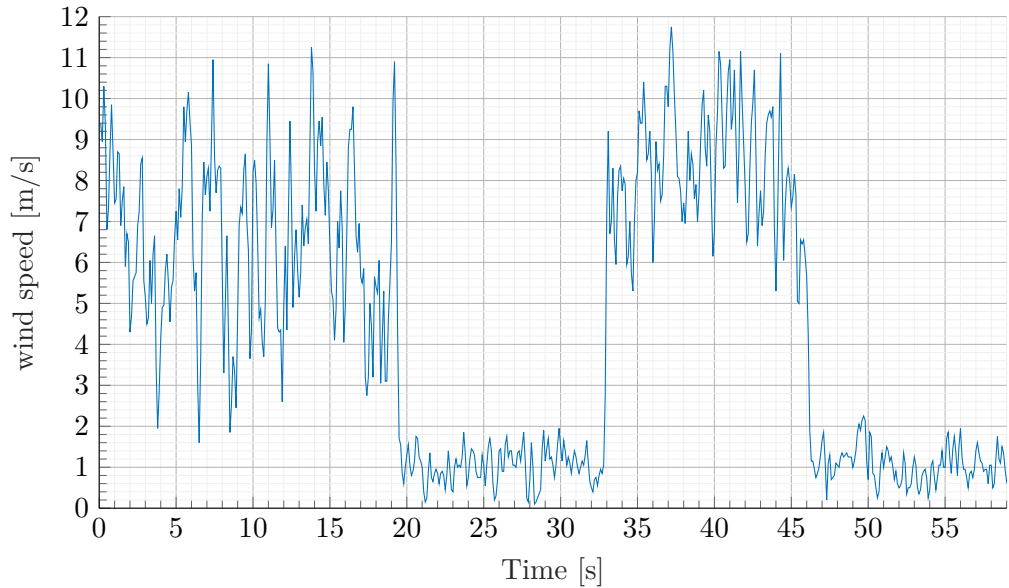


Figure E.9: The graph shows the wind speed versus time for configuration two. The grape have a high speed period and a low speed period, in the high speed period, the anemometer is in the wind approximately 30 cm from the windscreens where in the low speed period, the anemometer is inside the windscreens.

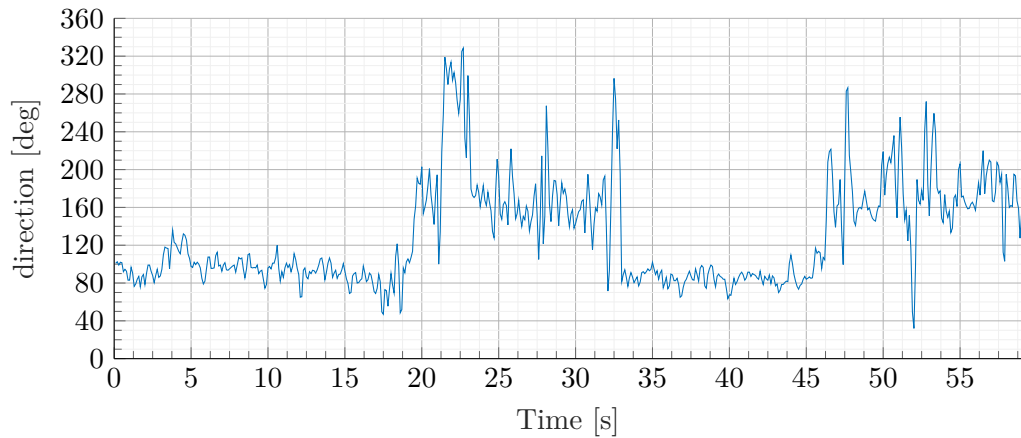


Figure E.10: The graph shows the synchronous direction of the wind with respect to the wind speed in Figure E.9

It is seen in Figure E.9 that the wind speed is lowered from approximately 7.5 m/s to 1 m/s. It is seen in Figure E.10 that the windspeed produces turbulence as high as with the small foam wedge in the windspeed and the direction of the wind change approximately 70°.

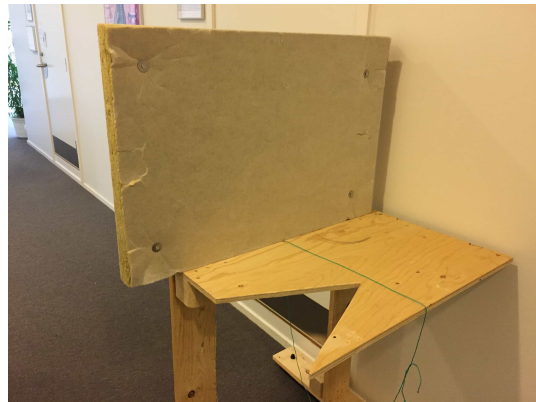


Figure E.11: The picture shows the measurement setup for the single rockwool bat, configuration four

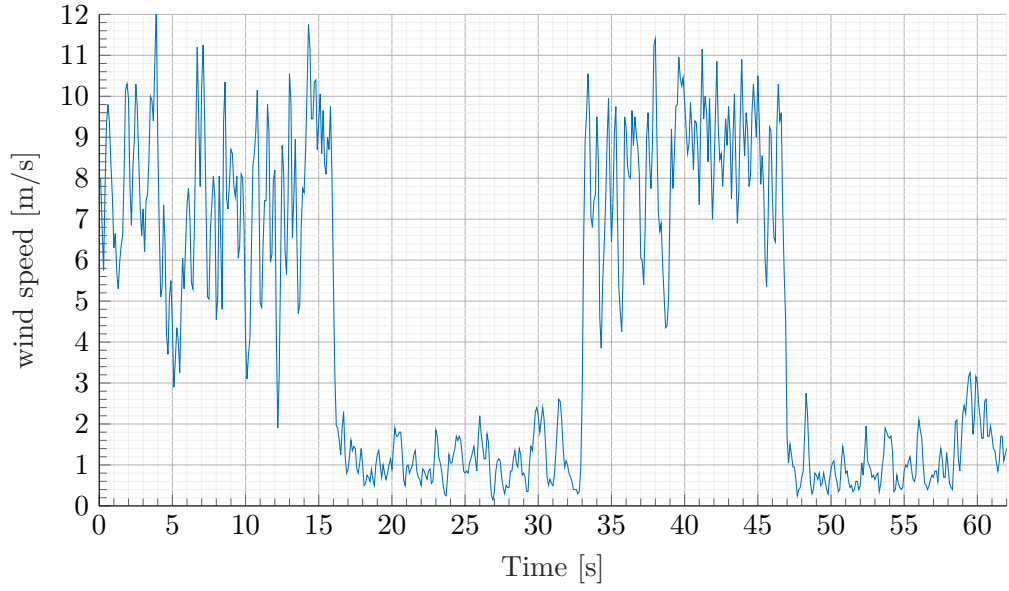


Figure E.12: The graph shows the wind speed versus time for configuration four. The grape have a high speed period and a low speed period, in the high speed period, the anemometer is in the wind approximately 30 cm from the windscreens where in the low speed period, the anemometer is inside the windscreens.

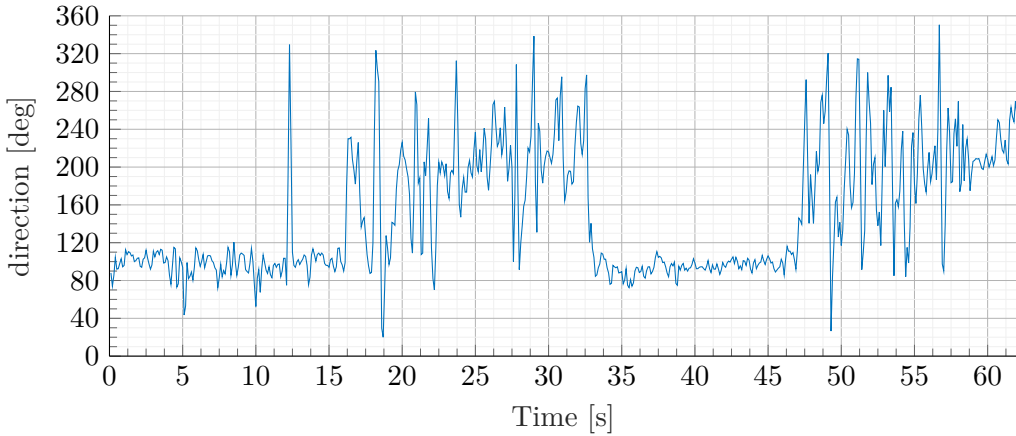


Figure E.13: The graph shows the synchronous direction of the wind with respect to the the wind speed in Figure E.12

It is seen in Figure E.12 that the wind speed is lowered from approximately 8 m/s to 1 m/s. It is seen in Figure E.13 that the windscreens produce higher turbulence

compare to the foam wedge windscreen. The direction of the wind change is approximately 100° .



Figure E.14: The picture shows the measurement with the large wedge and single rockwool bat, configuration five.

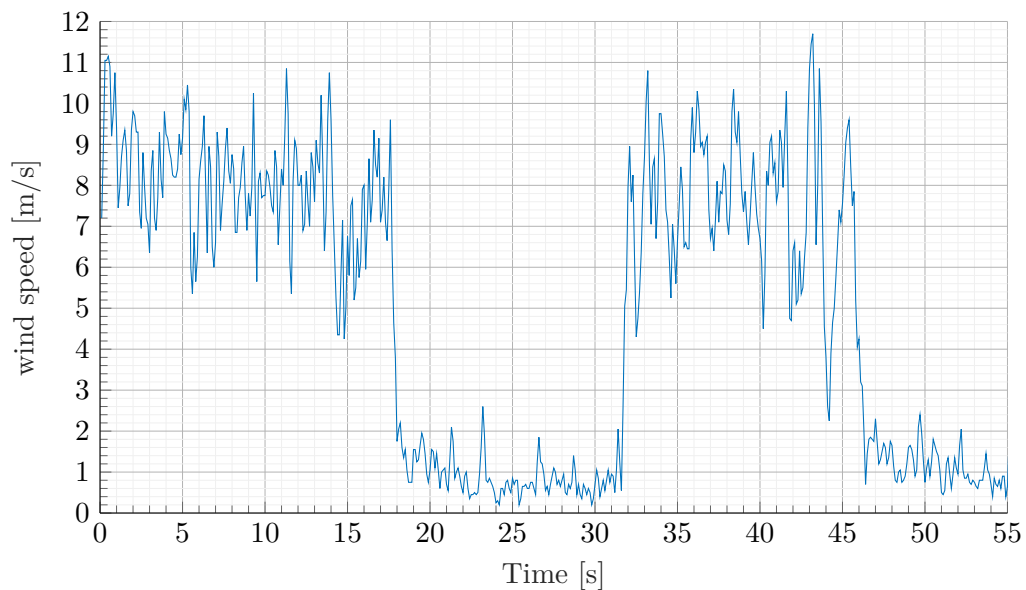


Figure E.15: The graph shows the wind speed versus time for configuration five. The graph have a high speed period and a low speed period, in the high speed period, the anemometer is in the wind approximately 30 cm from the windscreens where in the low speed period, the anemometer is inside the windscreens.

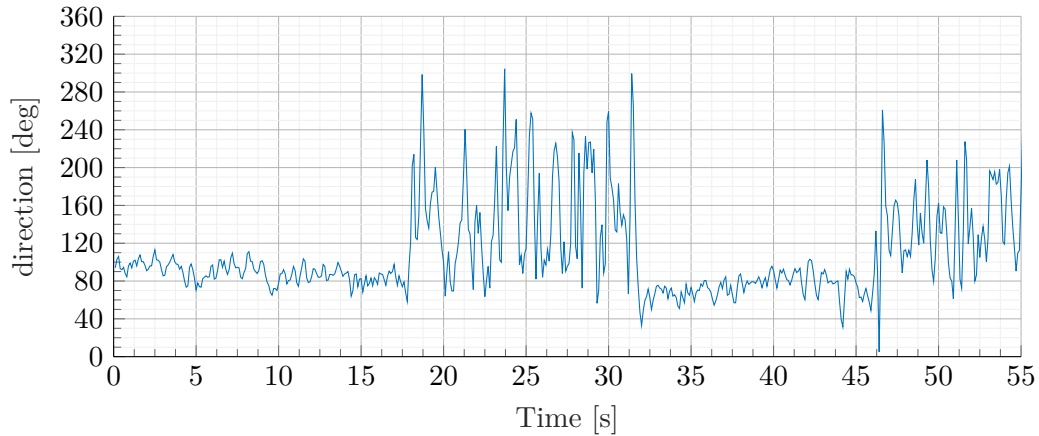


Figure E.16: The graph shows the synchronous direction of the wind with respect to the wind speed in Figure E.15

It is seen in Figure E.15 that the wind speed is lowered from approximately 8 m/s to 0.8 m/s. It is seen in Figure E.16 that this windscreens produces the highest turbulence of all windscreens. The direction of the wind change approximately 60°.

Summary

It is measured that all windscreens configuration lower the wind speed in the microphone position. The lowest attenuation of the wind is of the small foam wedge where the highest wind speed attenuation is attained by configuration five. Generally all windscreens yield turbulence wind direction, but the single rockwool bat configuration four seems to be the worst with respect to directional turbulence.

Appendix F

Windscreen attenuation measurement

A measurement was made to measure the wind attenuation in the microphone position with the difference windscreen configuration.

Materials and setup

To measure the wind attenuation of the windscreen configuration the following materials are used:

Table F.1: Equipment list

Description	Model	Serial-no	AAU-no
PC	Macbook	W89242W966H	-
Optimised windscreen	-	-	-
Fast fan	-	-	-
Fan control	tranformator	-	60398
Windspeed tools	FT technologies FT742-D-SM	9002-922	105634

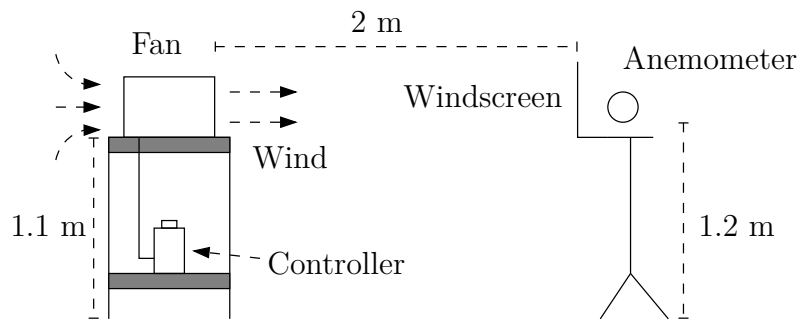


Figure F.1: The figure shows the measurement setup for the wind speed measurement in the microphone position

Test procedure

1. The materials are set up as in Figure F.1.
2. The fan is placed such that it produces crosswind.
3. The fan is activated.
4. The anemometer is activated to record.
5. The anemometer is placed in the wind for approximately 10 s.
6. Then the anemometer is moved into the microphone position for approximately 10 s.
7. Then the anemometer is moved back in the wind for approximately 10 s.
8. Then the anemometer is moved into the microphone position for approximately 10 s again.
9. The wind speed measurement is plotted in MATLAB® with a moving mean filter with 2 sample and as m/s versus s.
10. Next the wind direction measurement is plotted in MATLAB® with a moving mean filter with 2 sample and as ° versus s.

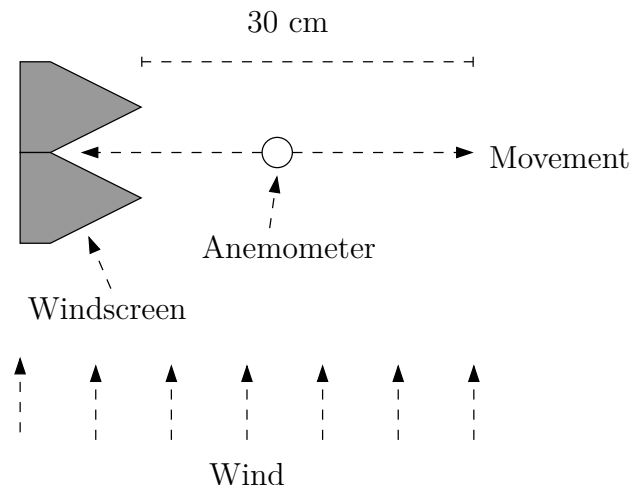


Figure F.2: The figure shows the movement of the anemometer doing the measurement

Measurement area

To be able to generate a controlled wind flow, the hall way in Fredrick Bajers vej 7B5, 9220 Aalborg is used. The following ?? shows a drawing of the area and the position of the fan and windscreens.

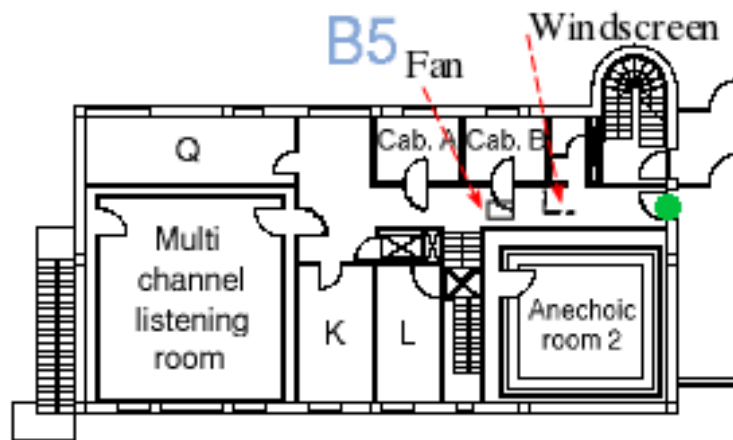


Figure F.3: The picture illustrate the area, where the wind flow is measured

Results

The following graphs shows the result of the measurement.

Figure E.5 shows the measurement setup of the foam wedge, where the ?? shows the result.



(a) The picture shows the measurement setup for the optimised windscreen configuration five from back

(b) The picture shows the measurement setup for the optimised windscreen configuration five in front

Figure F.4: ap:wind:large_opt_pic

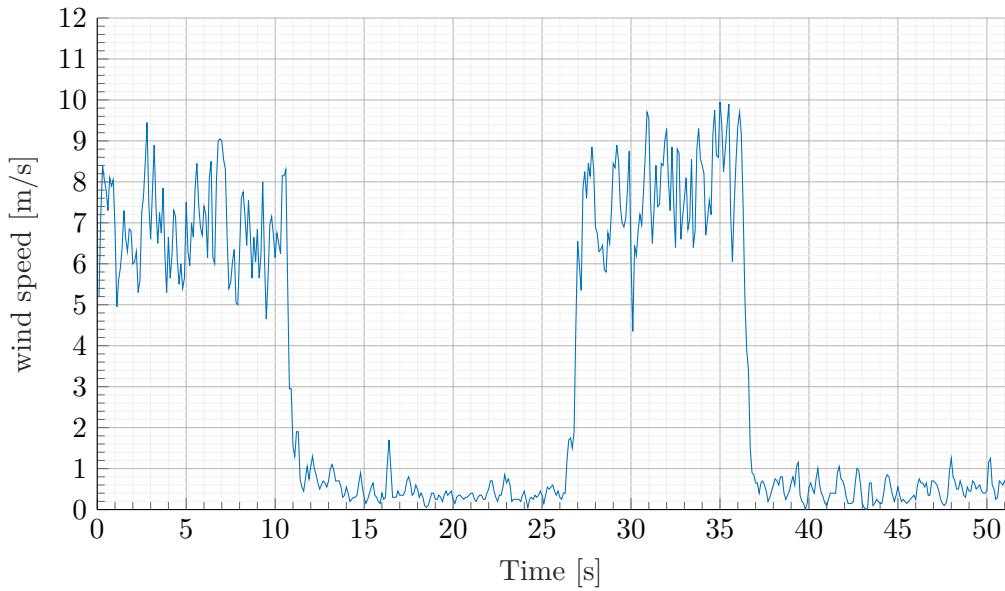


Figure F.5: The graph shows the wind speed versus time for the optimised configuration five. The graph have a high speed period and a low speed period. In the high speed period, the anemometer is in the wind approximately 30 cm from the windscreens where in the low speed period, the anemometer is inside the windscreens.

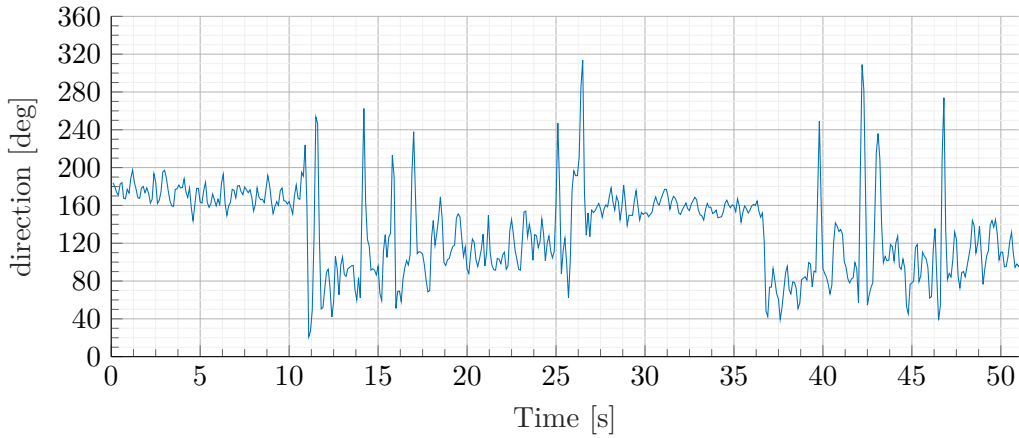


Figure F.6: The graph shows the synchronous direction of the wind with respect the the wind speed in Figure F.5

It is seen in Figure F.5 that the wind speed is lowered from approximately 8 m/s to 0.5 m/s. It is seen in Figure F.6 that the windscreen produces turbulence in the windspeed and the direction of the wind change approximately -100° . The reason that the angle is negative in this measurement is that the anemometer is turned 180° in the vertical plan for practical reason.

Summary

It is measured that the optimised windspeed lower the wind turbulence by optimising the aerodynamics with curved surface and small thin edges.

Appendix G

Outline ET 250-3D turntable control

In this appendix the control of an Outline ET 250-3D turntable will be described. The turntable can be controlled in three ways. the first which are Transistor–Transistor Logic (TTL) commands through a jack connector. Secondly, it can be controlled by specific Dynamic Link library (DLL) commands through Ethernet. All of those are included in a software pack available from the manufacturer. Thirdly the turntable can be controlled by User Datagram Protocol (UDP) commands through Ethernet. For controlling the turntable by MATLAB, the second Ethernet based control method is the easiest to do because MATLAB supports Ethernet access. The DLL method requires a complicated scripts which might only work on Windows operation systems. UDP can be sent and received by the vast majority of operating systems, which support IPv4 Ethernet connection. The usage of UDP leads to short and simple scripts, where the script opens a UDP channel as a file, and e.g. the script shall only edit the file in the right position to move the turntable. Because of the advantages in implementation, UDP is chosen over the other controlling methods for the turntable.

Materials and setup

The following materials are used:

Table G.1: Equipment list

Description	Model	Serial-no	AAU-no
PC	Macbook	W89242W966H	-
Turntable	Outline ET 250-3D	REIBO012	-
PC - software	MATLAB 2018b	-	-

The UDP setup of the computer

To establish connection between the turntable and computer, both have to run at the same SUBNET MASK. The turntable comes with a factory setting for Ethernet connection which is as follows:

Table G.2: Turntable network address

Internet Protocol (IP)	192.168.1.34
SUBNET MASK	255.255.255.0
DEFAULT GATEWAY	192.168.1.250
BROADCAST IP	192.168.1.255

Turtable control command

The software is implemented as a function, where the user can retrieve the turntable position, specify a position and stop the turntable. The function name is:

Code snippet G.1: The turntable control function | ET250_3D.m

```
1 function [angle] = ET250_3D(cmd, angle)
```

The function is made as a switch case with input variable "cmd", and an angle input. The following command can be send to the "cmd" of the function:

Table G.3: Function commands

cmd = 'udp_start'	Which start a connection on port 7000
cmd = 'set'	Which move the turntable to the specified angle
cmd = 'get'	Which get the position of the turntable
cmd = 'stop'	Which stop the turntable from moving
cmd = 'udp_stop'	Which stop the connection on port 7000

The MATLAB function

Code snippet G.2: The turntable control function | ET250_3D.m

```
1 function [angle] = ET250_3D(cmd, angle)
2
3
4 switch cmd
5
6   case 'udp_start'
7     echoudp('on', 7000)
8     u = udp('192.168.1.34', 7000);
9     fopen(u)
10
11
```

```

12     case 'set'
13         %request current position
14         fwrite(u,hex2dec(['04';'00';'00';'04']))
15         x = fread(u,7);
16         angle_current = (x(4)*256+x(5))/10;
17
18         %calc shortest way
19         angle_delta = angle-angle_current;
20         if angle_delta > 180
21             angle_delta = angle_delta - 360;
22         end
23         if angle_delta < -180
24             angle_delta = angle_delta + 360;
25         end
26
27         cmd(1) = uint8( 1.5-sign(angle_delta)/2 );
28             %1st byte = direction
29         cmd(2) = uint8( floor(abs(angle_delta*10)/256) );
29             %angle in degree*10
30         cmd(3) = uint8( mod(floor(abs(angle_delta*10)),256) );
30             %angle in degree*10
31         cmd(4) = 0;
32
33         fwrite(u,cmd)
34             %receive
35             ACK
36
37     case 'get'
38         %request current position
39         fwrite(u,hex2dec(['04';'00';'00';'04']))
40         x = fread(u,7);
41         angle = (x(4)*256+x(5))/10;
42
43     case 'stop'
44         fwrite(u,hex2dec(['03';'00';'00';'03'])) %send
45             stop stop
46         x = dec2hex(fread(u,2));
47
48     case 'udp_stop'
49         echoudp('off')
50         fclose(u)
51
52 end

```


Appendix H

Weather measurement

This appendix shows the arduino code for the weather samples.

The firmware

Code snippet H.1: The weather firmware | weather_program.ino

```
1 #include <math.h>
2 #include <dht.h>
3 dht DHT;
4 #include "TimerOne.h"
5
6
7 //Constants
8 #define DHT22_PIN 4      // DHT 22 (AM2302) - what pin we're
9     connected to
10
11 #define WindSensorPin1 (2) // The pin location of the anemometer
12     sensor
13 #define WindSensorPin2 (3) // The pin location of the anemometer
14     sensor
15
16 //Variables
17
18
19 volatile bool IsSampleRequired; // this is set true every 2.5s.
20     Get wind speed
21 volatile unsigned int TimerCount; // used to determine 2.5sec
22     timer count
23 volatile unsigned long Rotations1; // cup rotation counter used in
24     interrupt routine
25 volatile unsigned long Rotation_old1; // cup rotation counter used
26     in interrupt routine
27 volatile unsigned long ring1; // cup rotation counter used in
28     interrupt routine
```

```

21   volatile unsigned long ContactBounceTime1; // Timer to avoid
22     contact bounce in isr
23   volatile unsigned long Rotations2; // cup rotation counter used in
24     interrupt routine
25   volatile unsigned long Rotation_old2; // cup rotation counter used
26     in interrupt routine
27   volatile unsigned long ring2; // cup rotation counter used in
28     interrupt routine
29   volatile unsigned long ContactBounceTime2; // Timer to avoid
30     contact bounce in isr
31   volatile unsigned long timet1 = 0;
32   volatile unsigned long timet2 = 0;
33   float WindSpeed1; // speed miles per hour
34   float WindSpeed2; // speed miles per hour
35
36   int analogPin1 = A2;
37   int analogPin2 = A3;
38   int vaneValue1;
39   int vaneValue2;
40   int count1;
41   int count2;
42   int buffersize = 16;
43   int ringbuffer1[16];
44   int ringbuffer2[16];
45   float hum; //Stores humidity value
46   float temp; //Stores temperature value
47
48 void setup() {
49
50
51   IsSampleRequired = false;
52   TimerCount = 0;
53   count1 = 0;
54   count2 = 0;
55   Rotations1 = 0; // Set Rotations to 0 ready for calculations
56   Rotation_old1 = 0;
57   Rotations2 = 0; // Set Rotations to 0 ready for calculations
58   Rotation_old2 = 0;
59   ring1 = 0;
60   ring2 = 0;
61   Serial.begin(115200);
62   pinMode(WindSensorPin2, INPUT);
63   // Setup the timer interrupt
64   attachInterrupt(digitalPinToInterrupt(WindSensorPin1),
65     isr_rotation1, FALLING);
66   attachInterrupt(digitalPinToInterrupt(WindSensorPin2),
67     isr_rotation2, FALLING);
68   Timer1.initialize(26500); // Timer interrupt every 2.5 seconds
69     500000 (25000)
70   Timer1.attachInterrupt(isr_timer);
71 }

```

```

66 void loop() {
67     if(IsSampleRequired) {
68
69         ringbuffer1[count1] = Rotations1 - Rotation_old1;
70         Rotation_old1 = Rotations1;
71         ring1 = 0;
72
73         for(int i = 0; i <= buffersize; i++){
74             ring1 = ring1+ringbuffer1[i];
75         }
76
77         if(count1 == buffersize){
78             Rotations1 = 0; // Reset count for next sample
79             Rotation_old1 = 0;
80             count1 = 0;
81         }
82
83         else{
84             count1++;
85         }
86
87
88         ringbuffer2[count2] = Rotations2 - Rotation_old2;
89         Rotation_old2 = Rotations2;
90         ring2 = 0;
91
92         for(int i = 0; i <= buffersize; i++){
93             ring2 = ring2+ringbuffer2[i];
94         }
95
96         if(count2 == buffersize){
97             Rotations2 = 0; // Reset count for next sample
98             Rotation_old2 = 0;
99             count2 = 0;
100        }
101
102        else{
103            count2++;
104        }
105
106        IsSampleRequired = false;
107    }
108
109    int chk = DHT.read22(DHT22_PIN); //Read data and store it to
110    //variables hum and temp
111    vaneValue1 = analogRead(analogPin1);
112    vaneValue2 = analogRead(analogPin2);
113    temp = DHT.temperature;
114    hum = DHT.humidity;
115    WindSpeed1 = ring1*(2.25/2.960)*0.44704;
116    WindSpeed2 = ring2*(2.25/2.960)*0.44704;
117    Serial.print(WindSpeed1);

```

```
118 // Serial.print("\t");
119 // Serial.print(vaneValue1);
120 // Serial.print("\t");
121 // Serial.print(WindSpeed2);
122 // Serial.print("\t");
123 // Serial.print(vaneValue2);
124 // Serial.print("\t");
125 // Serial.print(temp);
126 // Serial.print("\t");
127 // Serial.println(hum);
128 delay(88);
129 }
130 }
131
132
133 // isr handler for timer interrupt
134 void isr_timer() {
135 TimerCount++;
136 if(TimerCount == 7) {
137   timet2 = millis();
138   IsSampleRequired = true;
139   TimerCount = 0;
140 }
141 }
142
143 // This is the function that the interrupt calls to increment the
144 // rotation count
145 void isr_rotation1() {
146   if((millis() - ContactBounceTime1) > 15 ) { // debounce the
147     switch contact.
148     Rotations1++;
149     ContactBounceTime1 = millis();
150   }
151 }
152 void isr_rotation2() {
153   if((millis() - ContactBounceTime2) > 15 ) { // debounce the
154     switch contact.
155     Rotations2++;
156     ContactBounceTime2 = millis();
157 }
```

Appendix I

Impulse response measuring software

The software measure the impulse response of a line source array while it read weather information on the serial bus.

The firmware

Code snippet I.1: The impulse and weather measuring software | IRmeas_fft.m

```
35 if ~isempty(instrfind)
36     fclose(instrfind);
37     delete(instrfind);
38 end
39
40 port = seriallist;
41 s = serial(port(5));
42 s=serial(port(5), 'InputBufferSize', 512, 'Baudrate', 115200);
43 fopen(s)
44 tic
45     while(toc<10)
46         buff=strsplit(fscanf(s), '\t');
47     end
48
49
50         % Perform capture
51         %audiowrite("sweep.wav", dataOut, fs)
52         L = 4096;
53         fileReader =
54             dsp.AudioFileReader('sweep.wav', 'SamplesPerFrame', L);
55         fs = fileReader.SampleRate;
56
56         aPR = audioPlayerRecorder('SampleRate', fs, ...
57             '% Sampling Freq.
58             'RecorderChannelMapping', inputChannel, ...
59             '% Input channel(s)
```

```

58         'PlayerChannelMapping',[1 2],... % Output
59             channel(s)
60         'SupportVariableSize',true,...    % Enable
61             variable buffer size
62         'BufferSize',L);                % Set
63             bufferSize
64
65         out = [];
66         data = [];
67         while ~isDone(fileReader)
68             audioToPlay = fileReader();
69             [audioRecorded,nUnderruns,nOverruns] =
70                 aPR(audioToPlay);
71             out = [out; audioRecorded];
72             dat=strsplit(fscanf(s,'%t'));
73             data = [data; dat];
74             if nUnderruns > 0
75                 fprintf('Audio player queue was
76                     underrun by %d
77                     samples.\n',nUnderruns);
78             res = 1;
79         end
80         if nOverruns > 0
81             fprintf('Audio recorder queue was
82                     overrun by %d samples.\n',nOverruns);
83             res = 1;
84         end
85         release(fileReader);
86         release(aPR);
87         fclose(s)
88         delete(s)
89         clear s
90
91
92     weather = str2double(data);
93     weather = weather(23:end,:);
94     weathertime = [0 ([1:length(weather)-1]./(fs/L))'];
95
96     load('calibration.mat')
97
98
99     for k=1:length(inputChannel)-1
100        % convolution of signal
101        input = out(:,k+1);
102        ref =
103            out(:,1)/(rms(out(:,1))/calibration.mic_sensitivity(k));
104        eps = 0.1;
105        L = numel(ref);
106        W = hann(L);

```

```
103     uz1f = fft(W.*input,L);
104     uz2f = fft(W.*ref,L);
105     ir(:,k) =
106         real(ifft((uz1f.*conj(uz2f))./(uz2f.*conj(uz2f)+eps*mean(uz2f.*conj(uz2f)))))'
107     irtime = ([1:length(ir)]./fs)';
108
109
110 end
```


Appendix J

The directionality of L-acoustics KUDO

A measurement was made to measure the directionality of a L-acoustics KUDO. The goal of this appendix is to measure the polar response and calculate transfer functions of the line source array element in a free field environment with calibrated measuring equipment. During the measurement of the polar response, impulse responses are measured with a specified degree step size all around the speaker. E.g. if the step is one degree, the loudspeaker will be turned 1 degree for every impulse response measurement, until 360° is achieved.

Materials and setup

To measure the directionality of the line source element, the following materials are used:

Table J.1: Equipment list

Description	Model	Serial-no	AAU-no
PC	Macbook	W89242W966H	-
Audio interface	RME Fireface UCX	23811948	108230
Microphone	GRAS 26CC	78189	75583
Preamp	GRAS 40 AZ	100268	75551
Speaker	L-acoustics KUDO	7733	-
Turntable	Outline ET 250-3D	REIBO012	-
PC - software	MATLAB 2018b	-	-

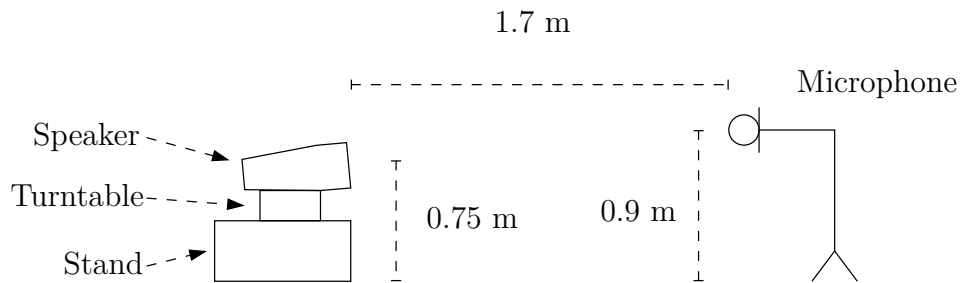


Figure J.1: The figure shows the measurement setup in the anechoic chamber

Test procedure

1. The materials are set up as in Figure J.1 where the microphone is connected to the audio interface.
2. The microphone is calibrated
3. The speaker is placed 1.7 m from the microphone and pointing in the direction of the microphone.
4. The impulse response is measured for every 5°
5. The -3 dB SPL step contour is calculated until -21 dB SPL and plotted.

Measurement area

To be able to measure the windscreen frequency response, the anechoic chamber in Fredrick Bajers vej 7B4, 9220 Aalborg is used. The following Figure J.2 shows a drawing of the area and the position of the fan and windscreens.

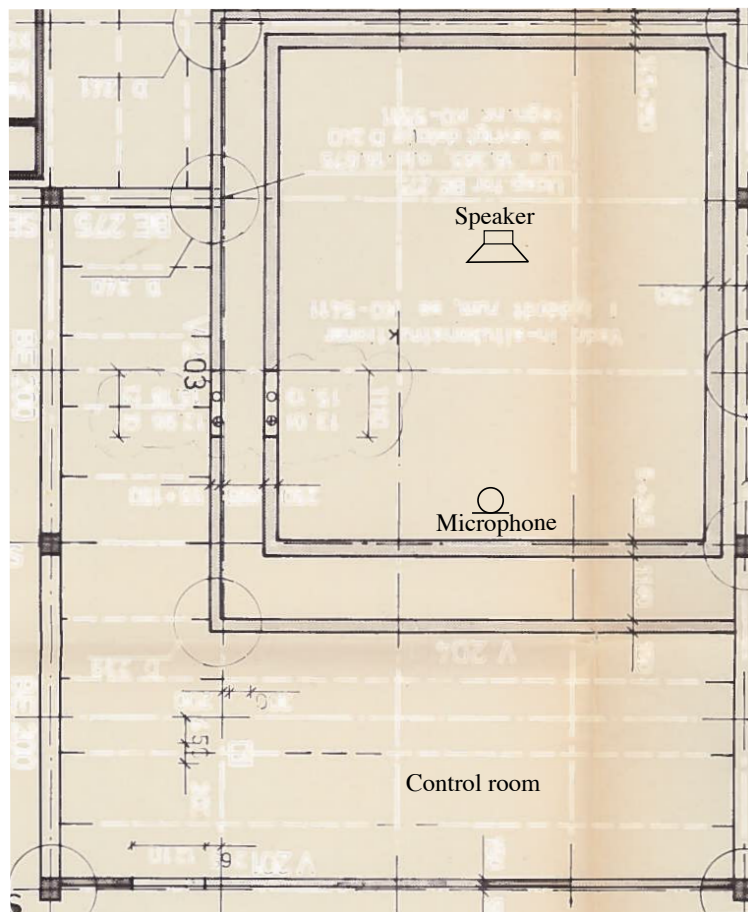


Figure J.2: The picture illustrate the position of the microphone and the speaker

Results

The following Figure J.3 shows the measurement setup.

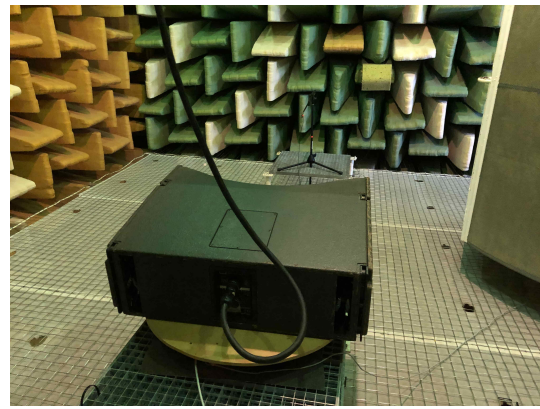


Figure J.3: The picture shows the measurement setup

The following graphs shows the result of the measurement.

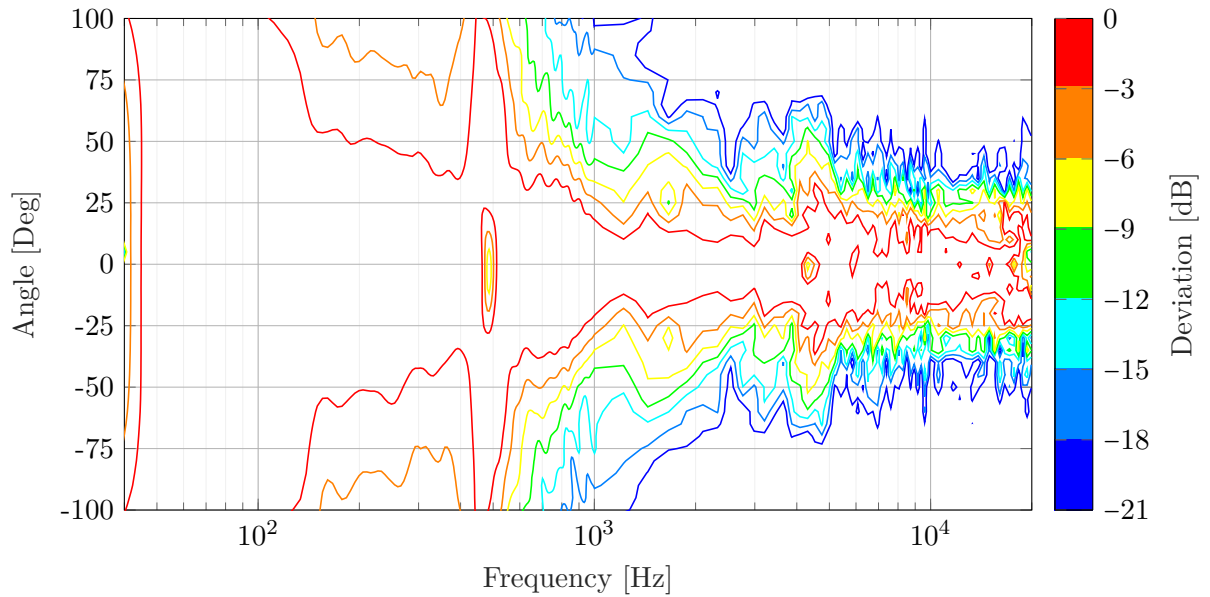


Figure J.4: The graph shows

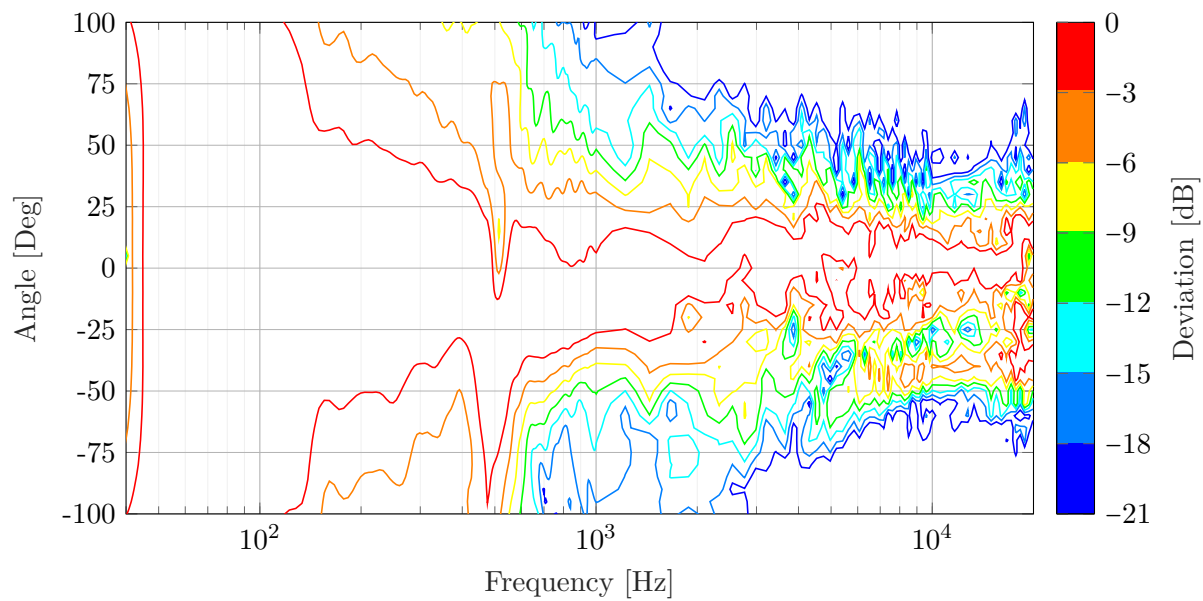


Figure J.5: The graph shows

Summary

Appendix K

cross wind effect on line source array

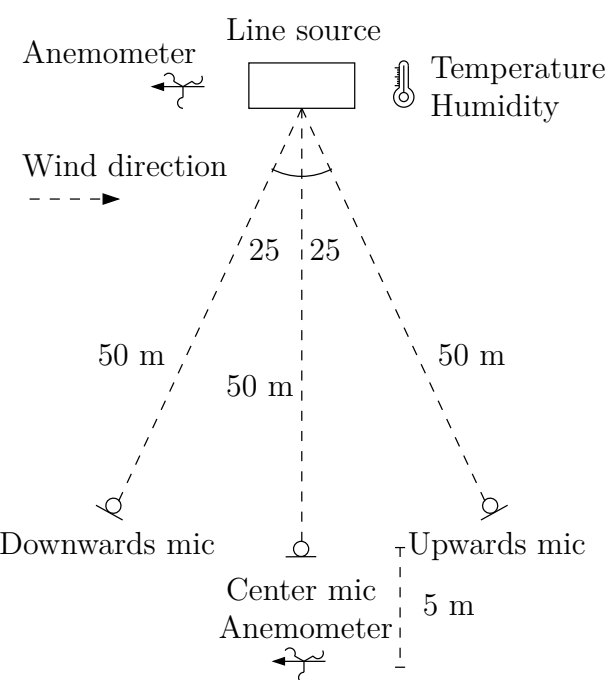
A measurement was made to measure the transfer function differences in three point in crosswind. One microphone situated in downwards direction, one microphone situated in upwards direction and one microphone situated in center, which is between the other two microphone. The used speaker have a horizontal dispersion pattern of 80°, but it is the 50° angle which is used as explained in ??

Materials and setup

To measure the transfer function in a crosswind situation, the following materials are used:

Table K.1: Equipment list

Description	Model	Serial-no	AAU-no
PC	Macbook	W89242W966H	-
Audio interface	RME Fireface UCX	23811948	108230
Microphone	GRAS 26CC	78189	75583
Preamp	GRAS 40 AZ	100268	75551
Microphone	GRAS 26CC	78186	75582
Preamp	GRAS 40 AZ	100267	75550
Microphone	GRAS 26CC	??	
Preamp	GRAS 40 AZ		
3 Windscreen	Author design	-	-
Line source element	L-acoustics KUDO		
Line source element	L-acoustics KUDO		
Line source element	L-acoustics KUDO		
Line source element	L-acoustics KUDO		
Line source element	L-acoustics KUDO		
Amplifier	Lab PLM10000Q		
Amplifier	Lab PLM10000Q		
Mixer	Yamaha LS9		
Wind measurement tools	Davis	-	
Angling tools flying tools	Author design	-	
	-	-	-

**Figure K.1:** The figure shows the microphone position versus the position of the line source, while the array is 0° horizontal turned



(a) The picture shows the speaker setup



(b) The figure shows the wind direction

Figure K.2: The figures shows the measurement set up for Appendix A and ??

Test procedure

1. The microphone is calibrated.
2. The wind direction is measured.
3. The materials are set up as in Figure K.1 where the speaker is placed in cross wind direction, such that the frontal wave direction is orthogonal to the wind. The microphone and speaker is connected to the audio interface.
4. The speaker is placed 2.92 m above the ground.
5. The speaker is tilted 5° pointing down against the ground.
6. The microphone is placed 1.68 m above the ground, 50 m from the speaker. One 25° to the left of the speaker, one 25° to the right of the speaker and one in center between the two other microphones.
7. The anemometer at the speakers is situated on the speaker tower in the same side as shown on the setup and a height of 4.64 m
8. The anemometer at the microphone position is lifted 1.68 m above the ground.
9. The wind direction goes from the upwards microphone to the downwards microphone.
10. The humidity and temperature is measured at the speaker position.
11. 10 sine sweep is performed with a length of 5 s each while the wind direction and speed is measured.
12. The impulse response is calculated and filtered with a 4th order highpass filter at 20 Hz.
13. The correlation is calculated for each impulse response to the first impulse response for time alignment [Gunness, 2001] of all microphone channels.
14. The mean impulse response is calculated for the 10 measurement of all three microphone.
15. The transfer function is calculated with a 10 sample moving mean filter.

16. The transfer function is down sampled to fit the plotting program.
17. The transfer function is calculated with a 5 sample moving mean filter.
18. The wind measurement is synchronised to the transfer function in time.
19. The measurement is repeated 6 times with different horizontal speaker angle from 0° to 30° in step of 5°

Measurement area

To be able to measure in a windy area, parking lot at Tryvej 13, 9320 Hjallerup is used. The following Figure K.3 shows a picture of the area and the approximate position of the speaker and microphone.



Figure K.3: The picture illustrate the area, where the wind flow is measured

Results

All measuring result is not shown here, the rest can be founded in the attached file. One synchronised measurement is shown for the upwards microphone where the speaker is turned 0° , 10° , 20° and 30° . The shown measurement result is for one measurement and is not a mean from 10. This shows the time synchronised result. The average result can be founded in ??.

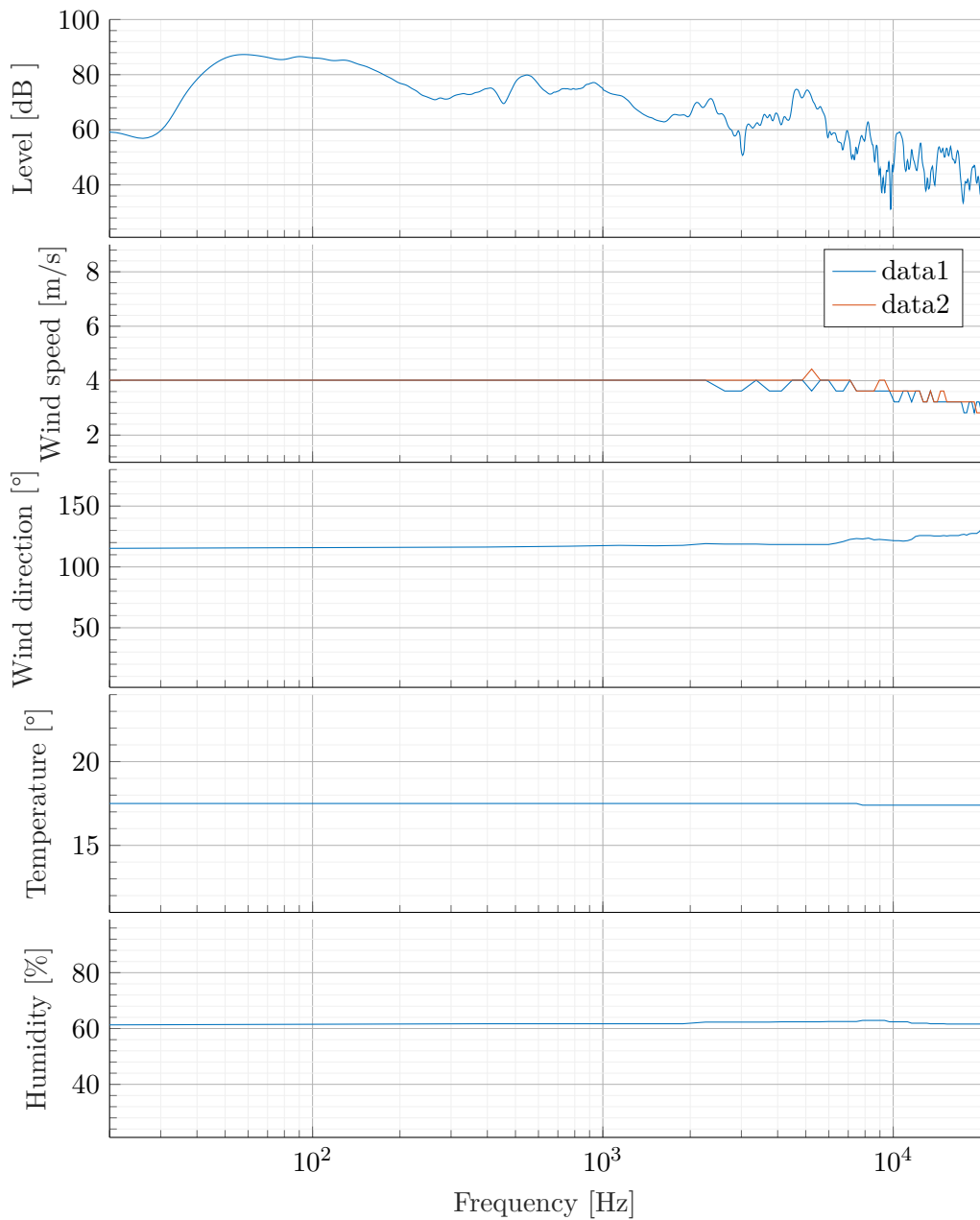


Figure K.4: the graph shows

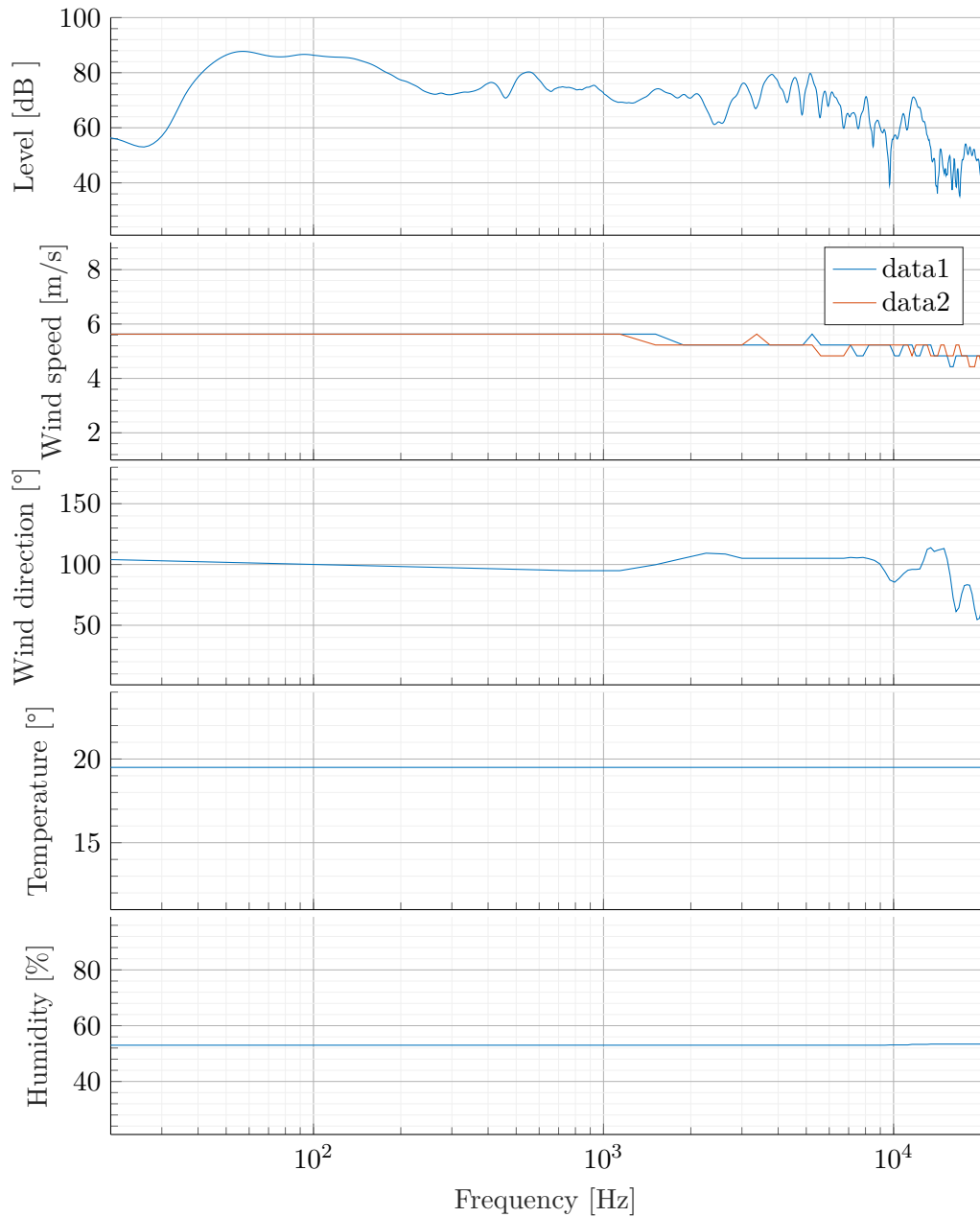


Figure K.5: the graph shows

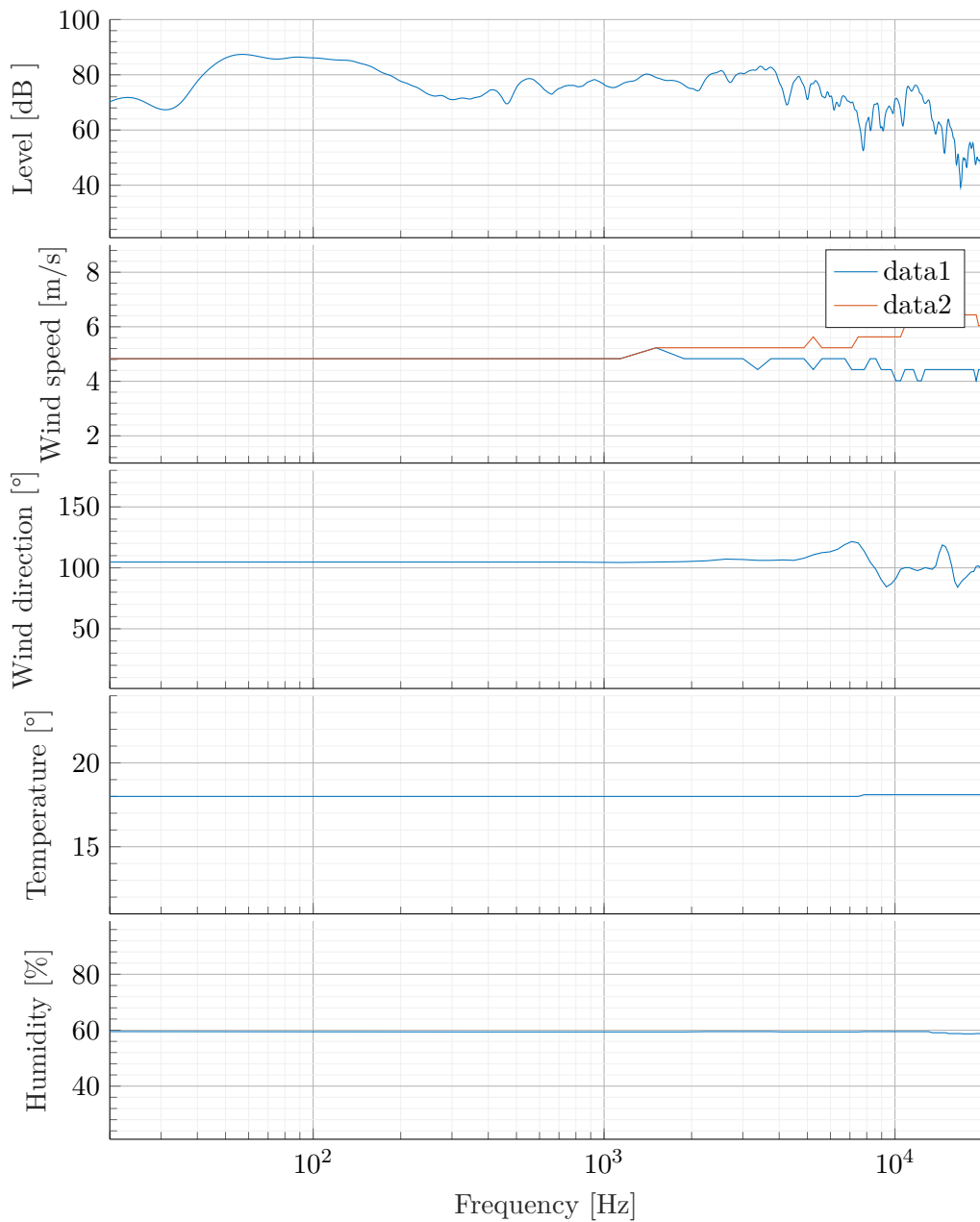


Figure K.6: the graph shows

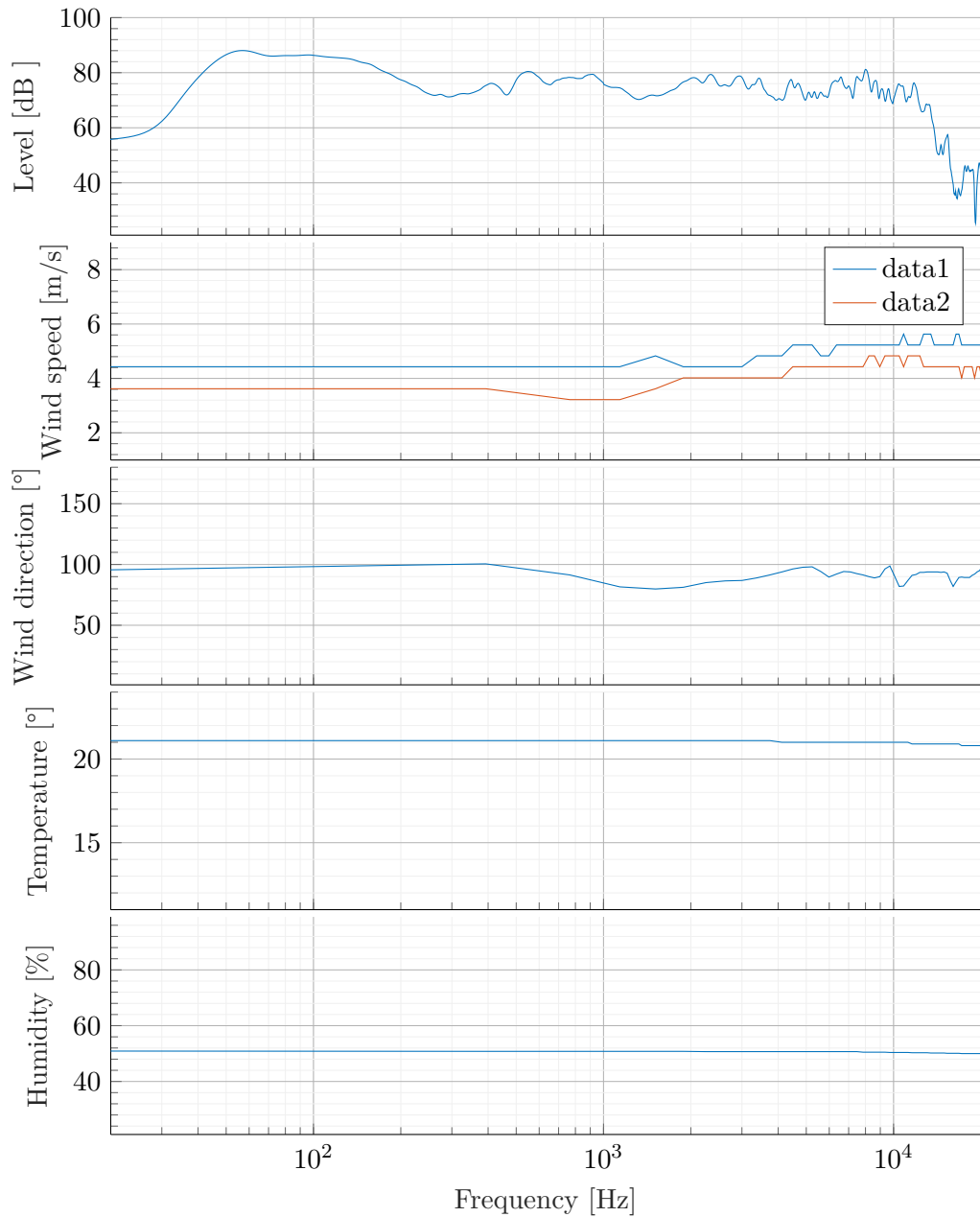


Figure K.7: the graph shows

Summary

Appendix L

Line source array angle measuring design

To measure the angle of the speaker, a angle plate with coloured laser indicator is designed.

Materials and setup

The following material is used

Table L.1: Equipment list

Description	Model	Serial-no	AAU-no
Laser pen	Red	-	-
Laser pen	Green	-	-
Angle plate	-	-	-
Laser pen holder	-	-	-



(a) The picture shows the angle finder plate
(b) The figure shows the lasers and the laser holder

Figure L.1: The figures shows the angle finder martial for the used line source array

Adjusting the line source horizontal angle

1. The materials are set up as in Figure L.1.
2. The line source array is turned until the laser pointers light is on the drawn line of the angle or with the same distance to the line.

Appendix M

Windscreen influence of frequency response

A measurement was made to measure the frequency influence of the designed windscreen. The configuration include the modified GRAS AM0069 windscreen. The measurement is done in the anechoic chamber. The measurement is done to analyse the effect of the windscreen in the frequency domain to find out if the observed frequency boost in ?? is an artifact of the windscreen.

Materials and setup

To measure the frequency response of the windscreen configuration the following materials are used:

Table M.1: Equipment list

Description	Model	Serial-no	AAU-no
PC	Macbook	W89242W966H	-
Audio interface	RME Fireface UCX	23811948	108230
Microphone	GRAS 26CC	78189	75583
Preamp	GRAS 40 AZ	100268	75551
Windscreen	GRAS AM0069	-	-
large foam wedge	-	-	-
Speaker stand	-	-	-
Speaker	Dynaudio	03508438	1441-0

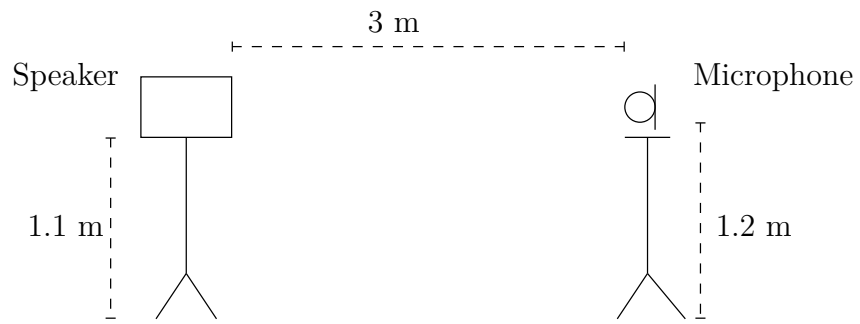


Figure M.1: The figure shows the measurement setup in the anechoic chamber

The following Figure M.2 shows the speaker.



Figure M.2: The picture shows the used speaker

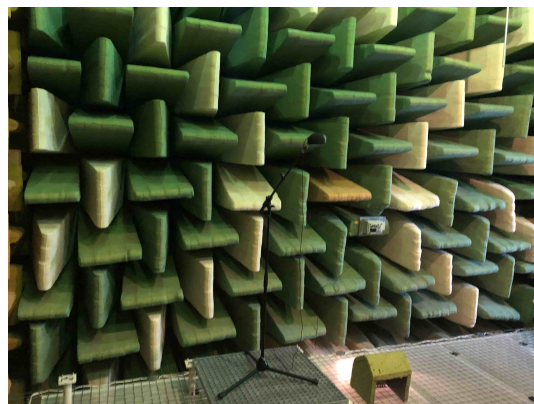


Figure M.3: The picture shows the measurement microphone with the original modified windscreens

Test procedure

1. The materials are set up as in Figure M.1 where the microphone is connected to the audio interface.
2. The microphone is calibrated
3. The speaker is placed 3 m from the microphone and pointing in the direction of the microphone.
4. The transfer function is measured of the speaker without the designed windscreen and with the modified windscreens.
5. The windscreens configuration is placed such that the microphone have approximately the same position as without the designed windscreens, (while the windscreens are tilted the microphone is closer to the speaker).
6. The transfer function is measured
7. The transfer function is calculated and plotted versus the transfer function without designed windscreens but with modified original windscreens MATLAB®.
8. The position of the windscreens is changed both with tilting and rotation while the measuring is repeated.
9. In the end the designed windscreens are measured without foam wedge.

Measurement area

To be able to measure the windscreens frequency response, the anechoic chamber in Fredrick Bajers vej 7B4, 9220 Aalborg is used. The following Figure M.4 shows a drawing of the area and the position of the fan and windscreens.

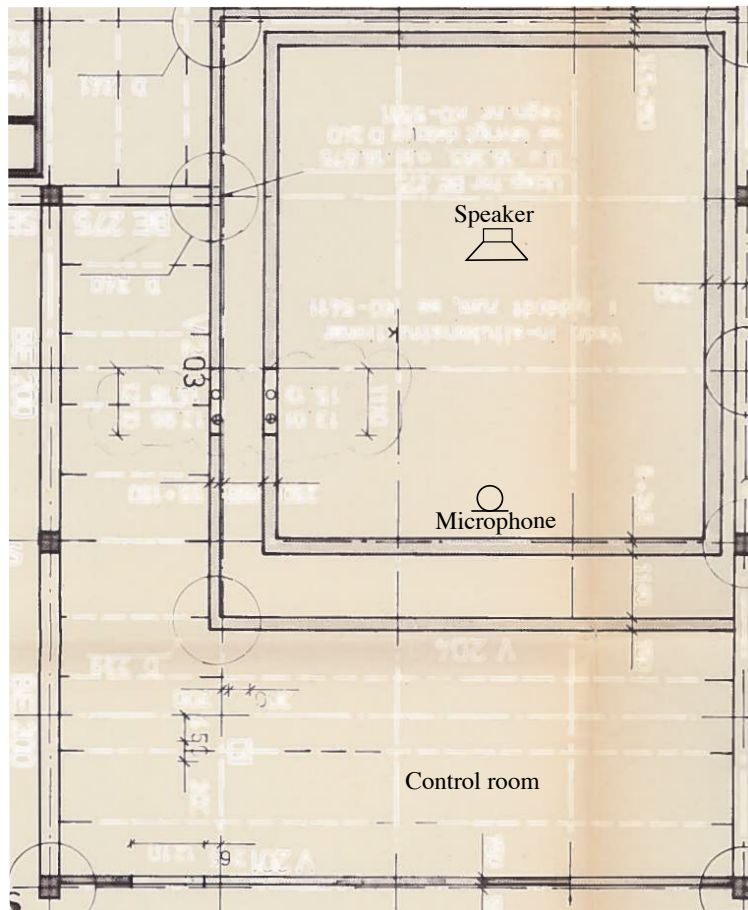


Figure M.4: The picture illustrate the area, where the wind flow is measured

Results

The following graphs shows the result of the measurement.

The first measurement in Figure M.5 shows the transfer function while the foam wedge is at its designed position and without tilting and rotation. Therefore the windscreens point with 0° to the speaker and the windscreens plate have vertical and horizontal of 0°

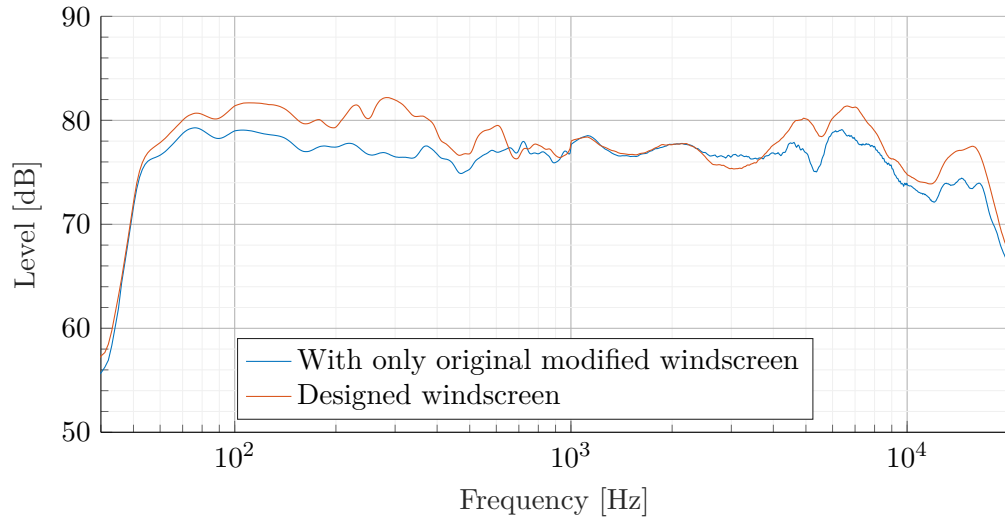


Figure M.5: The graph shows frequency response of the speaker measured without windscreen and with the designed windscreen with no rotation and no tilting

The next measurement in Figure M.6 shows the transfer function while the foam wedge is moved 20 cm back compare to its designed position and without tilting and rotation.

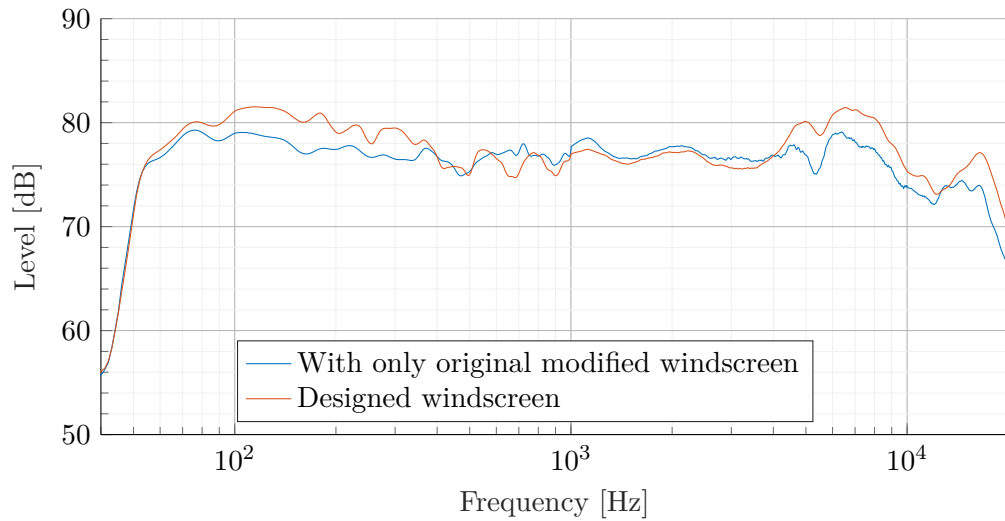


Figure M.6: The graph shows frequency response of the speaker measured without windscreen and with the designed windscreen with no rotation and no tilting while the foam wedge is moved 20 cm back

As seen in Figure M.6 the frequency response does not change markedly compare to Figure M.5. It is seen that the general level is 0.5 dB SPL lower as expected since the microphone is moved back.

The next measurement in Figure M.7 shows the transfer function while the foam wedge is at its designed position and without tilting and with 30° right rotation. Therefore the white PVC plate covers more the opening to the microphone and the windscreens have vertical and horizontal of 0°

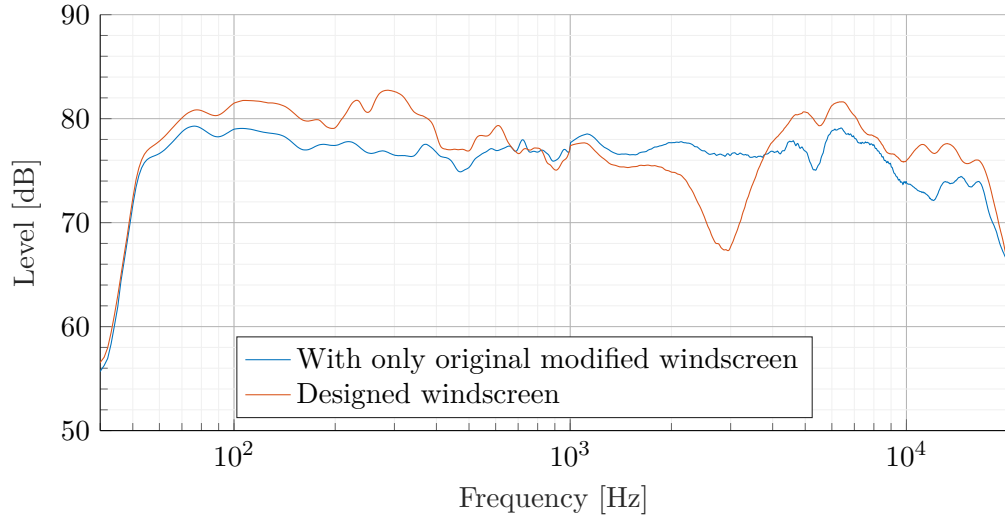


Figure M.7: The graph shows frequency response of the speaker measured without windscreens and with the designed windscreens with no tilting and a right rotation of 30°

It is seen in Figure M.7 that 30° right rotation gives a SPL depth between 1.0 kHz and 4.0 kHz otherwise the frequency response is similar to Figure M.5

The next measurement in Figure M.8 shows the transfer function while the foam wedge is at its designed position and without tilting and with 30° left rotation. Therefore the foam wedge covers more the opening to the microphone and the windscreens have vertical and horizontal of 0°

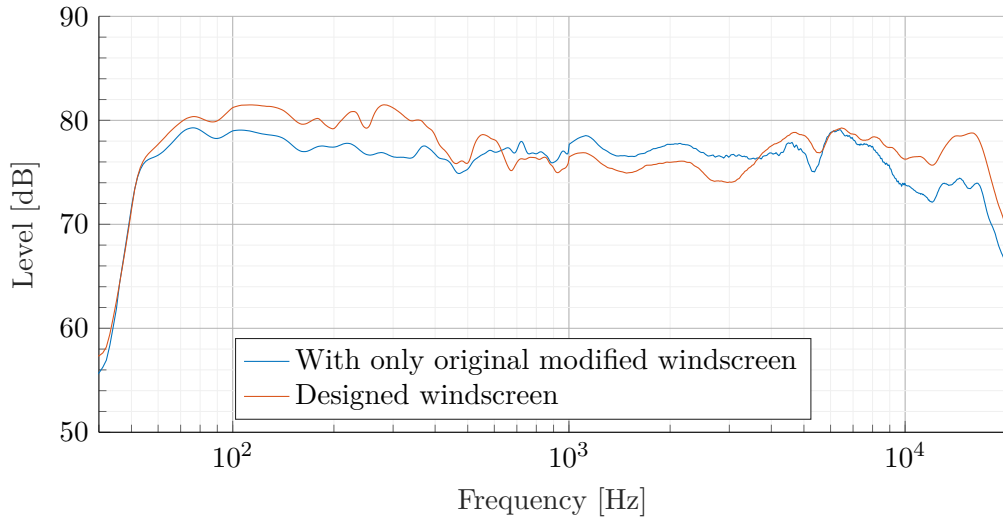


Figure M.8: The graph shows frequency response of the speaker measured without windscreens and with the designed windscreens with no tilting and a left rotation of 30°

It is seen in Figure M.8 that 30° left rotation also gives a SPL depth between 1.0 kHz and 4.0 kHz but much less than Figure M.7. Otherwise the frequency response is similar to Figure M.5

The next measurement in Figure M.9 shows the transfer function while the foam wedge is at its designed position and with a tilting of 9° and without rotation. Therefore the windscreens point with 0° to the speaker and the windscreens plate have horizontal of 0°

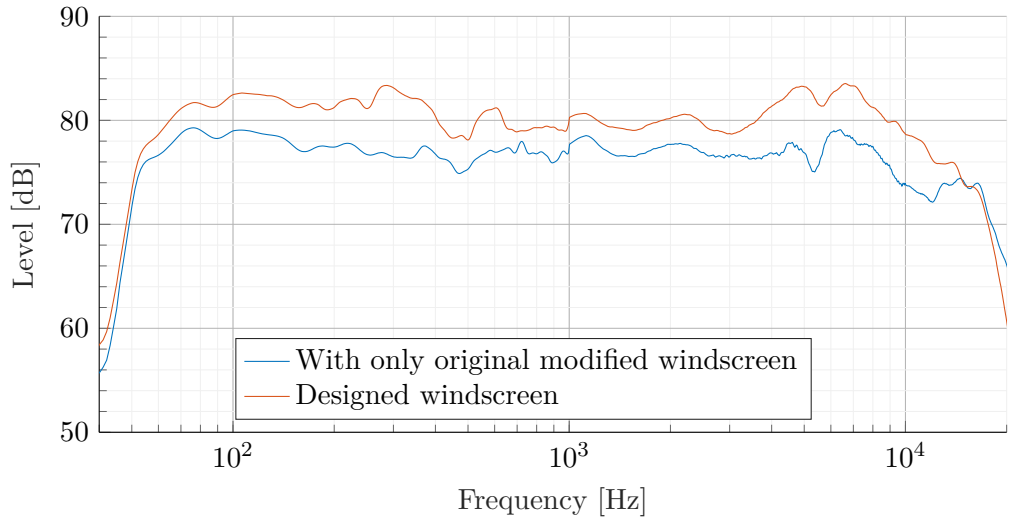


Figure M.9: The graph shows frequency response of the speaker measured without windscreen and with the designed windscreen with no rotation and a frontal tilting of 9°

As seen in Figure M.9 the frequency response does not change markedly compare to Figure M.5. It is seen that the general level is 2 dB SPL higher as expected since the microphone is moved closer to the speaker as shown in Figure M.10.



Figure M.10: The picture shows the measurement microphone with the tilted designed windscreen

Moreover there is a roll off in the frequency higher than 10 kHz which might result from a plate reflection of the sound since the microphone is lifted by the modified original windscreen. To research the roll off the tilting of the plate is raised to 20° . The result of tilting 20° is shown in Figure M.11

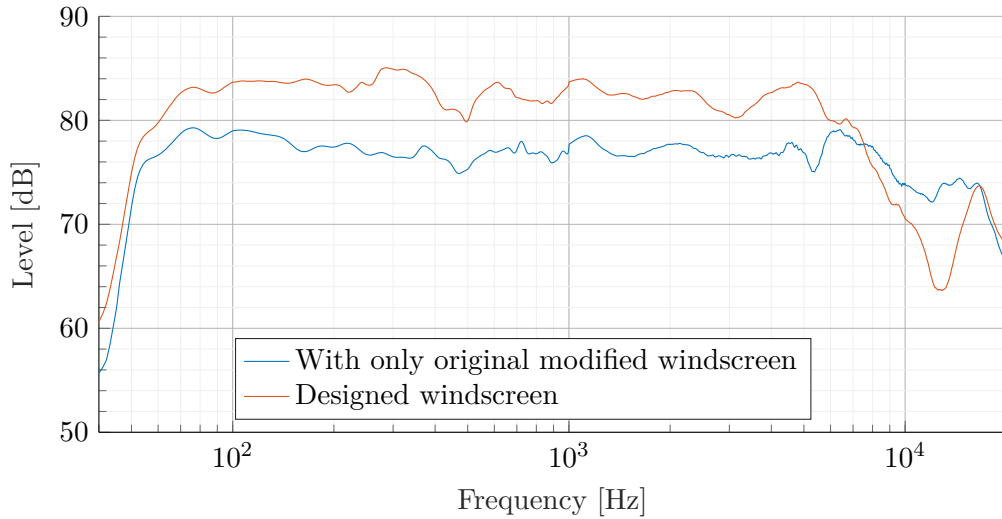


Figure M.11: The graph shows frequency response of the speaker measured without windscreen and with the designed windscreen with no rotation and a frontal tilting of 9°

As seen in Figure M.11, the roll off is due to a plate reflection. While tilting 20° the reflection frequency is lowered which means that the sound path differences of the reflected sound path grows.

A tilting of the windscreen while the foam wedge is moved 20 cm is measured as the last measurement while the foam wedge is on the plate. The following Figure M.12 shows the result with a tilt of 8° and no rotation.

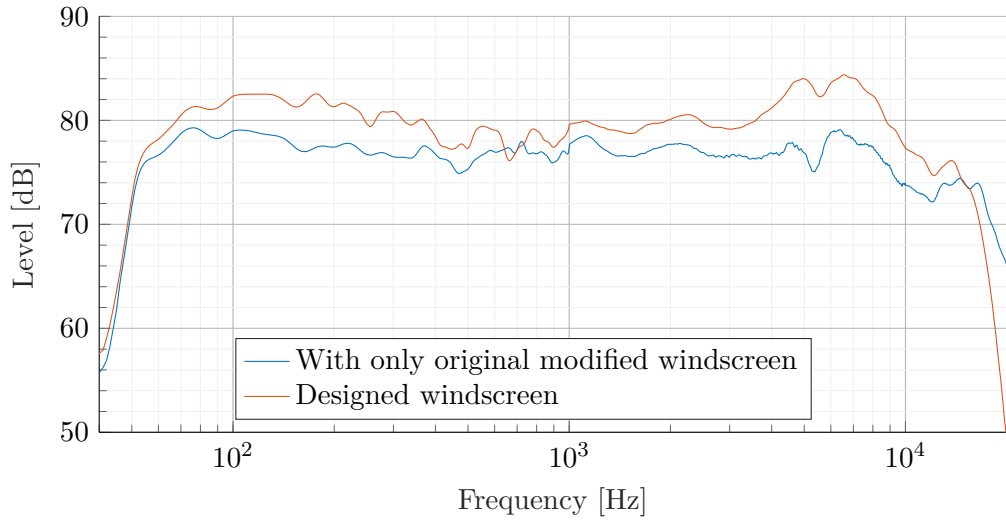


Figure M.12: The graph shows frequency response of the speaker measured without windscreen and with the designed windscreen moved 20 cm back with no rotation and a frontal tilting of 8°

The last two measurement shows the frequency response while the foam wedge is removed. The first measurement in Figure M.13 shows the frequency response without tilting and rotation. The second measurement in Figure M.14 shows the frequency response without tilting and a rotation of 30° to the right.

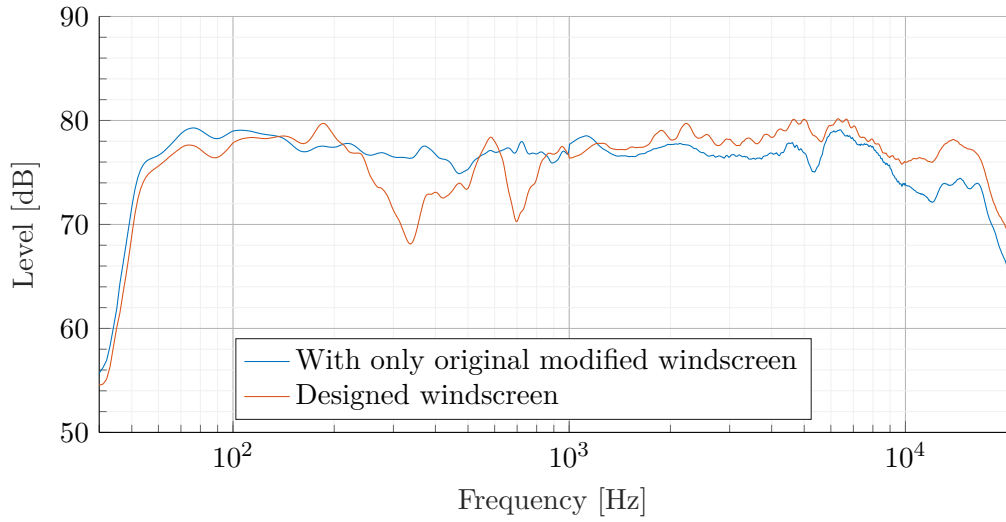


Figure M.13: The graph shows frequency response of the speaker measured without windscreen and without the designed windscreen without the foam wedge and with no rotation and no tilting

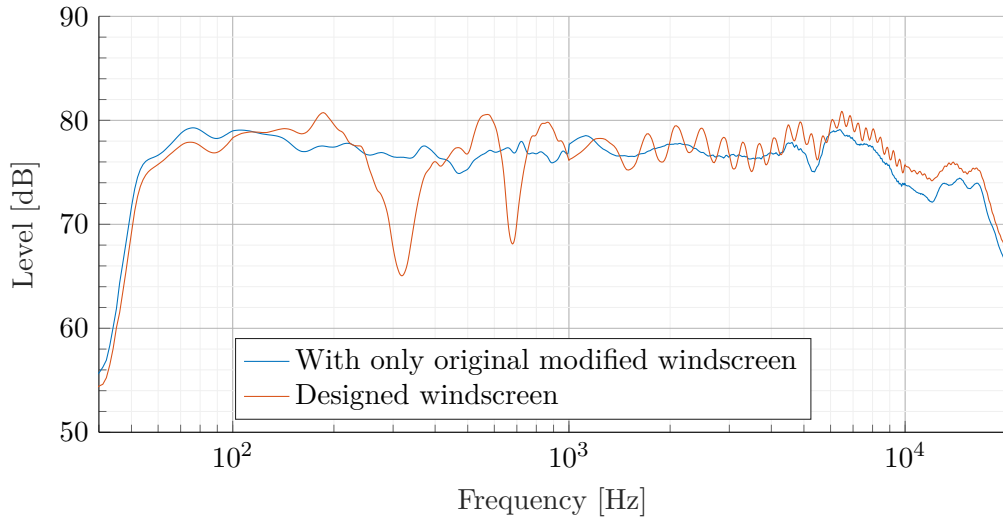


Figure M.14: The graph shows frequency response of the speaker measured without windscreen and with the designed windscreen without the foam wedge and with no tilting and a right turn of 30°

It is seen in measurement Figure M.13 and Figure M.14 that removing the foam wedge gives depth in 310 Hz and 690 Hz and the frequency response shows generally more reflections than with foam wedge.

Summary

The designed windscreen gives a small boost in frequency below 1.0 kHz and above 4.0 kHz but the boost is only approximately 2 dB SPL. Moreover tilting of the designed windscreen gives plate reflection in the high frequency, but tilting at 9° only affect frequency above 10 kHz. Rotating the windscreen ether to the left or right gives a depth within 1.0 kHz to 4.0 kHz. While moving the foam wedge backwards the frequency response of the designed windscreen have only negligible differences. Removing the wedge gives high reflection from the designed windscreen.

Appendix N

Wind noise in designed windscreen

A measurement was made to measure the wind attenuation of the designed windscreen. All measurement include the modified GRAS AM0069 windscreens. The measurement is done in real scenario outside on a flat area with above 5 m/s wind speed. The measurement is done to ensure that the measured wind does not overload the preamp of the microphone at the measured wind speed.

Materials and setup

To measure the wind attenuation of the windscreen configuration the following materials are used:

Table N.1: Equipment list

Description	Model	Serial-no	AAU-no
PC	Macbook	W89242W966H	-
Audio interface	RME Fireface UCX	23811948	108230
Microphone	GRAS 26CC	78189	75583
Preamp	GRAS 40 AZ	100268	75551
Windscreens	GRAS AM0069	-	-
Designed windscreens	-	-	-

Table N.2: Equipment list

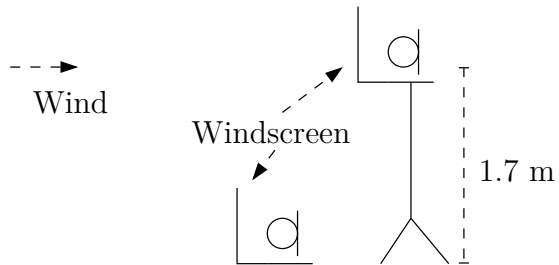


Figure N.1: The figure shows the measurement setup for the wind noise measurement.



Figure N.2: The picture shows the measurement set up

Test procedure

1. The materials are set up as in Figure N.1 where the microphone is connected to the audio interface.
2. The microphone is calibrated.
3. A 7 s time signal is measured.
4. The frequency content is calculated by `fft` after the time signal is windowed by a Hanning window.
5. The procedure is done with and without the windscreens.
6. The procedure is done where the windscreens are rotated 50° and -50°.
7. The result is plotted in MATLAB®.
8. The measurement is done over for every position until similar wind speed is measured with about 8.5 m/s.

Measurement area

To be able to measure in a windy area, the football stadium at Fredrick Alfred Nobels Vej 7, 9220 Aalborg is used. The following Figure N.3 shows a picture of the area and the approximate position of the speaker and microphone.



Figure N.3: The picture illustrate the area, where the measured is done

Results

The following graphs shows the result of the measurement.

The graph in Figure N.4 shows a measurement where the modified original wind-screen is on the ground and in the hight of 1.7 m.

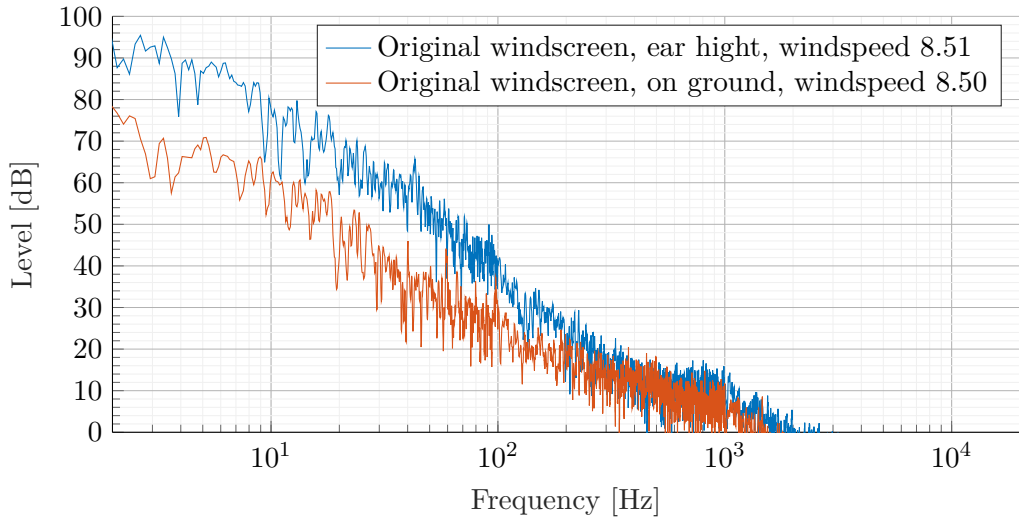


Figure N.4: The graph shows the frequency content of the measurement without the windscreen

As seen in Figure N.4, the wind noise is more than 10 dB SPL lower while the modified original windscreen is moved from the hight of 1.7 m to the ground.

The graph in Figure N.5 shows a measurement where the designed windscreen is on the ground and in the hight of 1.7 m. The windscreen is 90° to the wind in both measurement, which mean that the wind is orthogonal to the middle of the white PVC plate.

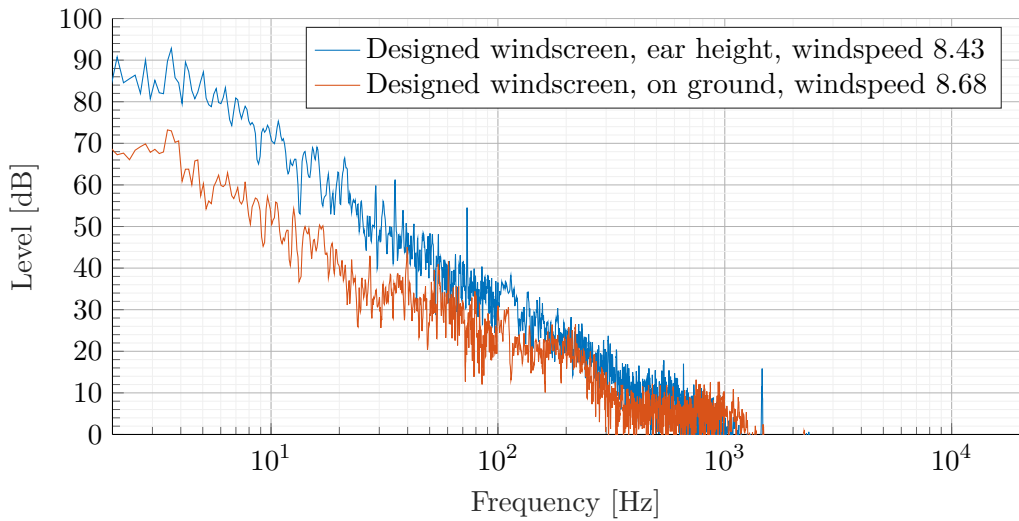


Figure N.5: The graph shows the frequency content of the measurement without the windscreen

As in Figure N.4 The wind noise is lowered more than 10 dB SPL in Figure N.5. Furthermore, the wind noise is lowered approximately 5 dB SPL to 10 dB SPL from 100 Hz and below while the designed windscreen is used. The highest attenuation is while the the windscreen is lifted above the ground.

Based on the observed ground reflection shown in section 8.1.1 and the high noise differences founded in the above measurement, only the measurement on the ground is shown in the rest of the measurement. The measurement in ear hight is chosen to be irrelevant since the measurement for the final test is done with microphone on the ground. The measurement in the hight of the ear can be founded in the file. The following measurement Figure N.6 shows the measurement with and without the designed windscreen.

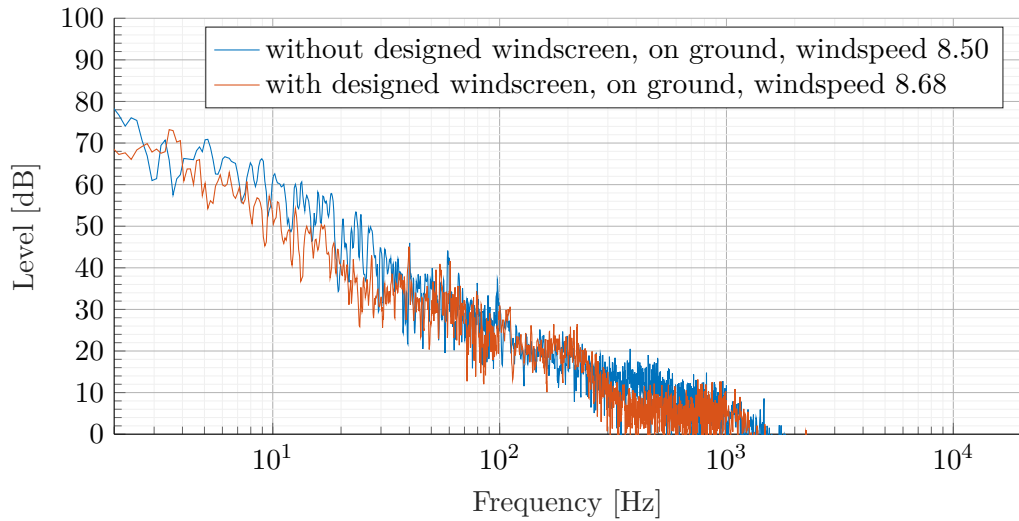


Figure N.6: The graph shows the frequency content of the measurement without the windscreen

As it is seen in Figure N.6 and explained above, it is clearly seen that the designed windscreen attenuate the wind noise. The next measurement Figure N.7 shows the differences in wind noise while the windscreen is ether rotated 50° to the left and to the right.

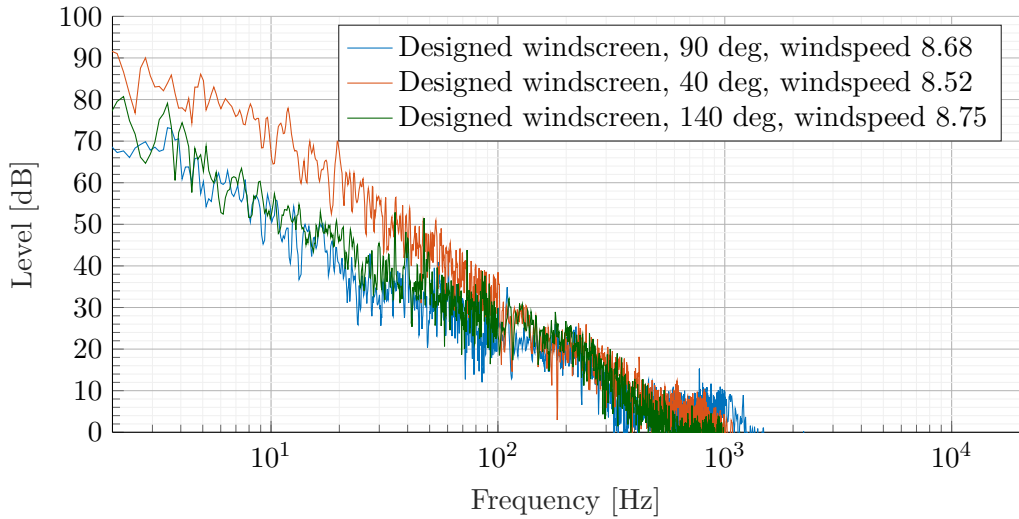


Figure N.7: The graph shows the frequency content of the measurement without the windscreen

As seen in Figure N.7 the wind noise depend on the angle of the wind to the designed windscreen. While the designed windscreen is rotated 50° to the left, the windscreen does not have any wind noise attenuation compare to the measurement with only the modified windscreen. While the designed windscreen is rotated 50° to the right, the wind noise follows the wind noise while the designed windscreen is non rotated unless around 2 Hz where the noise is 10 dB SPL higher.

Summary

It is founded that changing the position from the ear hight to the ground is have by it self a wind noise attenuation of more that 10 dB SPL and further the designed windscreen attenuate at less 5 dB SPL more while the designed windscreen is orthogonal to the wind, so non rotated and rotated such that the wind blows to the back of the designed windscreen. While the designed windscreen opening is rotated to the wind, the designed windscreen have no wind noise attenuation.

Appendix O

Hardware

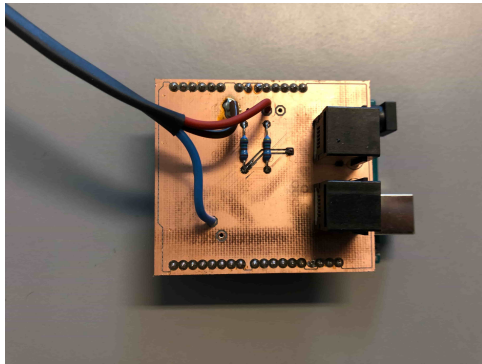


(a) The picture shows the anemometer.

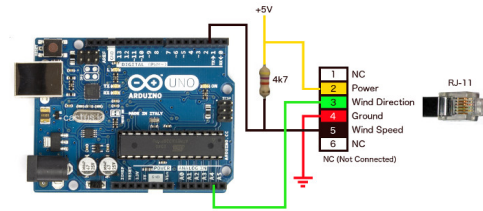


(b) The picture shows the temperature and humidity censor

Figure O.1: The figures shows the measurement sensors



(a) The picture shows the Arduino shield



(b) The picture shows the wire connection. The connection schematic is founded at [cactus.io, 2019]

Figure O.2: The figure shows the Arduino shield and the connection of the anemometer

Appendix P

Questionnaire

A questionnaire was made to find the maximum coverage distance for a line array.

Question	Answer	Unit
<i>Company</i>	Profox	
<i>What is the distances between the main stage to the first delay tower at large concert</i>	50	[m]
<i>How many audience attempt to a large concert you produces</i>	15000+	Number
<i>What is the distances between the main stage to the first delay tower at medium concert</i>	30	[m]
<i>How many audience attempt to a medium concert you produces</i>	5000+	Number
<i>Flying hight of top speaker</i>	12 - 16	[m]
<i>Does the wind direction and speed influence on the distance decision</i>	No	
<i>Do you want to know the end result</i>	Yes	

Question	Answer	Unit
<i>Company</i>	Nordic sales	
<i>What is the distances between the main stage to the first delay tower at large concert</i>	75	[m]
<i>How many audience attempt to a large concert you produces</i>	100000+	Number
<i>What is the distances between the main stage to the first delay tower at medium concert</i>	50	[m]
<i>How many audience attempt to a medium concert you produces</i>	30000	Number
<i>Flying hight of top speaker</i>	?	[m]
<i>Does the wind direction and speed influence on the distance decision</i>	Yes	
<i>Do you want to know the end result</i>	No	

Question	Answer	Unit
<i>Company</i>	Moto rental	
<i>What is the distances between the main stage to the first delay tower at large concert</i>	50-60	[m]
<i>How many audience attempt to a large concert you produces</i>	20000+	Number
<i>What is the distances between the main stage to the first delay tower at medium concert</i>	50	[m]
<i>How many audience attempt to a medium concert you produces</i>	5000+	Number
<i>Flying hight of top speaker</i>	12 - 16	[m]
<i>Does the wind direction and speed influence on the distance decision</i>	Yes	
<i>Do you want to know the end result</i>	Yes	

Question	Answer	Unit
<i>Company</i>	Roskilde festival	
<i>What is the distances between the main stage to the first delay tower at large concert</i>	73	[m]
<i>How many audience attempt to a large concert you produces</i>	100000+	Number
<i>What is the distances between the main stage to the first delay tower at medium concert</i>	?	[m]
<i>How many audience attempt to a medium concert you produces</i>	?	Number
<i>Flying hight of top speaker</i>	?	[m]
<i>Does the wind direction and speed influence on the distance decision</i>	No	
<i>Do you want to know the end result</i>	No	
Question	Answer	Unit
<i>Company</i>	AV-center Aalborg	
<i>What is the distances between the main stage to the first delay tower at large concert</i>	60	[m]
<i>How many audience attempt to a large concert you produces</i>	20000+	Number
<i>What is the distances between the main stage to the first delay tower at medium concert</i>	30	[m]
<i>How many audience attempt to a medium concert you produces</i>	5000+	Number
<i>Flying hight of top speaker</i>	14 - 16	[m]
<i>Does the wind direction and speed influence on the distance decision</i>	Yes	
<i>Do you want to know the end result</i>	Yes	
<i>comment: The biggest problem lays in the frequency range from 1.0 kHz to 7.0 kHz where the understanding of the music despisers and the music sound muddy</i>	-	

Question	Answer	Unit
<i>Company</i>	Kinovox	
<i>What is the distances between the main stage to the first delay tower at large concert</i>	60	[m]
<i>How many audience attempt to a large concert you produces</i>	20000+	Number
<i>What is the distances between the main stage to the first delay tower at medium concert</i>	30	[m]
<i>How many audience attempt to a medium concert you produces</i>	10000	Number
<i>Flying hight of top speaker</i>	14 - 16	[m]
<i>Does the wind direction and speed influence on the distance decision</i>	Yes	
<i>Do you want to know the end result</i>	No	
<i>comment: He use to rotate the line array agents the wind if he know that the wind is crosswind and the wind will continue along the concert time. Moreover he would stop the concert if the wind speed is above 10 m/s</i>	-	

Bibliography

AOSONG. *Temperature and humidity module*, AOSONG. Available at: <<https://akizukidensi.com/download/ds/aosong/AM2302.pdf>>.

Association, D. W. I., 2003. *The Geostrophic Wind*, Danish Wind Industry Association. [Website]. Available at: <<http://dr\T1\omst\T1\orre.dk/wp-content/wind/miller/windpower%20web/en/tour/wres/geostro.htm>>. [Accessed 18 feb 2019].

Ballou, G. Focal Press, Oxford, fourth edition edition, 2008. ISBN 978-0-240-80969-4. doi: <https://doi.org/10.1016/B978-0-240-80969-4.50002-X>. Available at: <<http://www.sciencedirect.com/science/article/pii/B978024080969450002X>>.

Bauman, P., Urban, M., and Heil, C. Wavefront Sculpture Technology. In *Audio Engineering Society Convention 111*, Nov 2001. Available at: <<http://www.aes.org/e-lib/browse.cfm?elib=9813>>.

Beranek, L. L., 2006. Analysis of Sabine and Eyring equations and their application to concert hall audience and chair absorption. *The Journal of the Acoustical Society of America*, 120(3), pp. 1399–1410. doi: 10.1121/1.2221392. Available at: <<https://doi.org/10.1121/1.2221392>>.

Bohn, D. A. Environmental Effects on the Speed of Sound. In *Audio Engineering Society Convention 83*, Oct 1987. Available at: <<http://www.aes.org/e-lib/browse.cfm?elib=4916>>.

cactus.io, 2019. *How to Hookup Davis Anemometer to Arduino (Part 1 of 3)*, cactus.io. [Website]. Available at: <<http://cactus.io/hookups/weather/anemometer/davis/hookup-arduino-to-davis-anemometer>>. [Accessed 21 maj 2019].

Corteel, E., Sugden, S., and Montignies, F. Large Scale Open Air Sound Reinforcement in Extreme Atmospheric Conditions (Engineering Brief). In *Audio Engineering Society Conference: 2017 AES International Conference on Sound Reinforcement – Open Air Venues*, Aug 2017. Available at: <<http://www.aes.org/e-lib/browse.cfm?elib=19184>>.

- Crocker, M. J. *Handbook of Acoustics*. John Wiley & Sons, New York, 1998. ISBN 978-0-471-25293-1.
- Czerwinski, E., Voishvillo, A., Alexandrov, S., and Terekhov, A., 1999. Air-Related Harmonic and Intermodulation Distortion in Large Sound Systems. *J. Audio Eng. Soc*, 47(6), pp. 427–446. Available at: <<http://www.aes.org/e-lib/browse.cfm?elib=12102>>.
- Davis. *Anemometer Vantage Pro2TM Accessories*, Davis. Available at: <https://www.davisinstruments.com/product_documents/weather/spec_sheets/6410_SS.pdf>.
- d&b audiotechnik, 2019. *d&b Soundscape*, d&b audiotechnik. [Website]. Available at: <<https://www.dbsoundscape.com/global/en/>>. [Accessed 21 feb 2019].
- de Oliveira, A. F. G. P., 2012. The effect of wind and turbulence on sound propagation in the atmosphere. Speciale, Instituto Superior Technico Universidad Tecnica de Lisboa. Available at: <<https://fenix.tecnico.ulisboa.pt/downloadFile/395144345754/dissertacao.pdf>>.
- Embleton, T. F. W., 1996. Tutorial on sound propagation outdoors. *The Journal of the Acoustical Society of America*, 100(1), pp. 31–48. doi: 10.1121/1.415879. Available at: <<https://doi.org/10.1121/1.415879>>.
- Gunness, D. W. Loudspeaker Transfer Function Averaging and Interpolation. In *Audio Engineering Society Convention 111*, Nov 2001. Available at: <<http://www.aes.org/e-lib/browse.cfm?elib=9850>>.
- ISO 9613-1:1993. *Acoustics – Attenuation of sound during propagation outdoors – Part 1: Calculation of the absorption of sound by the atmosphere*.
- L-Acoustics, a. *KUDO Multi-Mode WST Enclosure*, L-Acoustics. Available at: <<http://www.dreamsound.com/downloadable/211>>.
- L-Acoustics, b. *KUDO*, L-Acoustics. Available at: <http://impact-even.com/wp/wp-content/uploads/2012/03/procedure_d_accrochage_kudo.pdf>.
- L-Acoustics, 2019. *Live Sound*, L-Acoustics. [Website]. Available at: <<https://www.lisa-immersive.com/live-sound/>>. [Accessed 21 feb 2019].

- Letowski, T. R. and Scharine, A. A., 2017. Correlational Analysis of Speech Intelligibility Tests and Metrics for Speech Transmission, US Army Research Laboratory. [Online], DEFENSE TECHNICAL INFORMATION CENTER. Available at: <<http://www.dtic.mil/dtic/tr/fulltext/u2/1043203.pdf>>. [Accessed 27.09.2018].
- Levine, D. R., Calza, P., Di Cola, M., Martignon, P., and Chisari, L. Influence of Horn's Surface Temperature on its Directivity Control. In *Audio Engineering Society Convention 145*, Oct 2018. Available at: <<http://www.aes.org/e-lib/browse.cfm?elib=19746>>.
- Müller, S. and Massarani, P., 2001. Transfer-Function Measurement with Sweeps. *J. Audio Eng. Soc*, 49(6), pp. 443–471. Available at: <<http://www.aes.org/e-lib/browse.cfm?elib=10189>>.
- Ostashev, V. E., Wilson, D. K., Liu, L., Aldridge, D. F., Symons, N. P., and Marlin, D., 2005. Equations for finite-difference, time-domain simulation of sound propagation in moving inhomogeneous media and numerical implementation. *The Journal of the Acoustical Society of America*, 117(2), pp. 503–517. doi: 10.1121/1.1841531. Available at: <<https://doi.org/10.1121/1.1841531>>.
- Piercy, J. E., Embleton, T. F. W., and Sutherland, L. C., 1977. Review of noise propagation in the atmosphere. *The Journal of the Acoustical Society of America*, 61 (6), pp. 1403–1418. doi: 10.1121/1.381455. Available at: <<https://doi.org/10.1121/1.381455>>.
- Prospathopoulos, J. M. and Voutsinas, S. G., 2007. Determination of equivalent sound speed profiles for ray tracing in near-ground sound propagation. *The Journal of the Acoustical Society of America*, 122(3), pp. 1391–1403. doi: 10.1121/1.2764476. Available at: <<https://doi.org/10.1121/1.2764476>>.
- Roozen, N. B., Vael, J. E. M., and Nieuwendijk, J. A. Reduction of Bass-Reflex Port Nonlinearities by Optimizing the Port Geometry. In *Audio Engineering Society Convention 104*, May 1998. Available at: <<http://www.aes.org/e-lib/browse.cfm?elib=8519>>.
- Rossing, T. *Springer Handbook of Acoustics*. 01 2014. ISBN 978-1-4939-0754-0. doi: 10.1007/978-1-4939-0755-7.
- Vanderkooy, J. Nonlinearities in Loudspeaker Ports. In *Audio Engineering Society Convention 104*, May 1998. Available at: <<http://www.aes.org/e-lib/browse.cfm?elib=8432>>.
- Voishvillo, A. Comparative Analysis of Nonlinear Distortion in Compression Drivers and Horns. In *Audio Engineering Society Convention 117*, Oct 2004. Available at: <<http://www.aes.org/e-lib/browse.cfm?elib=12849>>.

- Wong, G. S. K. and Embleton, T. F. W., 1985. Variation of the speed of sound in air with humidity and temperature. *The Journal of the Acoustical Society of America*, 77 (5), pp. 1710–1712. doi: 10.1121/1.391918. Available at: <<https://doi.org/10.1121/1.391918>>.
- Yang, X. *Atmospheric Acoustics*. Walter de Gruyter GmbH Co KG, Berlin, 2016. ISBN 978-3-110-31153-2.